

**LITHOFACIES ASSEMBLAGES, DEPOSITIONAL ENVIRONMENTS AND
HYDROCARBON POTENTIAL OF A POTENTIAL RESERVOIR WITHIN THE
BANFF FORMATION IN NORTHEASTERN BRITISH COLUMBIA**

Daniel Swinden Haider

Submitted in Partial Fulfilment of the Requirements
for the Degree of Bachelor of Science, Honours
Department of Earth Sciences
Dalhousie University Halifax, Nova Scotia
March 2008

DATE: 18/04/2008

AUTHOR: Daniel Swinden Haider

TITLE: LITHOFACIES ASSEMBLAGES, DEPOSITIONAL ENVIRONMENTS,
AND HYDROCARBON POTENTIAL OF A POTENTIAL
RESERVOIR WITHIN THE BANEF FORMATION IN
NORTHEASTERN BRITISH COLUMBIA

Degree: BSC Convocation: SPRING, 2008 Year: 2008

Permission is herewith granted to Dalhousie University to circulate and to have copied for non-commercial purposes, at its discretion, the above title upon the request of individuals or institutions.

Signature of Author

THE AUTHOR RESERVES OTHER PUBLICATION RIGHTS, AND NEITHER THE THESIS NOR EXTENSIVE EXTRACTS FROM IT MAY BE PRINTED OR OTHERWISE REPRODUCED WITHOUT THE AUTHOR'S WRITTEN PERMISSION.

THE AUTHOR ATTESTS THAT PERMISSION HAS BEEN OBTAINED FOR THE USE OF ANY COPYRIGHTED MATERIAL APPEARING IN THIS THESIS (OTHER THAN BRIEF EXCERPTS REQUIRING ONLY PROPER ACKNOWLEDGEMENT IN SCHOLARLY WRITING) AND THAT ALL SUCH USE IS CLEARLY ACKNOWLEDGED.

ABSTRACT

The early Tournaisian - Viséan Banff Formation which accumulated as shallowing upward basinal, slope, shelf margin, and protected shelf deposits of a carbonate ramp system extends throughout the Western Canadian Sedimentary Basin (WCSB). In northeastern BC, the Banff Formation was divided by Richards (1993) into the informal members A and D. Basinal shale layers of Member A grade upward and laterally into interbedded layers of supratidal and shallow marine limestones and shales of member D. Well-log correlation and mapping of a 1700 km² area just northeast of Fort Nelson revealed a 5 m thick, potential carbonate reservoir unit, informally known as the Banff C which is particularly well developed over the Beatton High in the underlying bedrock. A cored interval within well d-A3-E/94-I-14 centered is upon the Banff C. Lithological interpretations of this core suggest that it consists of an upper, middle, and lower unit, each of which represents a different, relatively shallow marine environment.

The lower unit is an open-marine, mixed carbonate and siliciclastic deposit that consists of interbedded shale and massive carbonate rich in brachiopods and microfossils, including foraminifera and radiolarians. The unit represents sediments transported basinward by storms. The middle unit is a tidally influenced carbonate sand. It consists of stacked successions of tight skeletal and peloidal grainstones that coarsen upwards into porous oolitic grainstones. This unit correlates with the potential Banff C reservoir unit observed in the subsurface. The middle unit is interpreted as a sand-shoal barrier complex that formed on a tidally influenced shallow shelf margin. The upper unit formed in a protected setting landward of the shoal, and is represented by peloidal wackestones and mudstones with pelmatozoan and bryozoan fragments but generally lacking siliciclastic grains. Thin green paleosols represent brief periods of exposure during deposition of the upper unit. The upper unit accumulated in normal salinity conditions in a quiet, back-barrier environment.

Porosity is negligible in both the lower and upper units and ranks from negligible to good (0.1 to 18.5%) in the middle unit. Highest porosity levels are associated with the oolitic grainstone, where large moldic pores are prominent, along with ineffective micropores within micritized grains. Permeability levels rank from negligible to poor (<2.1 mD), and connectivity is generally poor. The middle unit sand belt is of low to moderate reservoir quality and may be capable of producing light oil or gas. Gas shows observed in strip logs are as high as 51 times background levels, indicating that the Banff C is a hydrocarbon-charged reservoir which probably belongs to a closed Late Devonian-Early Carboniferous petroleum system. Hydrocarbons probably originated from source rocks in the underlying Exshaw Formation and lower Banff correlatives.

TABLE OF CONTENTS

ABSTRACT	i
TABLE OF CONTENTS	ii
LIST OF FIGURES	vi
LIST OF TABLES	viii
ACKNOWLEDGEMENTS	v
CHAPTER 1 – Introduction	1
1.1.0 Introduction – The Banff Formation	1
1.2.0 Study area	1
1.3.0 Previous Work	2
1.4.0 Summer Work	4
1.5.0 Objectives	6
CHAPTER 2 – Regional Geology	7
2.1.0 Background	7
<u>2.1.1 DC Sea-Level</u>	7
2.2.0 Depositional Setting of the WCSB	8
2.3.0 Devonian Carboniferous (DC) succession	11
2.4.0 Banff Assemblage	12
<u>2.4.1 Exshaw Formation</u>	13
<u>2.4.2 Banff Formation</u>	14
2.5.0 Local Geology in Study Area	16
<u>2.5.1 Middle Banff C Unit</u>	16
<u>2.5.2 Interpretation</u>	20

CHAPTER 3 – Methodology	22
3.1.0 Introduction - Research Methods	22
3.2.0 Subsurface Mapping	22
3.3.0 Lithological Observations	23
<u>3.3.1 Megascopic Observations</u>	23
<u>3.3.2 Microscopic Observations</u>	24
3.4.0 Porosity and Permeability	24
<u>3.4.1 Porosity</u>	25
<u>3.4.2 Permeability</u>	25
3.5.0 X-Ray Diffraction	26
CHAPTER 4 - Lithofacies descriptions and depositional settings	28
4.1.0 Introduction	28
4.2.0 Lower Unit: open-marine mixed carbonate siliciclastics	31
<u>4.2.1 Lithofacies A Skeletal Mudstone/Wackestone</u>	33
<u>4.2.2 Lithofacies B Skeletal Wackestone</u>	34
<u>4.2.3 Lithofacies C Dark Siltstone Shale</u>	35
<u>4.2.4 Depositional Setting: Lower Unit</u>	37
4.3.0 Middle Unit: Tidal-influenced carbonate sand belt	37
<u>4.3.1 Lithofacies D Ooid Grainstone</u>	38
<u>4.3.2 Lithofacies E Peloidal Grainstone</u>	39
<u>4.3.3 Lithofacies F Skeletal Grainstone/Packstone</u>	40
<u>4.3.4 Depositional Setting: Middle Unit</u>	41
4.4.0 Upper Unit: Protected backshoal	44

<u>4.4.1 Lithofacies G Peliodal/Skeletal lime Wackestone</u>	45
<u>4.4.2 Lithofacies H Green Shale</u>	47
<u>4.4.3 Lithofacies I Lime Mudstone</u>	48
<u>4.4.4 Lithofacies J Skeletal Packstone</u>	50
<u>4.4.5 Depositional Setting: Upper Unit</u>	52
4.5.0 Well-log responses of Core Units	52
<u>4.5.1 Lower Unit</u>	52
<u>4.5.2 Middle Unit</u>	53
<u>4.5.3 Upper Unit</u>	53
4.6.0 Stratigraphic Succession	54
4.7.0 Modern Analogue –Bahamas Bank	57
CHAPTER 5 - Porosity, Permeability and Diagenesis	60
5.1.0 Diagenesis and Porosity Types:	60
5.2.0 Porosity Values:	63
5.3.0 Permeability Values:	64
5.4.0 Summary/Reservoir Quality middle core unit	65
CHAPTER 6 – Hydrocarbon Potential of Banff C, northeastern BC	66
6.1.0 Carboniferous Reserves	66
6.2.0 Petroleum Systems	66
<u>6.2.1 Exshaw Formation – potential source rock</u>	67
<u>6.2.2 Banff C – potential reservoir</u>	68
<u>6.2.3 Seal/ Cap rocks</u>	70
<u>6.2.4 Trapping Mechanisms</u>	71

<u>6.2.5 Type of petroleum system</u>	71
CHAPTER 7 – Conclusions	73
7.1.0 Core Observations	73
7.2.0 Recommendations for Further Analysis	75
7.3.0 Recommendations for Drilling	76
8.0 REFERENCES	77
APPENDIX A – Core Photographs	
APPENDIX B – Thin Section Descriptions	
APPENDIX C - XRD Data	

LIST OF FIGURES

Figure 1.1	Study Area	3
Figure 1.2	Informal Banff subdivisions – EnCana Nomenclature	5
Figure 2.1	Carboniferous Carbonate Ramp Model	8
Figure 2.2	Tectonic Model – northern Carboniferous WCSB	9
Figure 2.3	Regional Stratigraphic cross-section	10
Figure 2.4	Stratigraphic Devonian-Carboniferous log	12
Figure 2.5	Local cross-section	19
Figure 2.6	Banff C Isopach Map	20
Figure 3.1	Dunham’s Carbonate Classification Scheme	23
Figure 4.1	Summary log of Banff Cored Interval	30
Figure 4.2	Ternary Composition Diagram	31
Figure 4.3	Lithofacies A	33
Figure 4.4	Lithofacies B	35
Figure 4.5	Lithofacies C	36
Figure 4.6	Lithofacies D	39
Figure 4.7	Lithofacies E	40
Figure 4.8	Lithofacies F	41
Figure 4.9	Coarsening upward trends in middle core unit	43
Figure 4.10	Increasing porosity cycles in middle core unit	44
Figure 4.11	Lithofacies G	47
Figure 4.12	Lithofacies H	48
Figure 4.13	Lithofacies I	49
Figure 4.14	Lithofacies J	51
Figure 4.15	Gamma and Porosity log-response	54
Figure 4.16	3-D Depositional Setting model	57
Figure 4.17	Lithological Comparison of oolitic Grainstones from the Bahamas and the Banff Formation	59
Figure 5.1	Paragenesis of Middle Sand Unit	61

Figure 5.2	Ternary Pore-type Diagram	62
Figure 5.3	Total and effective Porosity Histogram	63
Figure 5.4	Permeability Histogram	65
Figure 6.1	Gas Show – strip log	69
Figure 6.2	Comparison of Banff C Net Pay and Isopach Maps	70

LIST OF TABLES

Table 2.1	Summary of Richards Members (Richards, 1989; Richards et al., 1993)	15
Table 2.2	Summary of local geology	18
Table 3.1	Qualitative Porosity Classification (North, 1985)	25
Table 3.2	Qualitative Permeability Classification (North, 1985)	26
Table 4.1	Summary of core units, lithofacies and associated thin section samples	29
Table 4.2	Lower Banff Core Unit	32
Table 4.3	Middle Banff Core Unit	38
Table 4.4	Upper Banff Core Unit	45
Table 5.1	Porosity and Permeability Data	60
Table 6.1	Tmax maturation levels	68
Table 6.2	Reserves analysis, parameters, and results (Banff C)	70

ACKNOWLEDGEMENTS

First of all, I would like to thank Dr. Martin Gibling. I never could have accomplished this without his guidance, patience, and endless enthusiasm. Many thanks to Rick Weirzbicki and the Fort Nelson Business Unit of EnCana Corporation for sparking my interest in carbonate sedimentology and petroleum geology and allowing me to develop what originally was a summer work-term project into the undergraduate thesis before you. I would also like to thank Dr. Grant Wach for bringing the project back to Halifax and setting me up with Dr. Gibling. My best regards go out to Dr. Yawooz Kettanah and Keith Taylor for helping out with the XRD data and apparatus and I can't forget Gordon Brown who provided me with thin sections. Finally I would like to thank my friends and family who stuck with me through the long sleepless nights and the maximum stress periods.

CHAPTER 1 - Introduction

1.1.0 Introduction

The Banff Formation represents one of the initial members of the Late Devonian to Early Carboniferous (D-C) carbonate ramp succession deposited in the Western Canada Sedimentary Basin (WCSB). The Banff, Rundle and Mattson assemblages make up this D-C shallowing-upward succession. The early Tournaisian – Visean Banff Formation of Western Canada lies within the Banff Assemblage and comprises shale, carbonate, and fine-grained mixed carbonate-siliciclastic sediments that extend throughout the WCSB. Basinal sediments from the lower Banff shallow upward into slope and shelf carbonate and siliciclastic sediments of the middle and upper Banff. Although gas shows within the Banff Formation have occasionally been encountered, few reservoir rocks have been found (Law, 1981).

Reservoirs account for one of the basic elements of a petroleum system and are generally defined by their relatively high levels of porosity and permeability. Magoon (1988) describes a petroleum system as one that includes all those geologic elements and processes that are essential for an oil and gas deposit to exist. This thesis is a continuation of the author's summer of 2007 work-term project with the EnCana Corporation. Using core data from a 15m cored interval through the Banff C unit (well: d-A3-E/94-I-14; Fig 1.1-C), it describes and interprets the geology of the potential Banff C petroleum reservoir, in northeastern British Columbia (BC) and assesses the effectiveness of its petroleum system.

1.2.0 Study area

Located slightly east of Fort Nelson in northeast BC, the 1700 km² study area falls in the map unit subdivision 94-I in sheets 11-14 (Fig 1.1). The drilling rights for

over 80% of this area belong to the EnCana Corporation. The boundaries of the study area were established during the summer work term, in 2007. The following data were available for evaluation within the study area. A total of 104 electric well logs (Fig 1.1-C) which penetrate the Banff Formation were used for the subsurface correlation and mapping of the Banff Formation. Also a 15 m core sample, taken at location D-A3-E/94-I-14 was available for lithological observations. (For core photographs, see Appendix I).

1.3.0 Previous Work

The Banff Formation was studied in the Fort Nelson area by Paul Barker of EnCana Corporation. He initially subdivided the formation into five units which were further subdivided to facilitate the author's summer 2007 project (Fig 1.2). GR Petrology Incorporated (2005) performed reservoir quality analysis including porosity and permeability measurements on 5 samples within the 5 m thick interval of the cored Banff C unit at location; d-A3-E/94-I-14 core sample. For each sample they reported porosity data using conventional core analysis and point count methods. Using point counts, GR Petrologies were also able to estimate mineral abundances. Using the properties of these samples, they assessed the reservoir quality of the middle Banff C unit. Brief, non-detailed lithological descriptions of the d-A3-E/94-I-11 well were created by Calin Dragoie of Cabra Consulting (2005). The reports listed above made little attempt to interpret depositional processes, paleoenvironments, and sequence stratigraphic context.

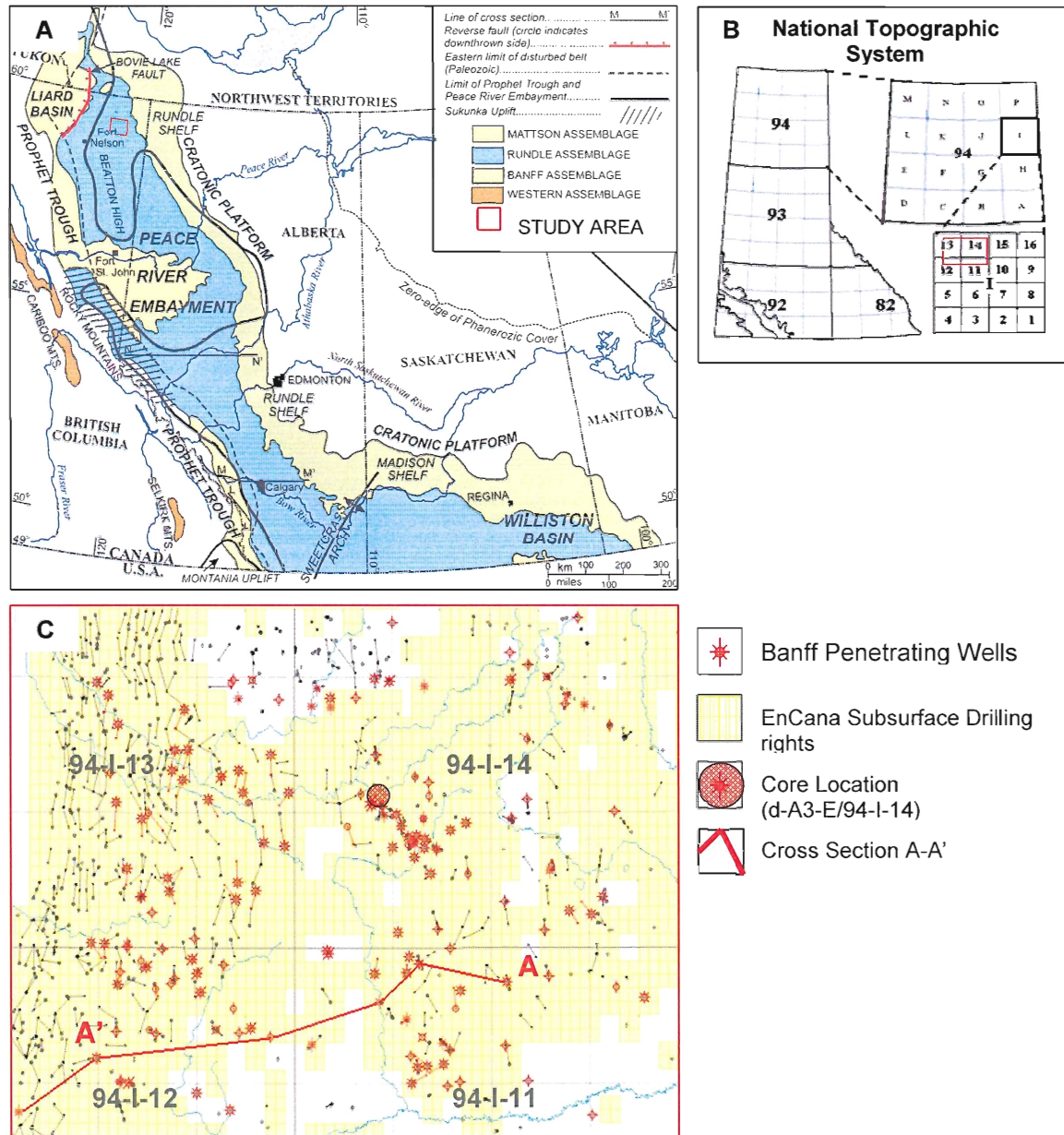
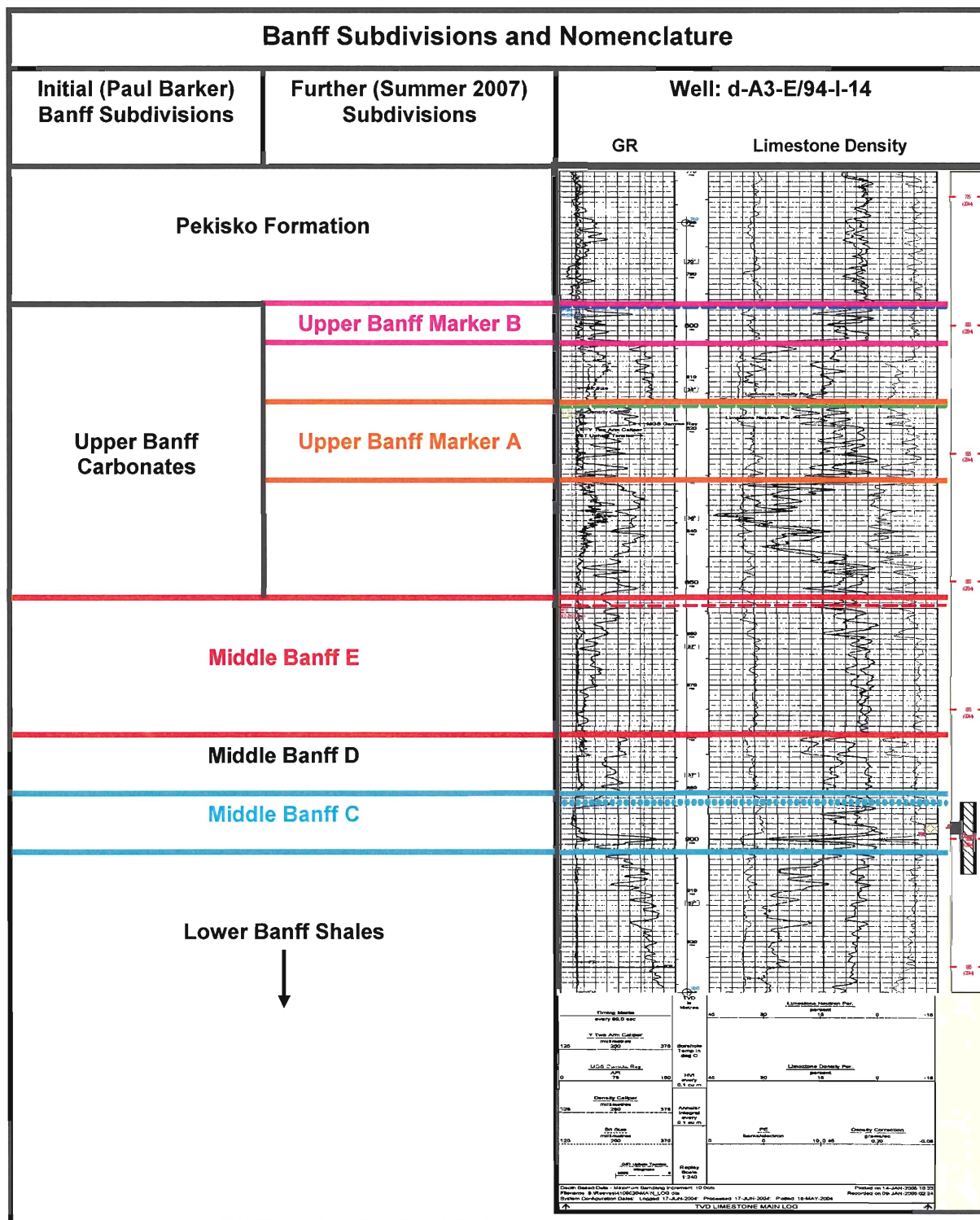


Figure 1.1- Location of Study area represented by the Red square. **A**, Map of Western Canada showing the study area location, extent of the D-C assemblages and the Tectonic elements of the D-C WCSB (after Richards et al, 2003). **B**, National Topographic System map of northeast BC showing location of study area (© Accumap). **C**, Map of study area displaying horizontal and vertical wells, Location of core D-A3-E/94-I-14 and the transect of Cross-section A-A'. Land whose subsurface mineral rights belonging to EnCana highlighted in yellow and wells with Banff penetration are enlarged and highlighted in red (© Accumap).

1.4.0 Summer Work

In 2007 the author took on a four month project as a junior geologist with the Fort Nelson Business Unit (FNBU) of EnCana Corporation's Foothills Division. The summer project was designed to identify any potential Banff reservoirs within the study area (Fig 1.1). During the project, 104 Banff penetrating well and strip-logs were analyzed within the study area using Accumap software (Fig 1.1-C). The analysis included creating a series of regional cross-sections, picking the lithological boundaries of low-gamma (presumably clean carbonate) units, and recording and mapping their thickness, porosity, and net pay values using Accumap and Geographix software packages (See Local Geology – Chapter 2). In total, five clean carbonate units were picked within the Banff Formation (Fig 1.2). Upon porosity assessment, two potential reservoirs were identified within the study area. The primary reservoir lies within the middle Banff C unit. A 15 m cored interval taken at location D-A3-E/94-I-14, centered on the Banff C unit, was examined and logged based on detailed lithological observations. The assessment of this reservoir will be the main focus of this thesis. A second potential reservoir lies within the upper Banff Channels. The channel systems are best recognized in confidential seismic amplitude maps and profiles, and lack sufficient lithologic and well data; they are not discussed in detail here.



1.5.0 Objectives

This thesis examines the petrography and interprets the depositional setting and the sequence-stratigraphic context of the potential middle Banff C reservoir. The entire cored Banff interval will be examined in an attempt to evaluate the reservoir quality of the Banff C unit. The five GR Petrology thin sections are re-evaluated and nine new samples from the cored interval are described using petrographic techniques and X-Ray diffraction (XRD) methods. The petrographic properties of these samples (e.g. matrices, cements, grain types and size, mineralization, porosity) yield information pertaining to the regional paleo-conditions and aid in setting up a stratigraphic model. Most importantly, the petrographic properties also provide indicators as to how well the Banff C and surrounding material might perform as a hydrocarbon reservoir and a hydrocarbon seal, respectively. This evidence will then be integrated with pre-existing structural, and well-log data, as well as relevant publications, to evaluate the effectiveness of the middle and lower Banff Assemblage as a petroleum system.

CHAPTER 2 - Regional Geology

2.1.0 Background

2.1.1 D-C Sea-Level

Several tectonic, oceanographic and biological events occurred globally during Late Devonian to Visèan time (Lasemi et al., 1998). According to Hallam (1984), Devonian sea-level began to rise at or slightly before the Devonian/Carboniferous boundary. The rise in sea-level is attributed to large-scale mid-ocean ridge building within the ocean basins causing a globally synchronous marine transgression which subsequently resulted in the widespread development of D-C sedimentary basins (e.g. the WCSB; Pysklywec and Mitrovica, 2000). The transgressive period yielded globally extensive deposits of latest Famennian to earliest Tournaisian black organic-rich shale (Caplan and Bustin, 2001). Records of this event are present within the late Famennian to early Tournaisian deposits of the lower Banff Assemblage in western Canada (Richards et al., 1994). Increased basin subsidence rates and a seaward shift in Tournaisian –early Visèan carbonate factories resulted in sedimentary basins dominated by ramp settings (Fig 2.1; Lasemi et al., 1998). Hallam (1984) described the late Visèan as the Carboniferous sea-level maximum which marks the last deposit of globally extensive neritic carbonates. Biologically, the Late Devonian marks a major faunal extinction of prolific frame-building organisms. Subsequently, carbonate factories were no longer dominated by reef complexes, allowing the widespread development of Early Carboniferous mud mounds and bryozoan-echinoderm build-ups (Lasemi et al., 1998).

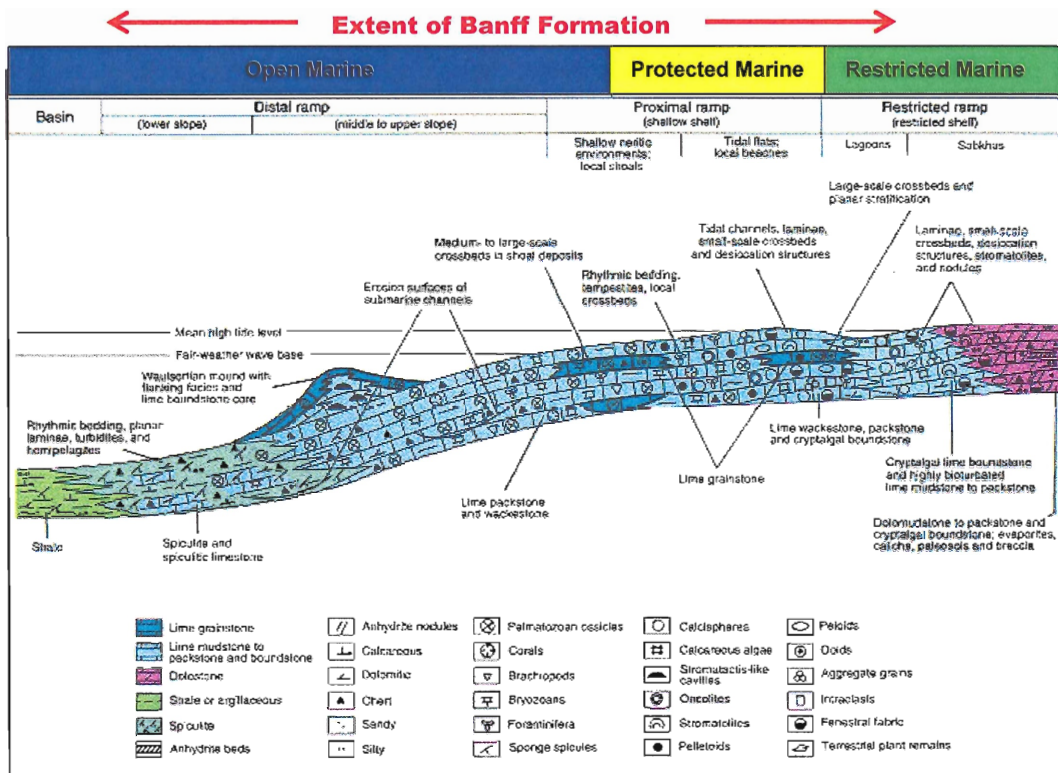


Figure 2.1. Generalized Carboniferous WCSB carbonate ramp model, after Richards et al. (1994).

2.2.0 Depositional setting of the WCSB

The late Devonian to early Carboniferous succession of the WCSB was deposited in a back-arc foreland basin. The western boundary of the D-C WCSB is described by Richards et al. (1994) as a poorly defined orogenic belt that was extensively exposed from the Famennian into the early Viséan. Late Devonian to Early Carboniferous volcanism, granitic plutonism, faulting and folding took place along the western rim (Fig 2.2; Richards, 1989, Parrish, 1992; Smith and Gehrels, 1992). Foreland basin systems are defined by DeCelles and Giles (1996) as elongate basins of sediment accumulation located between a contractional orogenic belt and the adjacent craton. Syn-orogenic clastic sediments derived from the rising orogen and the craton accumulate in four main structural depozones of foreland basins: the foredeep, the forebulge, the backbulge and

the craton (DeCelles and Giles, 1996; Fig 2.2). Within the D-C WCSB these four elements are known respectively as the Liard Basin, the Beatton high, the Pelloit Depression, and the Rundle shelf and are recognized in subsurface cross-sections based on well-logs (Figure-2.3).

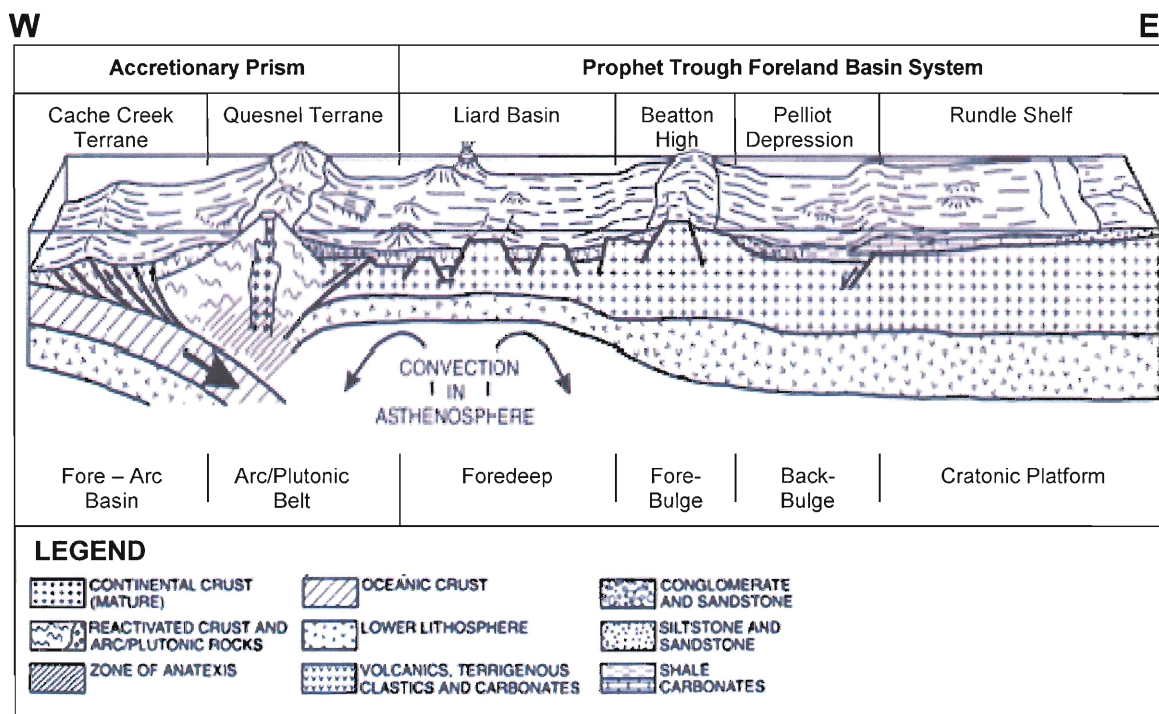


Figure 2.2- Generalized, schematic 3-D model of the tectonic mechanics of the northern WCSB (after Richards et al., 1989)

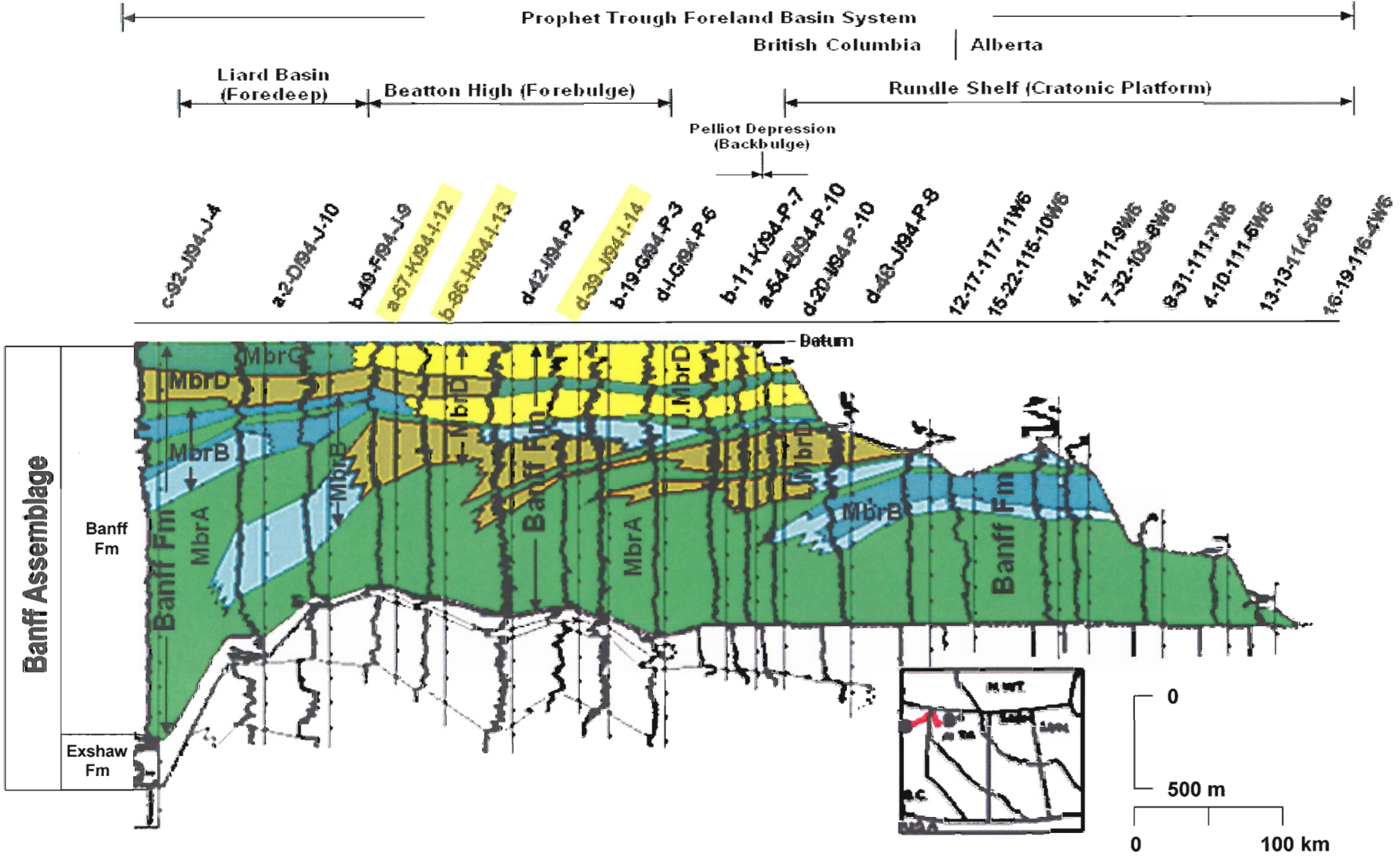


Figure 2.3. Stratigraphic cross section of Mississippian Banff and Exshaw strata in Northern BC and Alberta trending roughly E–W. The diagram illustrates the regional tectonic elements controlling the deposition of Mississippian strata, lithologies, and informal subdivisions. Wells highlighted in yellow are within or directly adjacent to study area and indicate the presence of informal Banff members A, B, and D. After Richards et al. (1994).

2.2.0 Devonian-Carboniferous (DC) succession

A thick, D-C system was deposited on the downwarped, downfaulted western margin of an ancestral North American plate and the central to western cratonic platform of the WCSB as described by Richards et al. (1994). The system lies disconformably above Famennian strata and was deposited in three main assemblages known as; the Banff, Rundle and Mattson Assemblages (Fig 2.4). Overall, two distinct lithofacies occur within the three assemblages. The lower lithofacies thickens basinward and is dominated by shale, spiculite and bedded chert of basin to slope origin. The upper lithofacies comprises platform and ramp carbonates and siliciclastic sandstone facies deposited in slope to continental settings. Both lithofacies contain multiple divisions that are typically separated by regional disconformities. Subaerial erosional episodes of pre-Permian, Triassic, Jurassic and Cretaceous age removed much of the Carboniferous strata, creating a major unconformable boundary at the top of the succession. Generally, the boundary is unconformably overlain by either Permian or Mesozoic strata (Procter and MacAuley 1968).

Lithofacies within the formations suggest a large-order shallowing upward sequence with distal ramp facies dominating the Banff Formation, slope and tidal facies dominating the Rundle group, and restricted marine and terrestrial facies dominating the Mattson Assemblage (O'Connell 1990; Richards et al, 1994).

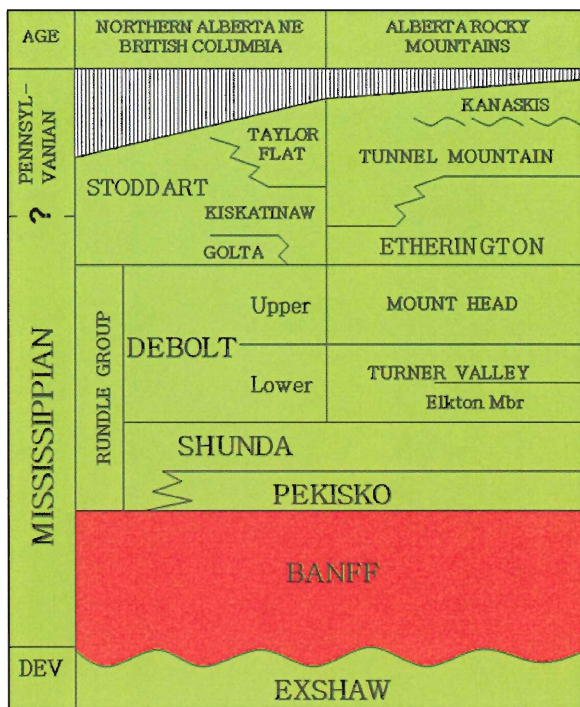


Figure 2.4 – Stratigraphic log of the DC succession in northern BC and Alberta. Note that all units overlying Rundle Group represent the Mattson assemblage.

2.3.0 Banff Assemblage

The uppermost Famennian – upper Tournaisian Banff Assemblage comprises carbonates and fine grained siliciclastics of the Bakken, Exshaw, Lodgepole, and Banff Formations. They developed in environments ranging from deep basin to restricted shelf on carbonate ramps and, less commonly, in carbonate platform settings. The Banff Assemblage extends from southern British Columbia, Alberta, and Saskatchewan into the southernmost areas of the eastern Yukon and western Northwest Territories (District of Mackenzie; Fig 1.1-A). Deposition of the Banff and Exshaw Formations took place within the Prophet Trough, Peace River Embayment and on the western edge of the cratonic platform. The remaining formations were deposited within the Williston Basin and the adjacent craton. Generally, the Banff assemblage disconformably overlies the Famennian Palliser assemblage and grades into the overlying Tournaisian to upper

Visèan Rundle assemblage. Regional sub-surface cross sections indicate that the Banff Assemblage was deposited in a gently inclined carbonate ramp setting (Fig 2.3; Richards et al., 1994). In northeastern BC, the Banff assemblage is represented by carbonates and siliciclastics of the Exshaw and Banff Formations (Richards, 1989, Richards et al., 1989; Richards et al., 1994).

2.3.1 Exshaw Formation

The Exshaw Formation comprises a thin (<50m) succession of Upper Famennian to middle (?) Tournaisian euxinic black shale overlain by neritic siltstone, sandstone and limestone (Richards, 1989; Richards et al., 1993). It occurs throughout most of the western interior platform and thickens basinward, towards the southwest (Fig 2.3; Richards, 1989). Stratigraphically, the Exshaw disconformably overlies upper Famennian strata of the Palliser Formation (Richards et al., 1989; Richards et al., 1994). The relationship between the Exshaw and the overlying Banff Formation varies from disconformable in the south to vertically and laterally gradational north of the southern portion of the Peace River Embayment (Richards et al., 1993).

The lower part of the Exshaw is a black, organic shale deposited in basinal euxinic conditions well below storm weather wave base (Richards, 1989; Richards et al., 1993). The black shale records a major regional transgression, rapid deepening and widespread anoxic conditions, which coincide with the latest Devonian eustatic rise in sea-level (Richards, 1989). Shallow-marine sandstones, siltstones and oolitic grainstones of the upper Exshaw record a regional shallowing event.

The black shale of the lower Exshaw Formation extends throughout the WCSB and correlates with the basal shale of the northern Banff Formation (Richards et al., 1994). Neritic deposits of the upper Exshaw Formation are only present in the southern Banff Assemblage and correlate with northward neritic deposits of the Banff Formation.

2.3.2 Banff Formation

Latest Famennian to late Tournaisian deposits of the Banff Formation consist of shales, carbonates, and silt to sand-sized siliciclastics of deep-basin to restricted shallow marine environments that prograde southwestward and thin eastward (Richards, 1989; Richards et al., 1993). The formation ranges in thickness from <150 m in west-central Alberta to >500 m in the southwestern district of Mackenzie (Richards et al., 1993). In southern regions the Exshaw / Banff contact is disconformable, but in northern regions, the contact is gradational (Richards et al., 1993). Typically, coarse carbonates of the Pekisko and Livingstone formations from the Rundle Group overlie the Banff Formation with a boundary generally described as sharp and erosional.

Carbonate deposits of the Banff Formation indicate a basinal to restricted carbonate ramp setting (Fig 2.1). Throughout the WCSB the Banff Formation displays multiple high-order Transgressive-Regressive (T-R) sequences. In the northwest, basinal Banff shales correlate with those of the Exshaw formation and grade-upward into rhythmically bedded and cross-stratified, slope to shallow shelf, siltstone, sandstone and limestone. Common T-R sequences in the eastern and upper parts of the Banff Formation consist of skeletal and oolitic carbonates of shallow shelf origin grading upward into more restricted deposits of marine carbonates and siliciclastics.

Richards (1989) and Richards et al. (1993) divided the Banff into five members (A, B, C, D, E and F) which are summarized in table 2.1. Of these units, Richards et al. (1994) inferred the coexistence of members A and D within the study area (Fig 2.3). Note that these formally recognized members are not correlative with the informal EnCana nomenclature described in chapter 1 (See table 2.2).

Member	Thickness (m)	Boundaries	Lithology	Depositional Interpretation	Extent/ Occurrence
A	8 – 490 m	Conformably – disconformably overlies Exshaw Formation, or disconformably overlies Palliser Formation, gradationally overlain by member B or D	Black shale interbeds of siltstone and silty carbonates.	Basinal – deep to moderately deep-water environment	Southwestern Alberta to the southwestern district of Mackenzie
B	50 – 250 m	Gradationally overlain by and grades laterally into either members C or D	Cherty to argillaceous spiculite, dolostone, and lime mudstones and wackestones, grade both vertically and laterally (towards the northeast) into cherty lime packstones and grainstones.	Basin and slope to shelf margin, protected shelf and shallow shelf	Southern Alberta into northeastern BC
C	<100m	Grades and passes southwestward into the upper member B or member D	Limestone, dolostone, and shale.	Restricted shelf, shallow shelf and protected shelf	Southern Alberta to east-central British Columbia, poorly developed south of Calgary
D	<40 - >135m	Overlies member B or C, passes into basinal shales of member A	Interbedded shale, siltstone, silty to sandy dolostone and sandstone with minor developments of skeletal limestone and other carbonates.	Shallow marine to supratidal environments	Southern Alberta to the southwestern district of Mackenzie
E	n/d	Overlies member B and underlies member F	Rhythmically bedded cherty, spiculitic, pelmatozoan - lime wackestone and packstone with subordinate grainstone, dolostone and spiculite	Moderately deep-water slope environments	Eastern Cordillera of southwestern Alberta and the western portion of the southern plains
F	n/d	Overlies member E	Rhythmically bedded, spiculite dolostone, marlstone and cherty to dolomitic skeletal lime wackestone and packstone	Moderately deep-water slope environments	Same as member E

Table 2.1- Summary of the informal subdivisions by Richards (1989; 1993). Units within study area are highlighted in red.

2.4.0 Local Geology in Study Area

According to subsurface cross-sections created by Richards et al. (1994), Banff strata within the study area developed over the Beaton High platform and down the gently dipping ramp or platform margin (Fig 2.2). The ramp can be detected in the subsurface by dips of sedimentary packages determined through well correlation and interpreted as southwesterly dipping clinoforms (Fig 2.3) which seem to present themselves locally in the informally defined Banff C unit (Fig 2.5). According to Richards et al. (1994), members A and D occur within the study area (Fig 2.3), the Banff C unit corresponds with grainstones occurring in the Banff Member D (Table 2.2).

All response curves for logs penetrating the Banff Formation within the study area were examined and mapped, leading to an informal subdivision of the Banff Formation into five, low responding gamma units interpreted as carbonate dominant layers (Fig 1.2). The clean-responding units are typically separated by approximately 10m thick high-responding gamma-ray layers interpreted as shale. All the units encountered within the study area are summarized in table 2.2. Strip log analysis suggests a range in facies types within the study area from basinal shale deposits to slope and restricted shelf limestone and paleosol facies. The middle Banff C unit represents the potential Banff reservoir in question, and is centered upon the cored interval from well d-A3-E/94-I-14.

2.4.1 Middle Banff C Unit

The middle Banff C unit is defined as a blocky low-gamma unit with a consistently strong gas show, ranging in thickness from 2 m to 10 m (average thickness ~5 m; Figs 2.5; 1.2). Isopach maps and local cross-sections reveal a laterally extensive NNW – SSE trending unit which is most prominent in the central and eastern portions of

the study area and appears to thin and pinch-out along the western edge (Figs 2.5 and 2.6). This represents the westerly passing of the shelf-deposited lower Member D into slope deposits of member B which occurs directly adjacent to the study area (Fig 2.3). The unit is white to buff wackestone with local packstone and grainstone. It is partially silty, with a very fine sucrosic granular cement and compact crystalline matrix. Porosity, described as poor to fair and intergranular, ranges from 5 -15% and is greatest within the local grainstone unit. Thick layers of light grey to black, fissile, platy basinal shale become increasingly carbonaceous as they grade upward into the Banff C unit (Transitional zone; Fig 2.5). The material overlying the Banff C is white to buff mudstone with minor wackestone, interbedded with thin layers of grey-green shale.

Banff Units (EnCana)		Available Data	Thickness (m)		Gamma-log Response	Extent	Lithology	Stratigraphic relationships	Interpretation	Members	
Paul Barker	Daniel Haider										
Upper Banff Carbonates	MRK B	Electric well-logs and strip log lithological descriptions	40-50	5-17	Alternating high-low gamma-response	Throughout study area	Carbonate mudstone interlayered with green shale	Disconformably overlain by Pekisko Formation	Repeating cycles of Restricted lime mudstones and wackestones interlayered with green shale	D	
	Shale			CHNL	2-15	High, blocky gamma-response (shale) Clean, blocky gamma-response (Channel)					Throughout study area (shale)
					MRK A	10-30	Alternating high-low gamma-response	Throughout study area			Carbonate mudstone interlayered with Green shale
	Shale				10-15	Blocky, high gamma	Green Shale				Gradationally overlies Banff E
Banff E		Electric well-logs and strip log lithological descriptions	17-31		Blocky, clean gamma-log fines-up into shale layer	Throughout study area	Carbonate Mudstone and Wackestone	Abrupt log signature change marks base of Banff E			
Banff D		Electric well-logs and strip log lithological descriptions + core sample d-A3-E/94-I-14	10-30 (thickens basinward)		High-gamma response with local lows		Carbonate mudstone interbedded with green shale layers	Unconformably overlain by Banff E			
Banff C		Electric well-logs and strip log lithological descriptions + core sample d-A3-E/94-I-14	2-10m		Blocky, clean gamma-log	Throughout study area, poorly defined to the west	Carbonate skeletal, peloidal, and oolitic grainstone	Abrupt Facies change into Banff D	Shelf margin and protected shelf		
Lower Banff Shale		Electric well-logs and strip log lithological descriptions + core sample d-A3-E/94-I-14	100-200m		High-gamma response, coarsens upward into Banff C,	Throughout study area	Black shale interbeds of siltstone and silty carbonates.	Grades upward into Banff C Gradationally overlies Exshaw Formation	Distal ramp	A	

Table 2.2- Summary table of the log response, lithologies, and interpretations of the units encountered within the study area as well as their correlative, informal members defined by Richards (right hand column; 1989; 1983). Dashed-black line represents the representative lithologies and units of the Banff cored interval well: d-A3-E/94-I-14. Units labeled 'Shale' represent unnamed, unmapped shale beds encountered throughout the entire study area. Note for well-log signatures see figure 2.3.

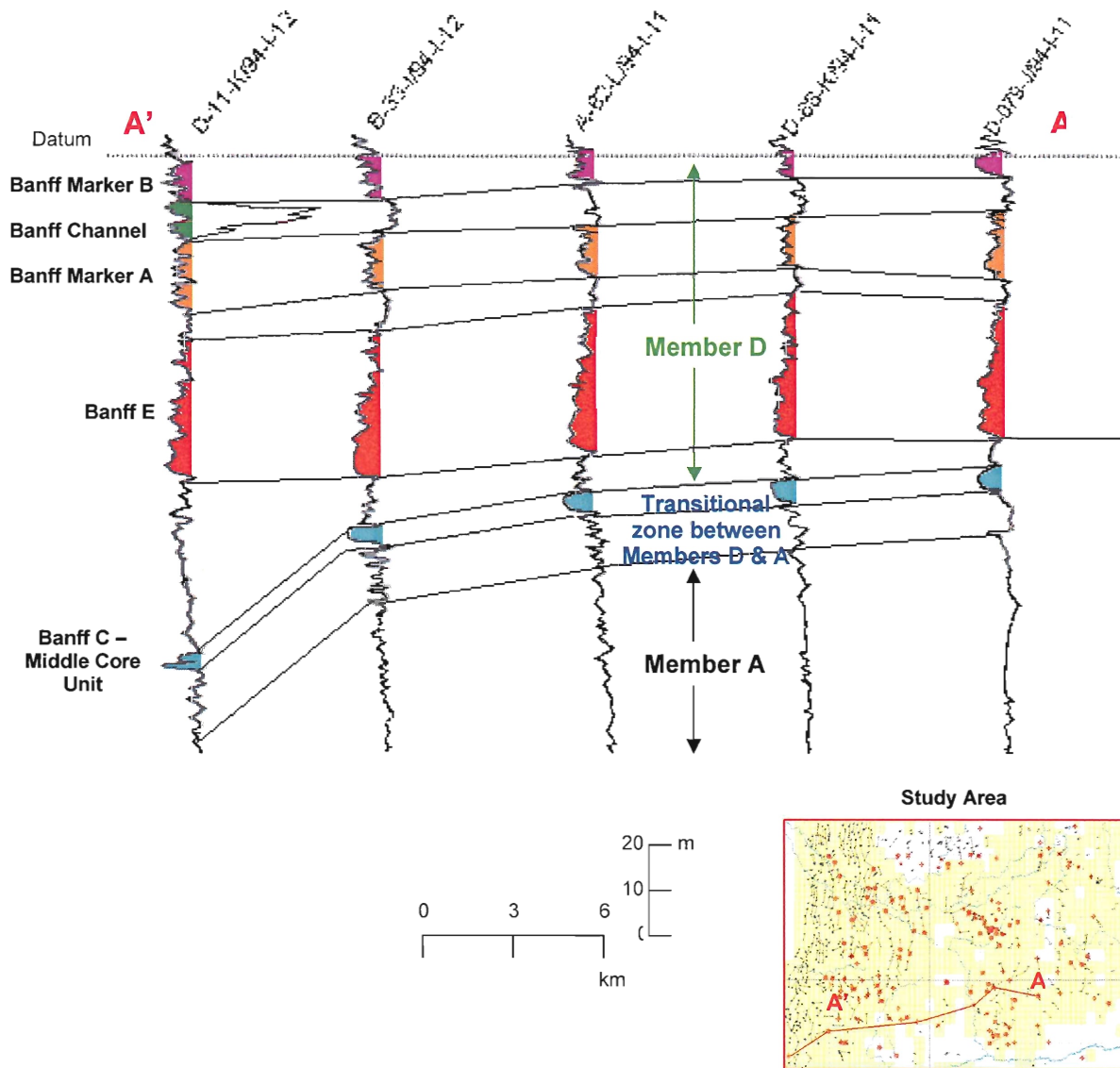


Figure 2.5: Typical local gamma-ray cross-section through the upper and middle Banff Formation trends approximately E-W within the study area. Datum was placed at the top of the Banff Formation. Note the presence of the Banff Channel (well D-11-K/94-I-12) and the westerly thinning and dipping of the middle Banff “C” unit. Note Member A continues downward for ~100m until it contacts the Exshaw Formation.

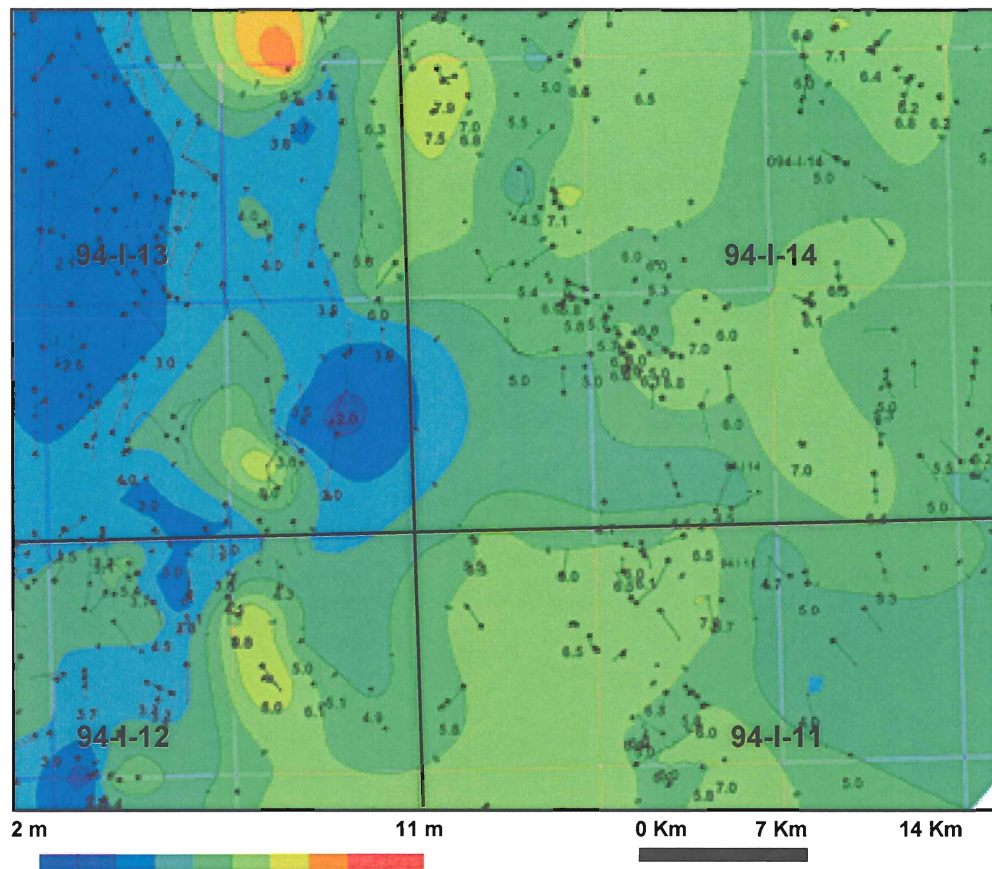


Figure 2.6- Local Banff C isopach map based on subsurface well-logs. Postings represent recorded thickness values. Note the approximate N-S trend of the body and the westward thinning.

2.4.2 Interpretation

Thick layers of shale which gradationally overlie the Exshaw Formation and underlie and grade into the Banff C unit correspond to the Banff Member A (Table 2.2; Fig 2.5). The Member A unit is described by Richards et al. (1993) as a dominant shale layer with turbidite-like beds of silty carbonates and shale present in the upper portion indicating a deep to moderately deep basin to slope origin of deposition (Table 2.1). Banff units C,D,E and the upper Banff carbonates correspond with Richards Member D. Member D was described by Richards et al. (1993) as shallow marine to supratidal deposits which gradationally overlie Member A in the northwest. Member D comprises

interbedded shale, siltstone, silty – sandy dolostone and sandstone with commonly developed skeletal limestone and other carbonates.

The upward transition from deep-water to restricted facies indicates a prograding sequence resulting from a regressing shoreline. Minor T-R sequences occur within the upper member D unit as repeating cycles occur of clean, dominantly mudstone units fining upwards into layers of green shale interpreted as arially exposed clay deposit. The T-R sequences correspond with those described by Richards et al. (1989).

CHAPTER 3 - Methodology

3.1.0 Introduction - Research Methods

Isopach and net pay data were gathered primarily from gamma and sonic logs obtained using Accumap software produced by IHS Energy Company. Maps of these data were created using Geographix subsurface mapping software. Lithologic data was derived from one 14 m long drill core located at D-A3-E/94-I-14 (Fig 1.1-C). Core samples were examined in both hand sample and thin section, using several methods of investigation. The emphasis of the testing was to determine the petrology of the Mississippian carbonates, and to evaluate how these characteristics may affect the petroleum system.

3.2.0 Subsurface Mapping

Eight regional well-log cross-sections were created within the limits of the study area. Gamma-ray, neutron/density, sonic and resistivity log signatures aided in the correlation of different stratigraphic units. Stratigraphic units within Banff-penetrating wells located in the study area, but not incorporated in the eight cross-sections, were then picked and named based on the cross-sectional units. In total, 104 wells within the study area were evaluated. Thickness, porosity, and net pay values for each unit within every well were recorded and mapped. Net pay values can be defined as the thickness of a particular reservoir. When evaluating net pay values, the industry standard carbonate cutoff values for gamma-ray and porosity logs (30 API and 3%, respectively) were applied.

Gamma-ray logs indicate the radioactivity of the subsurface units. Clean, low-gamma responding (low radioactivity) units are interpreted as pure carbonates which may

potentially form reservoirs. For this reason, they were the main focus of mapping.

Limestone neutron/density are sonic logs that measure the density of the lithological unit which will be less dense if porous. Clean carbonate units with high porosity levels are interpreted as units capable of accumulating hydrocarbons (reservoirs).

3.3.0 Lithological Observations

3.3.1 Megascopic Observations

A detailed stratigraphic log of the D-A3-E/94-I-14 drill core was compiled and core samples were examined on a centimeter scale. The core log lithology was correlated with well log responses and lithological strip log records. Macrofossils, matrix, cement, grain size, structures and mineralization were evaluated using a low-powered microscope. Particular attention was paid to the middle Banff “C” shoal unit. A dilute acid solution was used to test for the presence of calcite cement. Grain size was determined microscopically, and the carbonates were classified based on the Dunham (1962) classification scheme (Fig 3.1).

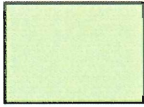
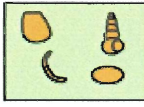


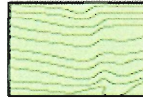
Original Components not bound together at deposition				Original Components bound together at deposition. Intergrown skeletal material, lamination contrary to gravity, or cavities floored by sediment, roofed over by organic material but too large to be interstices
Contains Mud		Lacks Mud		
Mud-Supported		Grain Supported		
Less Than 10% Grains	More Than 10% Grains			
Mudstone 	Wackestone 	Packstone 	Grainstone 	Framestone 

Figure 3.1 – Dunham’s Carbonate Classification Scheme (1962). After USC Sequence Stratigraphy Web (2006).

3.3.2 Microscopic Observations

In total, 15 thin sections were cut from the core plugs. Five samples were cut between 895.0 and 899.0 m by GR Petrology Consultants Incorporated (2005) for initial reservoir study and are referred to here as the GR sample series. The GR sample series were stained red and mounted with blue epoxy to emphasize porosity and photographed. The remaining 12 thin sections were selected visually based on varying structures and lithologies and cut at the Dalhousie University thin-section preparation facilities.

The thin sections aid in refining the facies descriptions, highlighting subtle but important differences between the facies that are relevant to fine-scale reservoir properties. Documented microscopic properties include types and quantities of matrix, grains and cements, and faunal assemblages – features of importance for determining depositional environments. Matrix and cement relationships were a key factor in determining depositional relationships (chapter 4). Detailed thin section descriptions are located in Appendix B.

3.4.0 Porosity and Permeability

GR Petrology (2005) analysed the pore size, type and percentage of the GR sample series using both point count and conventional core analysis. They also obtained permeability data using conventional core analysis. Porosity and permeability values play an important role in the mechanics of a petroleum system, in particular the quality and effectiveness of the system's reservoir and seal rocks.

3.4.1 Porosity

Approximate porosity values can be obtained from sonic and density logs. GR Petrologies (2005) compared both point count and conventional core analysis porosity values of the GR sample series to determine accuracy. The porosity values of the GR sample series (see Chapter 5 table 5.1 and Fig 5.3) were ranked according to North's (1985) qualitative evaluation system (Table 3.1; 1985). The porosity data documented in the well and strip-logs representative of the GR sample interval correlate well with the values obtained by GR Petrologies. Furthermore, the well and strip-log porosity values for the Banff C unit remain consistent throughout the central and eastern portion of the study area (where the Banff C unit is most prominent). Porosity types and diagenetic factors controlling porosity can be inferred from thin-section observation of pores (Fig 5.2).

Porosity (%)	Qualitative evaluation
0 – 5	Negligible
5 – 10	Poor
10 – 15	Fair
15 – 20	Good
20 +	Very good

Table 3.1 – North's (1985) qualitative porosity evaluation.

3.4.2 Permeability

The degree of interconnectedness of the pore spaces in the reservoirs is important because poorly connected pores restrict the flow of hydrocarbons, affecting their migration and accumulation. These factors play a key role when determining

hydrocarbon extraction methods. Permeability data for samples Gr-001-GR-005 were measured by GR Petrologies and ranked according to North's Qualitative permeability evaluation (Table 3.2; Chapter 5; Table 5.1 and Fig 5.4).

Permeability Value (mD)	Qualitative Description
< 1.0 – 15	Poor to fair
15 – 50	Moderate
50 – 250	Good
250 – 1000	Very good
> 1000	Excellent

Table 3.2- North's (1985) qualitative permeability description.

3.5.0 X-Ray Diffraction (XRD)

X-Ray diffraction (XRD) studies aid in determining mineral assemblages.

According to Nesse (2000), the wavelengths used in X-ray diffractometers are similar to the atom spacing in most mineral structures. The similarity in dimensions enables the diffraction of X-rays by regularly spaced atoms which comprise a crystal lattice.

Diffraction maxima produced by layers of atoms transmit the incident X-rays effectively given an appropriate angle of incidence (θ). If the X-ray wavelength and the interplanar spacing between crystals in a crystal structure are known, reflection angles can be predicted using the Bragg equation:

$$n\lambda = d \sin\theta$$

where n represents the order of reflections, λ represents the X-ray wavelength, and d represents the interplanar spacing of atoms within a crystal lattice.

A few tenths of a gram of sample were ground into a fine powder using a mortar and mounted on a slide. This ensures that every possible reflection plane is presented parallel to the specimen surface. The sample is mounted on a holder that pivots relative to the X-ray tube, allowing the angle of incidence of the X-ray beam to vary from zero to 90° . To record the reflections, the electronic X-ray detector is placed at the angle 2θ . In order to achieve this angle, the electronic X-ray detector is mounted on a concentric goniometer which moves at twice the angular speed between sample and X-ray tube. As the sample and detector are rotated through the desired range of θ and 2θ angles the intensity of the reflected X-rays is electronically recorded in the form of an X (2θ) – Y(Intensity-counts/second) graph. Intensity peaks indicate that the sample contains a mineral with atomic planes the d-spacing of which is appropriate to reflect X-rays for the particular angle θ . Each mineral possesses a different diffraction pattern that can be identified using the graphic records.

X-Ray Diffraction techniques were used to confirm minerals identified in thin section, to test for the presence of dolomite, and to test for minerals such as clay types that are difficult to identify in thin sections. Semi-quantitative mineral proportions were obtained by measuring the areas of the diagnostic peaks for identified minerals and then multiplying their peak areas by an intensity factor (Mann and Muller, 1980). The raw numbers for each mineral were summed and converted to percentages (See chapter 4). XRD data are present in Appendix C.

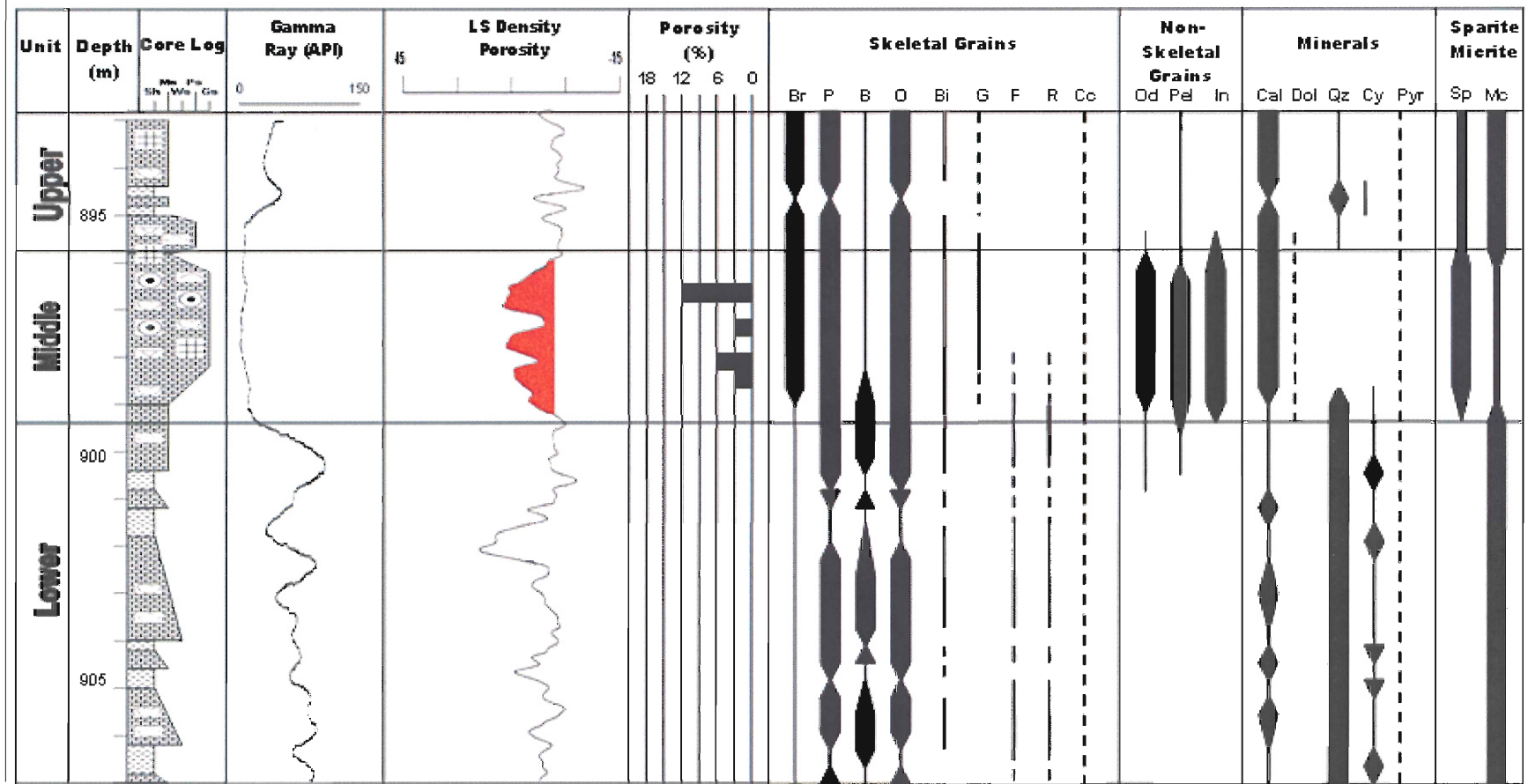
CHAPTER 4 – Lithofacies descriptions and depositional settings

4.1.0 Introduction

Based on a megascopic analysis, the core can be divided into lower, middle, and upper units. Upon further investigation it was determined that each unit contains multiple lithofacies indicating different, relatively shallow depositional settings within the inferred carbonate ramp system (Table 4.1). The different settings were inferred based on variations in both lithological and biological components as well as grain, matrix, and cement ratios observed using both hand samples and thin-section microscopy (Figs 4.1, and 4.2 respectively). The bio-lithological variations are mainly a function of wave-energy and, to some degree, water depth and salinity. Included below are descriptions of each unit and their associated lithofacies.

Core Unit	Depositional Setting	Lithofacies	Name	Thin Section	Thin Section Sample Depth (m)	Notes
Upper	Protected Backshoal	G	Peloidal-Skeletal Lime Wackestone	01	894.35	Lithofacies are interlayered. Beds range from 5 cm – 120 cm in thickness. Lithofacies G & J are the most prominent.
		H	Green Shale	02	894.45	
		I	Lime Mudstone	03	894.90	
		J	Peloidal-Skeletal Packstone	GR-001 04	895.00 895.36	
Middle	Tidal – Influenced Sand belt	D	Oolitic Grainstone	GR-002 GR-004	896.50 898.00	Lithofacies are interlayered and evenly distributed. They occur in repeating coarsening-upward cycles. Cycles range in thickness from 50 cm – 100 cm
		E	Peloidal Grainstone	GR-003	897.50	
		F	Skeletal Grainstone	GR-005	899.00	
Lower	Open Marine Mixed Carbonate-Siliciclastic	A	Skeletal Mudstone/Wackestone	05	900.50	Lithofacies occur in repeating, fining-upward cycles. Cycles range in thickness from 1.0 m – 1.5 m. Lithofacies A is the most prominent.
				06	902.36	
		B	Skeletal Packstone	07	904.36	
		C	Dark Shale	08	904.73	
09	905.70					

Table 4.1- Summary table of the depositional setting and lithologies, that correspond with the three core divisions illustrated in Figure 4.1 Thin section petrography of each core unit enables the definition of multiple lithofacies within each unit.



Legend

Core Log		Skeletal Grains				Non-Skeletal Grains			Minerals			Sparite/Micrite	
	Limestone		Br - Bryozoan		G - Gastropod		Od - Ooid		Cal - Calcite		Sp - Sparite		Mc - Micrite
	Shale		P - Pelmatozoan		F - Foraminifera		Pel - Peloid		Dol - Dolomite				
	Pelmatozoan		B - Brachiopod		R - Radiolarian		In - Intraclasts		Qz - Quartz				
	Ooid		O - Ostracod		Cc - Coccolid Cells				Cy - Clay				
			Bi - Bivalve						Pyr - Pyrite				

Figure 4.1- Lithological, electronic log, porosity, skeletal and non-skeletal grain occurrence and abundance, mineralogical occurrence and abundance, and matrix and cement data of the d-A3-E/94-I-11 cored interval. Red colour in density-porosity log indicates porous intervals in a clean carbonate layer – potential reservoir.

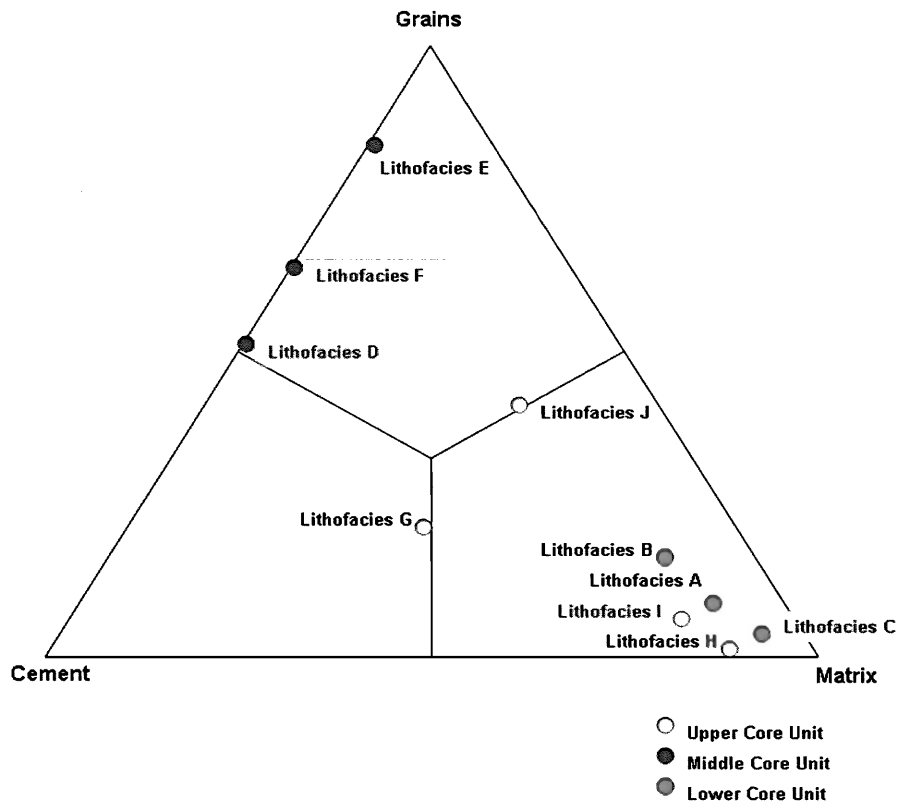


Figure 4.2- Ternary Composition diagram of the d-A3-E/94-I-12 Banff cored interval suggesting that each core unit have their own distinct grain-to-cement-to-matrix ratios. Lithofacies of the lower unit lack grains and cements compared to the lithofacies of the middle unit which are lacking in matrix. The dominant lithofacies (J & G) of the upper unit share relatively equal grain-to-cement-to-matrix ratios. Data based on estimates from petrographic thin sections (Table 4.1).

4.2.0 Lower Unit: open-marine mixed carbonate siliciclastic

The lower mixed carbonate-siliciclastic unit displays distinct rhythmic bedding. Cycles of packstone/wackestone grading into layers of dark, fissile shale repeat multiple times, with abrupt but not erosional contacts. On a first order observation the lithologies of the lower facies appear quite similar to those of the upper facies, the only major difference being the colour of the shale interbeds. Petrographically, the lower unit is different from the upper. The matrix is generally siliciclastic-rich with sub-angular to sub-rounded quartz grains approximately 0.02 mm in size mixed with micrite and

microsparite. A diverse range of bioclastic material occurs within the lower unit, which generally contains fragmented pelmatozoans, brachiopods, bivalves and bryozoans.

Although bryozoans are present, they are considerably less abundant within the lower unit than in the middle and upper units. Three lithofacies were identified within the lower unit, described below and summarized in table 4.2.

Lithofacies	A	B	C
Classification	Skeletal Mudstone/ Wackestone	Skeletal Wackestone	Dark Silty Shale
Occurrence	Lower Core Unit	Lower Core Unit	Lower Core unit
Carbonate/ Clastic	Mixed	Mixed	Clastic
Thickness (cm)	20 – 70 cm	5-10 cm	5 – 40 cm
Grain Size	< 88 µm	< 88 µm	< 88 µm
Color	Light - dark grey	Light – Dark Grey	Dark Grey, with light grey lenticular beds
Fossils	Ostracods, brachiopods, radiolarian, foraminifera, rugose corals	Brachiopods, pelmatozoans, coccooid cells, sponge spicules, and minor amounts of bryozoans	Pelmatozoans, ostracods, bryozoans
Fossil Abundance	Moderate locally common	Common	rare
Non-Skeletal Grains	Detrital quartz grains	Detrital quartz grains	Detrital quartz grains
Non-Skeletal Abundance	Abundant	Abundant	Abundant
Matrix	Micrite	Micrite	Micrite and microspar
Cement	N/A	N/A	N/A
Other Minerals	Traces of pyrite, local dolomite	Traces of pyrite	Minor heavy minerals and dolomite
XRD results	Calcite -68% Quartz – 26% Kaolinite – 6% Pyrite – Trace Illite – Trace	Quartz – 44% Kaolinite – 21% Calcite – 20% Illite – 15%	Illite – 36% Kaolinite – 21% Calcite – 21% Quartz – 20% Montmorillonite – 2%
Comments	Dominates lower core unit, Grades into lithofacies C	Grades into lithofacies A, solution seams	Caps off fining upward sequences
Depositional environment	Foreshoal	Foreshoal	Foreshoal

Table 4.2- Summary of lithofacies A, B and C within the Lower core unit.

4.2.1 Lithofacies A Skeletal Mudstone/Wackestone

The lithofacies is dark grey and massive, matrix-supported and with abundant pelmatozoans and minor rugose corals (Fig 4.3-A). Intraclasts, fragmented ostracods, brachiopods, and radiolarians are present, along with well preserved, chambered foraminifera. These grains are encompassed by a matrix of brown micrite mixed with sub-angular to sub-rounded silt-sized quartz grains. The lithofacies lacks sparry cement (Figs 4.3-B & C). XRD analysis revealed a strong presence of quartz and calcite, with minor occurrences of kaolinite and illite clays and traces of pyrite.

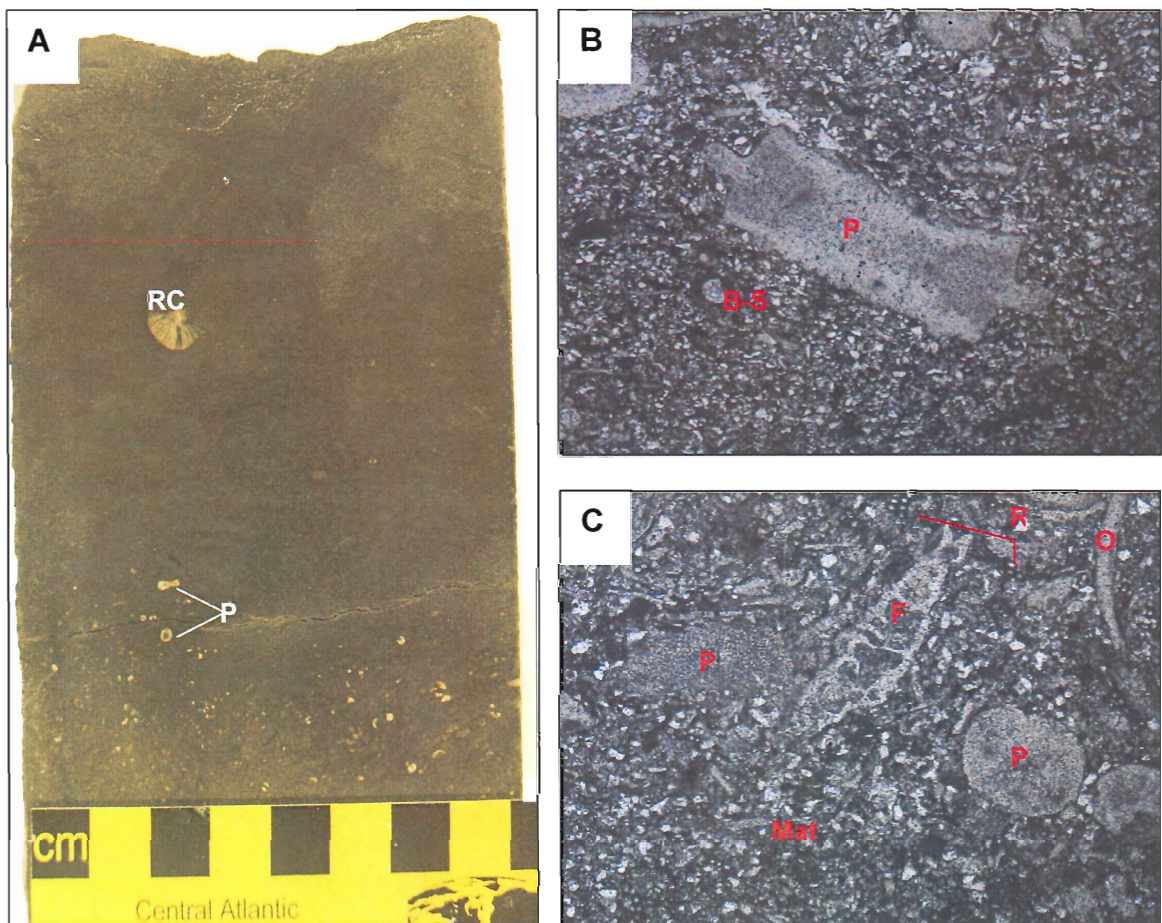


Figure 4.3- Cored and thin section samples of lithofacies A. **A**, typical cored sample of lithofacies A, note the presence of graded bedding, pelmatozoans (P) and solitary rugose corals (RC). **B**, x6.3 – PPL. Photo of thin section 05 displaying the presence of relatively coarse pelmatozoan grains, and brachiopod spines (B-S) in a mixed carbonate-siliciclastic matrix. **C**, x6.3 – PPL. Photo of thin section 06, shows presence of pelmatozoan fragments, chambered foraminifera (F), ostracod fragments (O), and radiolarians (very-fine, dark mesh-like networks-R) in a mixed carbonate-siliciclastic matrix (Mat).

4.2.2 Lithofacies B Skeletal Wackestone

The skeletal nature of this dark grey, highly fractured lithofacies is easily visible in hand sample (Fig 4.4-A). Long (~2.0 cm) shell fragments (mainly brachiopods) are aligned in layers with a preferred orientation approximately parallel to bedding. Coarse brachiopod shell and spine fragments are abundant, ranging from impunctate to punctate, with some shells highly ornamented. Pelmatozoans, coccoid cells, sponge spicules, and minor amounts of bryozoans are also present (Figs 4.4-B & C). Solution seams commonly occur between contacting grain boundaries. XRD analysis showed quartz as the primary mineral with secondary occurrences of calcite, kaolinite and illite. The matrix is similar to that of the above described lithofacies A. Minor amounts of sparry cement occupy the centers of brachiopod spines. Traces of pyrite are scattered throughout the matrix.

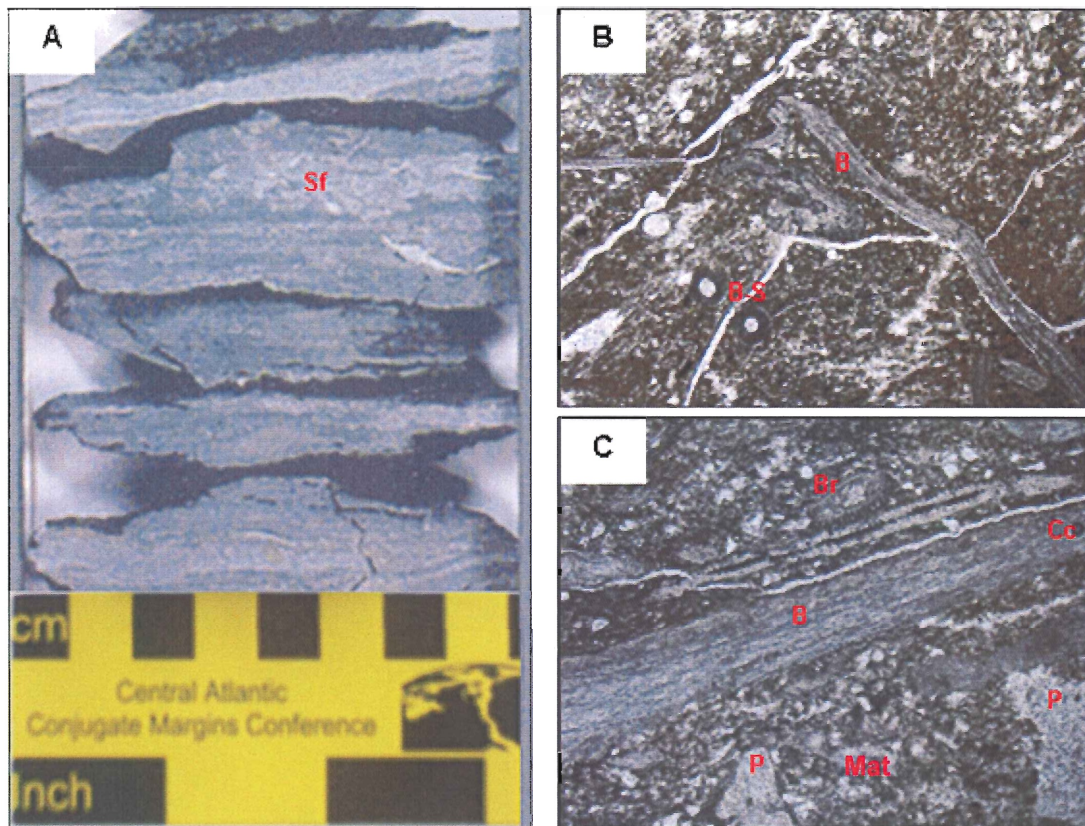


Figure 4.4- Representative hand sample photo and photomicrographs of lithofacies B. **A**, cored sample of lithofacies B **B**, x6.3 – PPL. Thin section photograph of sample 07 showing coarse brachiopod shell (B) and spine (B-S) fragments. **C** x6.3 – PPL. Thin section photograph of sample 07 shows coarse brachiopod shell fragments (B), evidence of pelmatozoan grains (P), minor bryozoan fronds (Br) and coccoid cells (Cc) in a mixed carbonate-siliciclastic matrix (Mat).

4.2.3 Lithofacies C Dark Silty Shale

The contact between lithofacies C and lithofacies A is typically gradational, through lenticular-bedded limey shale. The rock is dark (almost black) and extremely fissile (Fig 4.5-A). The limey shale contains layers with a matrix similar to that of lithofacies B (Fig 4.5-B) alternating with layers or lenses of shaley material of lithofacies C (Fig 4.5-C & D). The dominant material within the matrix is silt-sized, sub-angular to sub-rounded quartz grains which are mixed with minor amounts of micrite and microspar. Bioclastic material is rare but occasional pelmatozoans, brachiopods,

bryozoans and ostracods are present. XRD analysis detected a strong presence of illite, kaolinite, quartz and calcite with traces of montmorillonite. Also present within the matrix are traces of dolomite, muscovite, chlorite, pyroxenes and biotite.

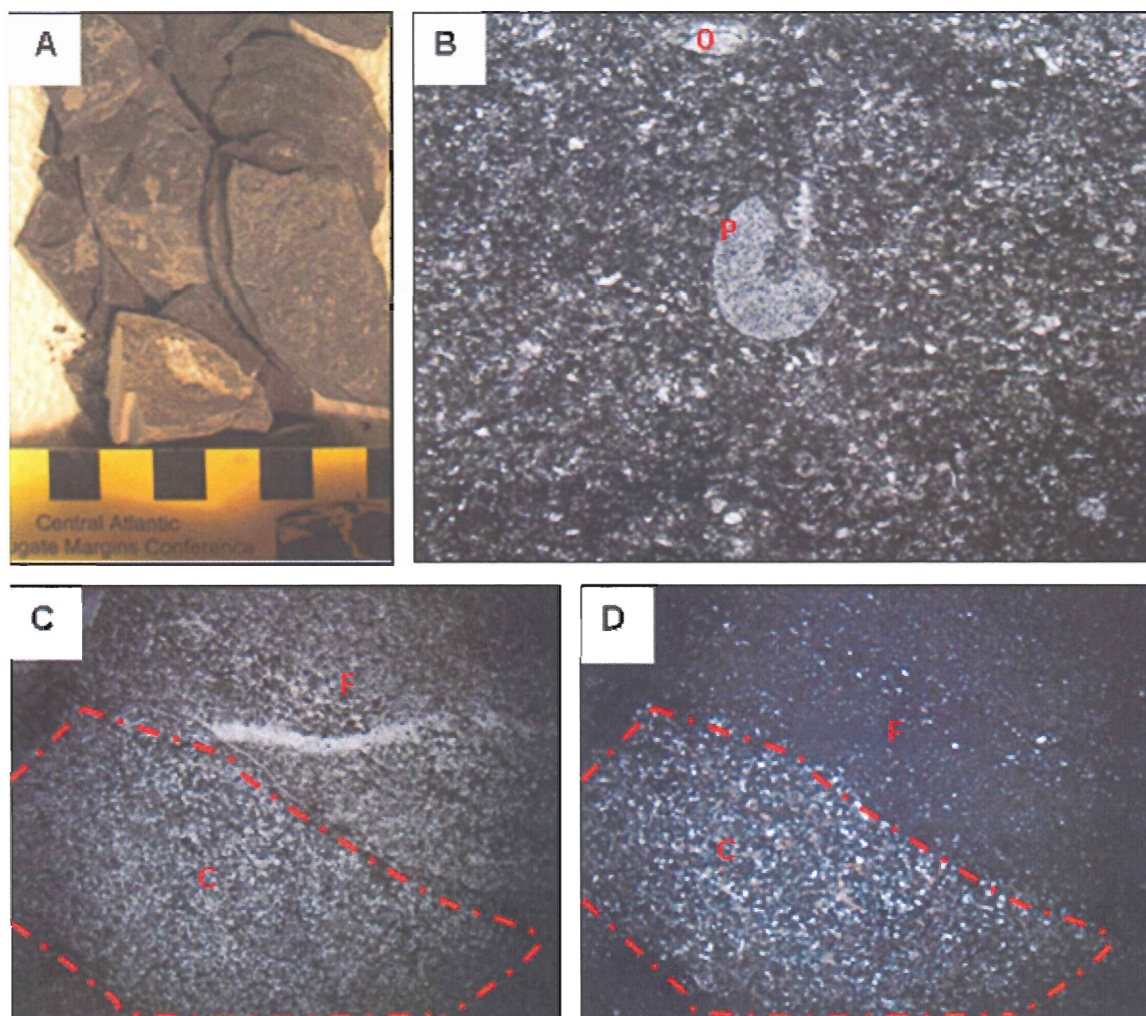


Figure 4.5- Representative cored samples and photomicrographs of lithofacies C. **A** cored, fissile sample of lithofacies C shale. **B** x6.3 – PPL. Thin section 09 shows rare pelmatozoan (P) and ostracod (O) grains in a mixed carbonate-siliciclastic matrix. **C and D**, Photomicrographs in plane polarized light (**Figure 4.5-C** – x6.3 – PPL) and crossed-polarizers (**Figure 4.5-D** – x6.3 – XP) of a coarse lens representing the transitional zone between massive carbonates (C) of lithofacies A and fissile shale (F) of lithofacies C.

4.2.4 Depositional Setting: Lower Unit

The lower unit comprises mixed carbonate-siliciclastic wackestone and mudstone rich in foraminifera, interlayered with shale beds that occur in six repeating, meter-scale, fining-upward successions. The relatively poorly preserved nature of the fossils, the scarcity of fragile grains (e.g. bryozoans), and graded bedding suggests transport by a high-energy mechanism, with settling under quieter settings, probably representing storm events. The storm events washed fine-grained sediments out from landward settings and transported them basinward, where they gradually settled and accumulated at the lower-energy base of the barrier complex (Fig 4.16).

4.3.0 Middle Unit: Tidal-influenced carbonate sand belt:

The middle unit is a light grey-brown grainstone-packstone, containing both skeletal and non-skeletal grains. It gradationally overlies the lower unit and is overlain abruptly by the upper unit. Minor occurrences of thin, dark laminae are interpreted as dissolution seams. The grain size ranges from fine (0.125-0.25 mm) to coarse (0.5-1.0 mm). Skeletal grains include pelmatozoans, bryozoans, bivalves, ostracods, and gastropods. Non-skeletal grains include intraclasts, ooids, and micritic peloids with typical dimensions ranging from 0.25 - 0.5 mm in diameter. Generally, micrite forms a coating around the boundaries of the well-sorted skeletal grains and intraclasts, resulting in the formation of incipient to well-developed ooids. The main porosity type is secondary, resulting from the leaching of micrite within ooids. Sparry calcite cement typically infills intergranular, intraparticle and shelter porosity. Minor dolomite and pyrite are present. Three lithofacies are described in Table 4.3.

Lithofacies	D	E	F
Classification	Ooid Grainstone	Peloidal Grainstone	Skeletal Grainstone/ Packstone
Occurrence	Interlayered with lithofacies E and F	Interlayered with lithofacies D and F	Interlayered with Facies D and E
Carbonate/ Clastic	Carbonate	Carbonate	Carbonate
Thickness (cm)	5- 10 cm	5- 10 cm	5- 10 cm
Grain Size	>500 μm	>500 μm	>500 μm
Color	Tan – light brown	Tan – light brown	Tan – light brown
Fossils	Pelmatozoans, bryozoans and gastropods	Bryozoans, pelmatozoans, bivalves and ostracods	Bryozoans, pelmatozoans, ostracods, bivalves, and brachiopods
Abundance	Rare - Moderate	Moderate	Abundant
Non-Skeletal Grains	Ooids, Intraclasts	Peloids, Intraclasts, ooids	Intraclasts, peloids, ooids
Abundance	Common – Abundant	Common – Abundant	Rare
Matrix	Micritic	Micritic	Micritic
Cement	Sparite	Sparite	Sparite
Minerals (GR Petrology)	97.5 - 99.2% - Calcite Trace – 2.1% Dolomite Trace Pyrite	93.9% - Calcite 6.1% - Dol	98.0% - Calcite 1.7% - Dolomite Trace Pyrite
XRD results	N/A	N/A	N/A
Comments	Caps shoaling-upward sequences		Represents base of shoaling-up sequence
Depositional Environment	Shallow-shelf barrier	Shallow – shelf barrier	Shallow-shelf barrier

Table 4.3- Summary of lithofacies D, E and F within the middle cored unit.

4.3.1 Lithofacies D Ooid Grainstone

The oolitic grainstone is tan in color and can be recognized by the predominance of well-preserved, undeformed ooids and the relative lack of skeletal grains (Fig 4.6-A). Moderate to small amounts of pelmatozoans, bryozoans and gastropods are the major biological constituents, and intraclasts are also present. The grains are typically well-sorted and their long axes are randomly oriented (Fig 4.6-B). The ooid cortex formed around a fragmented bioclastic or intraclastic nucleus (Fig 4.6-C). Also present are minor occurrences of microcrystalline dolomite and pyrite. Dolomite tends to occur within partially leached micritic ooid grains, whereas pyrite tends to border the outer

grain boundaries. This lithofacies is described as a poor-good quality reservoir (GR petrologies) with typical effective porosity values ranging from 5-12% (see chapter 5).

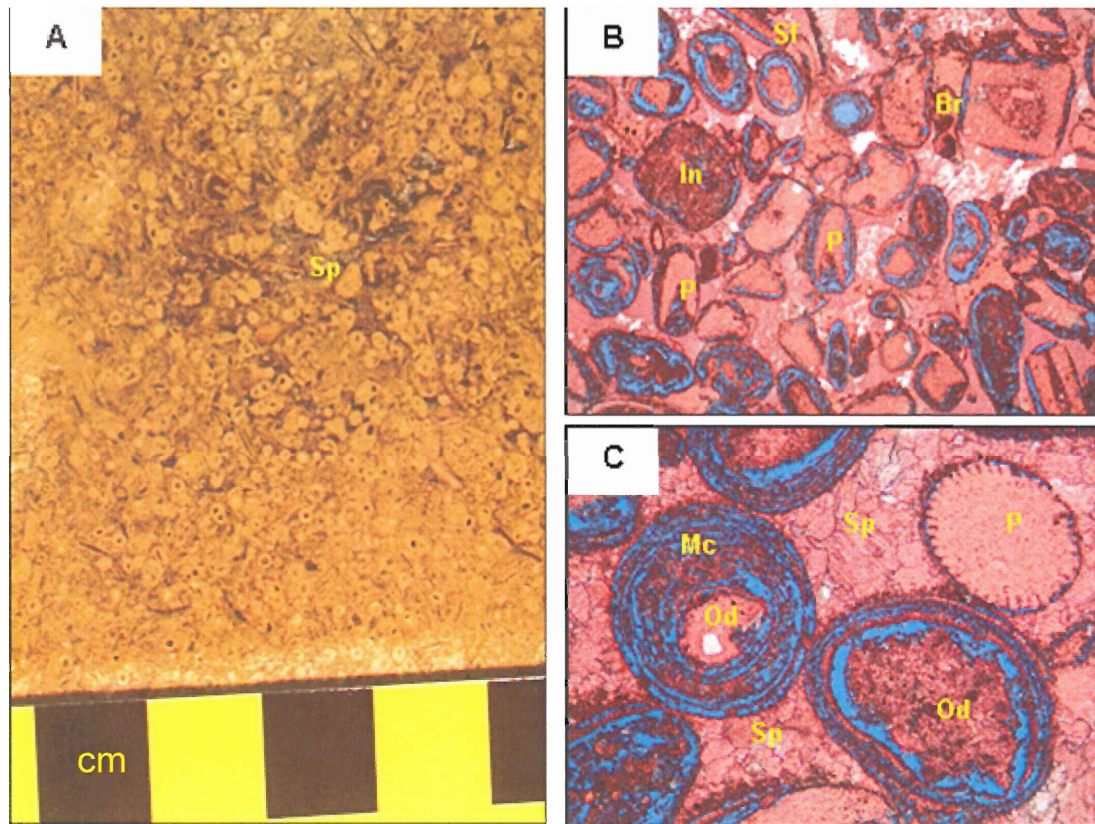


Figure 4.6- Cored and thin section samples of lithofacies D. **A**, oosparite hand sample showing abundant ooids (brown, circular grains with dark centers) and the formation of sparite cements (Sp). **B**, x32 PPL. Thin section sample Gr-002, showing interparticle porosity (blue background) and a variety of skeletal (bryozoans, pelmatozoans and shell fragments-Sf), and non-skeletal grains (intraclasts-In). **C**, x100-PPL. Thin section photo of sample Gr-002, showing a close up look at the interparticle porosity and interparticle micritization (Mc) within the ooid grains (Od), and the intraparticle sparry cement (Sp). Note the porosity in the photomicrographs documented by the blue epoxy background.

4.3.2 Lithofacies E Peloidal Grainstone

Distinguishing lithofacies E from lithofacies D and G was only possible using petrographic techniques. Lithofacies E is rich in micritic peloids whereas D and G are rich in oolitic and skeletal grains, respectively. Similar grain types are present in all three facies, with bryozoans, pelmatozoans, bivalves and ostracods. The facies contains micritic peloids, intraclasts and ooids (Figs 4.7-A and B). Micrite forms within grains and

around their boundaries. Sparite cement occupies former inter- and intraparticle pore spaces, and sparite is locally replaced with dolomite crystals ranging in size from 0.01 – 0.05 mm. Minor, small (<0.05 mm) crystals of pyrite occur throughout the sample.

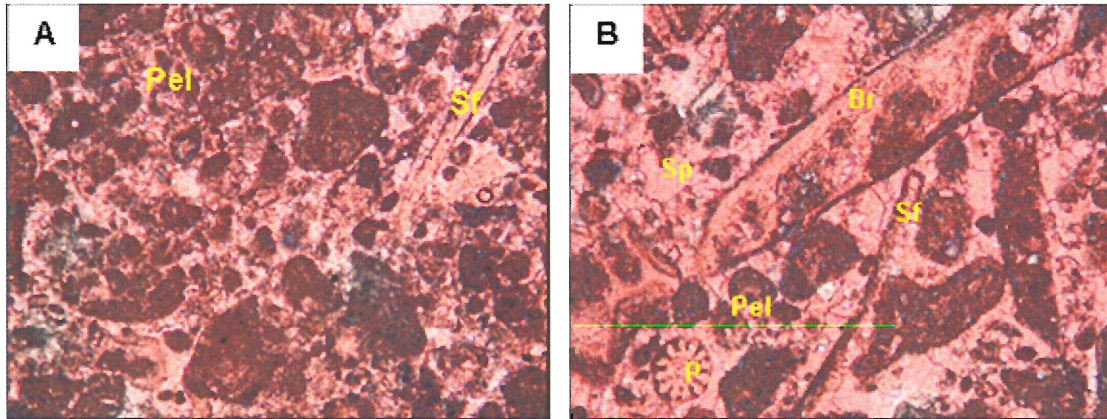


Figure 4.7- Representative thin section samples of lithofacies E. **A**, x100 – PPL. Photograph of this section sample GR-003 showing overall peloidal nature of lithofacies E. **B** x100 – PPL. Grain, and cement types associated with lithofacies E which is abundant in micritized peloids (Pel), with occurrences of bryozoans (Br), pelmatozoans (P), and shell fragments (Sf) all encompassed by sparite cement (Sp).

4.3.3 Lithofacies F Skeletal Grainstone/Packstone

The rock is light brown with abundant skeletal grains (Fig 4.8-A). The samples are generally rich in well to poorly sorted bryozoan, pelmatozoan, and ostracod grains with moderate amounts of bivalves and brachiopods and occasional gastropods. Non-skeletal grains are generally rare with local abundances of intraclasts, micritic peloids and ooids. Shells are well-preserved to fragmented, with degree of preservation commonly linked to shell strength (thickness and internal structure) (Fig 4.8 B & C). Micrite is present around and within grains. Blocky sparite infills sheltered, intragranular, and intergranular pore spaces, especially within fenestral organisms (principally bryozoans). Microporosity within micrite is the dominant porosity type and occurs in leached micritic layers. Microcrystalline dolomite occurs within partially-leached micritic grains. Porosity

is low and ineffective according to GR petrologies data and consequently, so are permeability values (see chapter 5). Minor amounts of pyrite accumulated within coarser calcite cements and range in size from 0.01 – 0.03mm.

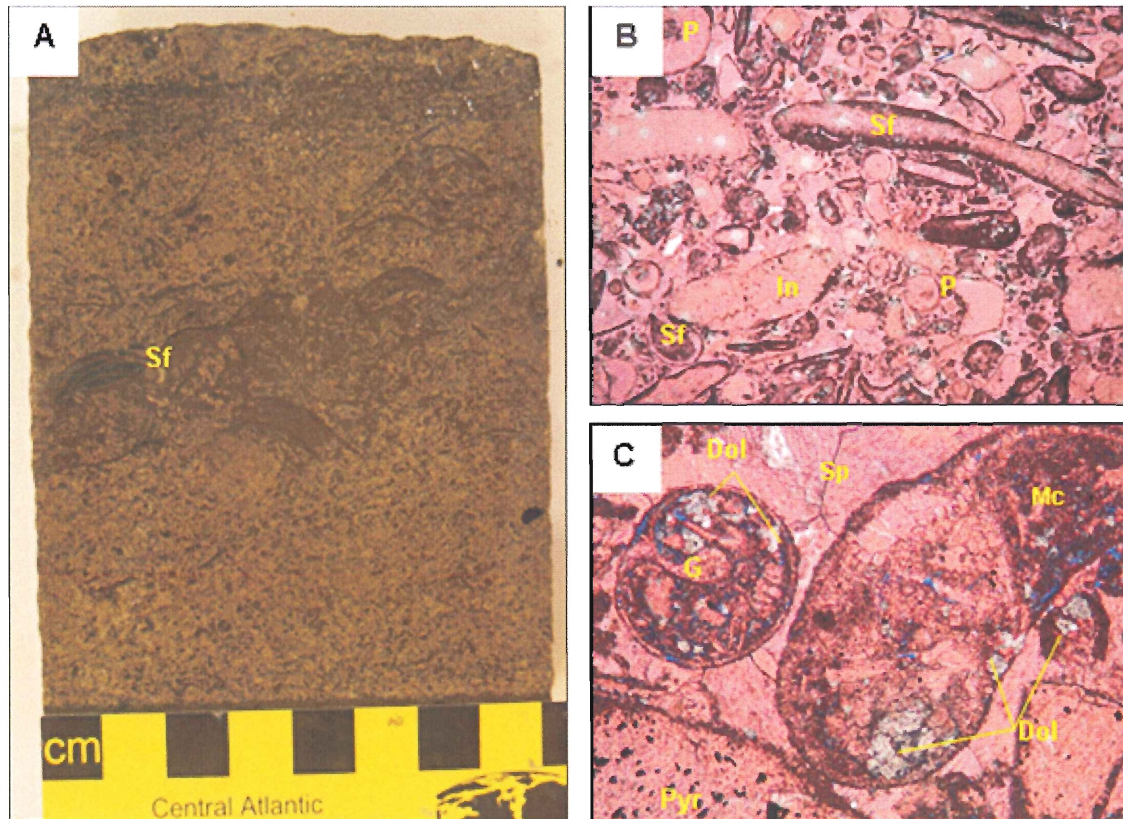


Figure 4.8- Cored and thin section samples of lithofacies F. **A**, Cored sample of the coarse-grained lithofacies F, showing large (1-2 cm long) shell fragments (Sf). **B**, x10 – PPL photo of thin section sample GR-005 showing dominant grain types including shell fragments (Sf) and pelmatozoans (P). Also present are intraclasts (In). **C**, x100 – PPL. Close-up photo of sample GR-005 showing a coarse gastropod grain (G), inter and intraparticle sparite cements (Sp), interparticle micritization and the presence of dolomite (Dol) and Pyrite (Pyr-opaque crystals, bottom left corner).

4.3.4 Depositional Setting: Middle Unit:

The middle unit has been mapped regionally as a linear, laterally extensive sedimentary body trending NNE-SSW (approximately parallel to the former paleo-shoreline; Fig 2.4). It averages nearly 5m in thickness, is approximately 40 km wide and

has been mapped throughout the WCSB. Local isopach maps of the middle unit reveal abrupt changes in thickness resulting in thick lenses in the center of the unit. The morphology and orientation of this body suggests that it was a tidal-influenced barrier complex which accumulated as a long, thin, narrow sand body parallel to the shoreline in shallow marine settings. The lenses are attributed to tidal currents creating erosional ebb and flood-tidal channels over the surface of the complex creating irregular thicknesses.

The nature of the lithofacies in the middle unit lends support to the geometry-based interpretation of a barrier complex. The lithofacies contain well-sorted grains coated in layers of micrite with variable thicknesses, with sparite cement. Relatively well sorted, coated grains are typical of a high-energy setting, as is the general absence of micrite and presence of cement (Fig. 4.2).

The skeletal facies (F) grades vertically into the oolitic facies (D). Four stacked successions, each 0.5 to 1.0m thick (Fig 4.9). These successions are recorded by the limestone density log, which records increasing-upward porosity cycles. The peaks of the porous intervals correspond with the sample interval of the most porous lithofacies D (Fig 4.10). Each succession commenced with flooding, allowing for the accumulation of skeletal grainstone which amalgamated with overlying oolitic material, interpreted here to represent shallower conditions. The stacked successions formed an amalgamated sand barrier complex (Fig 4.16).

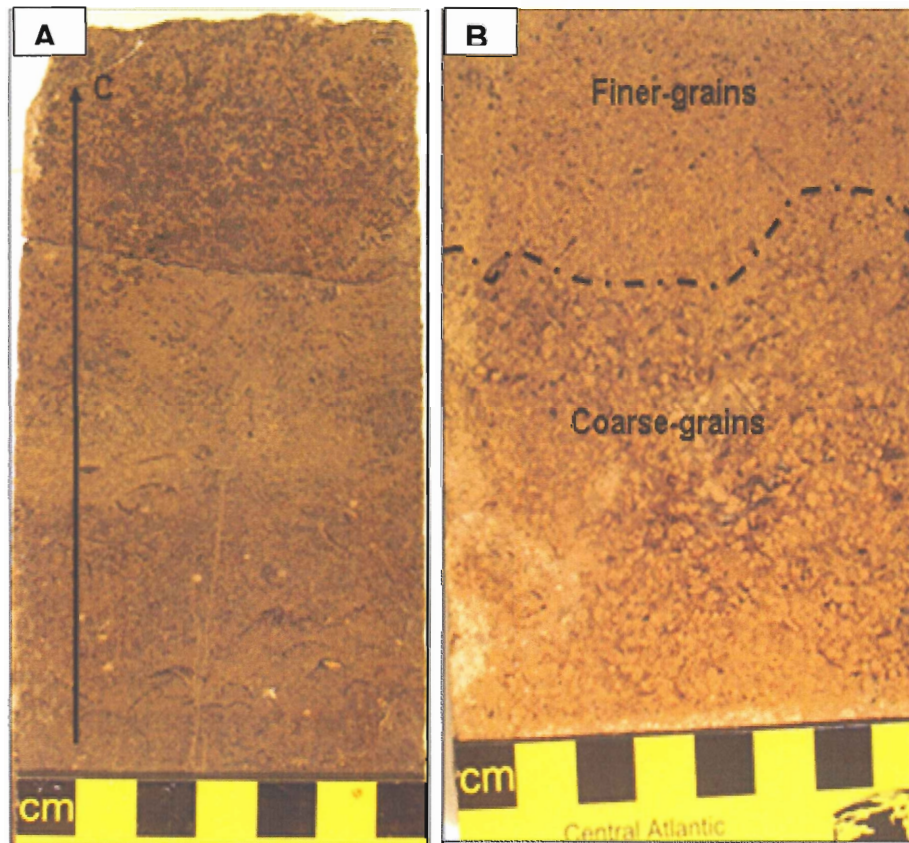


Figure 4.9- Hand sample photographs of middle core unit. **A**, Example of coarsening-upward cycles of finer skeletal material grading-upward into coarser oolitic grains. **B**, Finer-grained skeletal-grains of lithofacies F erode the underlying ooid grainstones of lithofacies A.

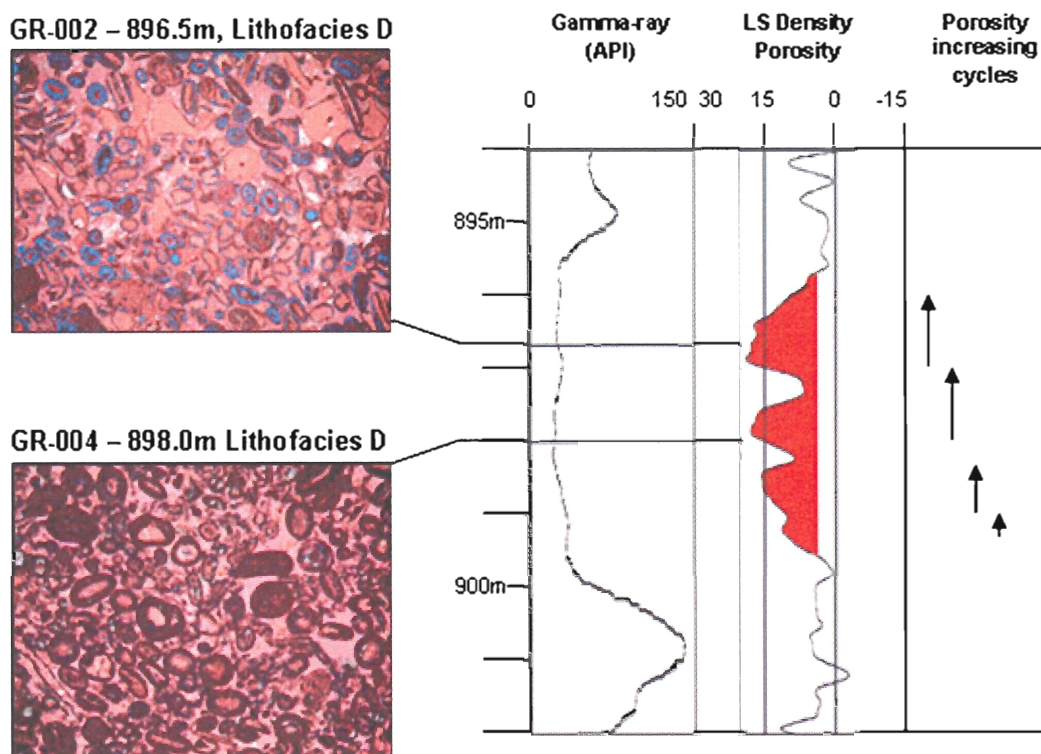


Figure 4.10- Gamma-ray and limestone density porosity log for the middle unit of the d-A3-E/94-I-14 well compared with the depths of representative thin sections of the porous lithofacies D. The depths of GR-002 (total $\Phi = 18.5\%$) and GR-004 (total $\Phi = 12.6\%$) correspond with the porosity peaks on the limestone density logs.

4.4.0 Upper Unit: Protected backshoal

The upper unit consists mainly of light grey mudstone/wackestone layers with minor interbeds of green shale. An abrupt contact separates the middle and upper units. The major constituents of the limestone layers include a variety of reasonably well-preserved skeletal grains and peloids, in micritic matrices with blocky sparite infilling former pore spaces. The grains are generally poorly sorted. The green shale has soil-like microtextures and lacks any biotic evidence. Four major lithofacies are described in Table 4.4.

Lithofacies	G	H	I	J
Classification	Peloidal-Skeletal Lime Wackestone	Green Shale	Lime Mudstone	Peloidal-Skeletal Lime Packstone
Occurrence	Upper portion of upper core unit	Inter-bedded with lithofacies G	Middle of upper core unit	Lower portion of upper core unit
Carbonate/Clastic	Carbonate	Clastic	Carbonate	Carbonate
Thickness (cm)	120 cm	5-10 cm	5 cm	20 cm
Grain Size	< 62 μm	< 62 μm	< 62 μm	< 62 μm
Color	Light gray to light brown	Green-grey	Grey	Light brown – grey
Fossils	Bryozoans, pelmatozoans, bivalves, brachiopods and minor gastropods	N/A	Pelmatozoans, ostracods, bryozoans, coccooid cells, minor brachiopods, gastropods, and peloids	Bryozoans, pelmatozoans, ostracods, bivalves and brachiopods
Abundance	Common-locally Abundant	N/A	Rare to locally common	Abundant to locally common
Non-Skeletal Grains	Peloids	N/A	Peloids	Peloids, rare ooids
Abundance	Rare to locally Common	N/A	Trace to locally common	Rare to locally common
Matrix	Micritic	Clay	Micritic	Micritic
Cement	Sparite	Calcareous	Sparite (rare)	Sparite
Other Minerals	Pyrite	N/A	Pyrite	Pyrite
XRD results	Calcite – 89% Quartz – 10%	Quartz – 75% Illite – 19% Kaolinite – 4% Calcite – 2% Chlorite -Tr	Calcite – 66% Quartz – 17% Illite – 9% Pyrite – 5% Kaolinite – 3%	Calcite – 88% Quartz – 12%
Comments				
Depositional Environment	Back-shoal (low energy)	Back Shoal paleosol	Back-shoal (low energy)	Back-shoal (low energy)

Table 4.4- Summary of lithofacies G, H, I, and J of the lower core unit.

4.4.1 Lithofacies G Peloidal-Skeletal Lime Wackestone:

Samples appear light grey/brown with thin (2.5 cm) occurrences of dark laminae every 5-10 cm between layers of massive wackestone (Fig 4.11-A). Well-preserved fenestrate bryozoans and bryozoan fronds, along with whole and fragmented ostracod

shells, are the dominant biological components (Fig 4.11-B & C). Also present are pelmatozoans, bivalves, brachiopods and minor gastropods. Micritic peloids are present and well-preserved (Fig 4.11-B). The wackestone consists of a micritic matrix which forms within and around grains. Abundant sparry calcite cement occupies former intergranular and intragranular pore spaces and large irregular void spaces. The large void spaces may have originated in some cases as soft-bodied organisms which lacked any hard skeleton and therefore are not well-preserved, or as large dissolved grains. The grains are sorted into alternate layers of coarse grains with dominant sparry cements and finer layers dominated by a micritic matrix. Large, elongate grains are aligned parallel to bedding. XRD analysis indicates that this unit consists purely of calcite and quartz although traces of pyrite observed optically are scattered throughout the entire sample, ranging in size from 0.10 – 0.02 mm.

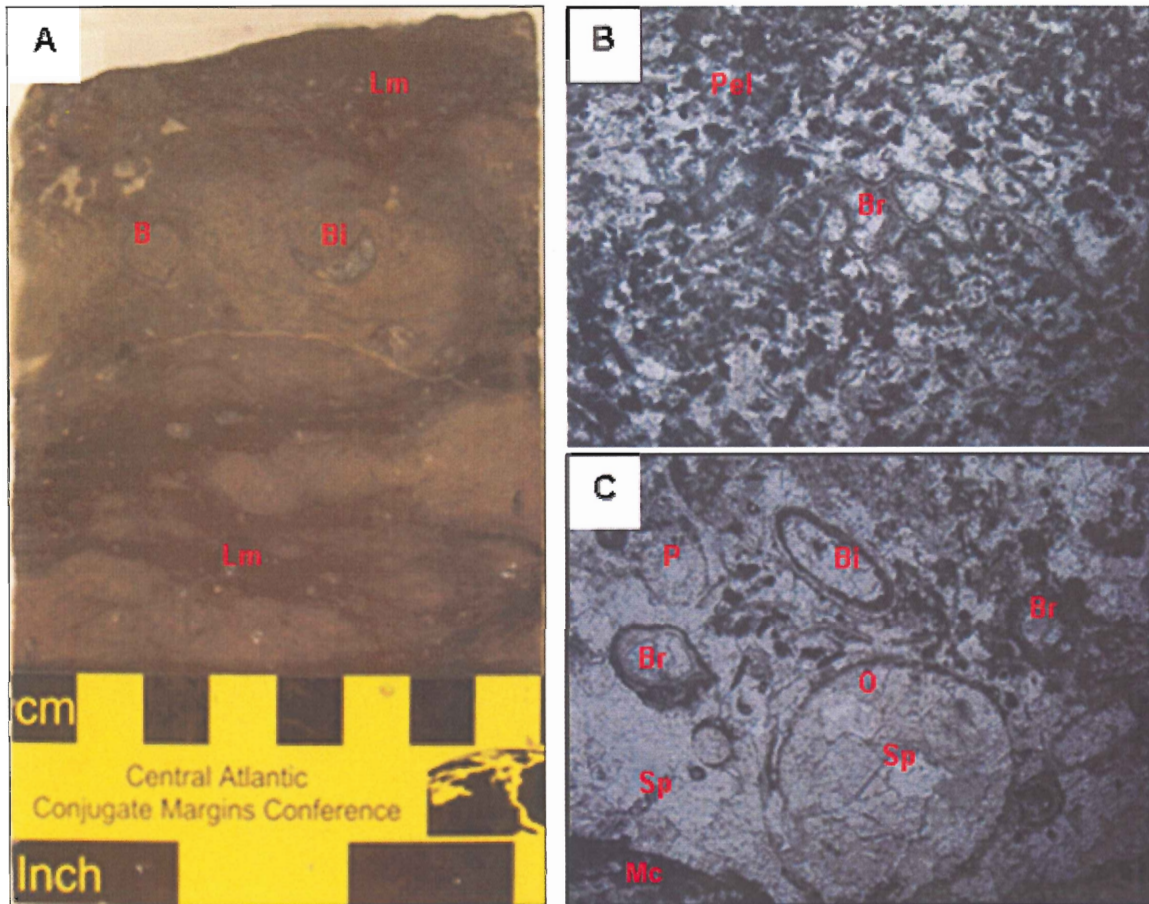


Figure 4.11- Representative core photo and photomicrographs of lithofacies G. **A**, cored sample of lithofacies G showing massive skeletal wackestone with dark laminae (Lm) and well preserved brachiopods (B) and bivalves (Bi). **B**, x6.3 – PPL. Thin section sample 01 showing a well preserved bryozoan (Br) and abundant peloidal material (Pel – black, circular shapes throughout the photograph) **C**, x6.3 – PPL. Thin section sample 01 showing abundant skeletal material including a coarse, well preserved ostracod (O), some bryozoan fronds (Br), a pelmatozoan grain (P) and a bivalve (Bi). The grains are infilled, and surrounded by sparite cement, dark micritic accumulations occur in the bottom left corner.

4.4.2 Lithofacies H Green Shale

In hand sample, lithofacies D appears light greenish grey and very fissile (Fig 4.12-A). Petrographic analysis reveals a matrix of brown clay flakes, coarse lenses rich in kaolinite and quartz, and soil-like microtextures (Fig 4.12-B). The formation of the microtextures is attributed to shrinking and swelling of clay minerals which creates sets or “domains” of parallel, linear fabrics within the matrix that trend perpendicular to one another. Void spaces within the green shale are coated with micro-laminated illuvial clay.

According to the XRD data, quartz is the dominant mineral accounting for approximately 75% of the sample. Illite is the dominant clay mineral with trace amounts of kaolinite and chlorite.

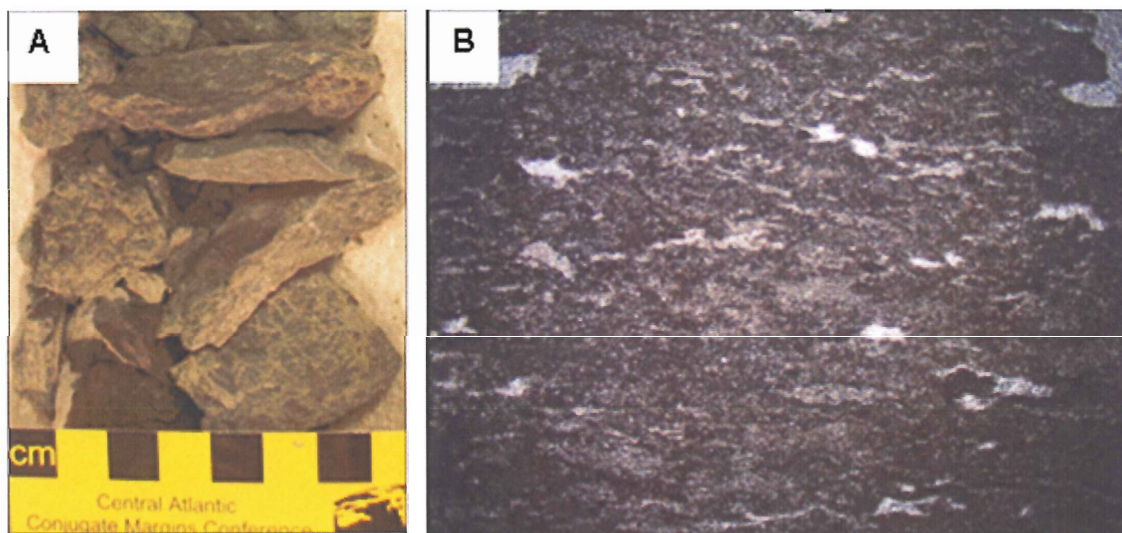


Figure 4.12- Representative core photo and photomicrograph of lithofacies H. **A**, cored interval showing the fissility and greenish color of lithofacies H. **B** x6.3 – PPL. Thin section sample 02 showing the clay-rich, poorly oriented material.

4.4.3 Lithofacies I Lime Mudstone

The rock is light grey, possesses a greasy texture, and is highly fractured, and lacks any observable grains in hand specimen (Fig 4.13-A). Petrographic examination reveals a dominant micritic matrix relatively poor in grains, with minor thin, brown, laterally extensive, wavy laminae. The matrix encompasses lenticular layers and/or lenses with high concentrations of fragmented skeletal grains, pyrite, and sparry cement (Fig 4.13-B). Grain types include pelmatozoans, ostracods, bryozoans and coccoid cells, with minor occurrences of brachiopods, gastropods, and peloids (Fig 4.13-C). Minor sparite occurrences fill intergranular pore spaces within the coarser lenses. According to XRD

analysis, calcite is the dominant mineral within the lithofacies, common occurrences of quartz, minor amounts of illite and pyrite and trace amounts of kaolinite are also present. Pyrite is recognized optically throughout the sample and is most abundant in the coarser, lenticular layers. Pyrite also tends to accumulate in sparry cemented areas. The pyrite grains range in size from 0.03 – 1.0 mm.

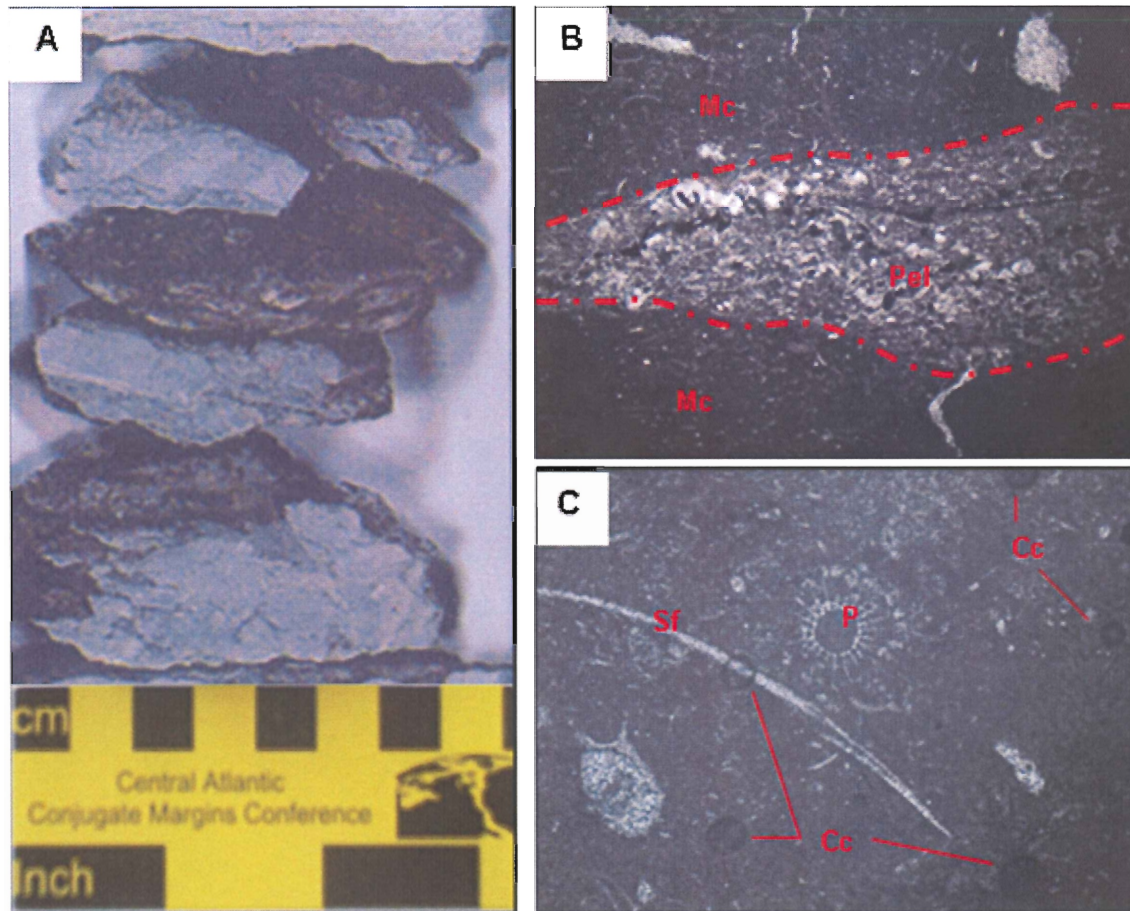


Figure 4.13- Representative core photo and photomicrographs of lithofacies I. **A**, cored sample of lithofacies I, showing its light grey color, lack of grains and tendency to fracture. Note that this lithofacies possesses a greasy texture in the dark areas along the fracture plains. **B**, x6.3 PPL. Thin section sample 03, showing the burrow structures represented by coarse-grained, peloid (Pel)-rich lenses, surrounded by heavily micritic (Mc) layers with very fine skeletal fragments (white specs). **C**, x 6.3 – PPL. Micritic layer of thin section sample 03 showing a strong presence of coccooid cells (Cc) with thin shells (Sf) and pelmatozoan (P) fragments.

4.4.4 Lithofacies J Skeletal Packstone:

The rock has a light grey matrix and is rich in skeletal grains that are poorly sorted with large variations in size (Fig 4.14-A). Abundant grain types include bryozoans, pelmatozoans, ostracods, bivalves and brachiopods (Figs 4.14-B, C, D, &E). Micritic peloids occur throughout the facies whereas oolitic grains are extremely rare (Figure 4.14-E). The preservation of the grains ranges from well-preserved to fragmented, and generally depends on shell strength (thickness and internal structure). Micrite tends to form around and within grains and sparite tends to infill sheltered, intragranular and intergranular pore spaces, as well as fenestral organisms (Figs 4.14 B & C). Micrite and sparite are present in about equal proportions (Figs 4.14-C &E). XRD analysis indicates that the calcite accounts for nearly 88% of the sample and quartz is also present. Traces of dolomite occur within the micritic matrix, the crystals ranging in size from 0.01 – 0.05mm. Minor pyrite accumulations range in crystal-size from 0.01 – 0.03mm, within the coarser calcite cements. Porosity is almost non-existent, resulting in low permeability values (See chapter 5).

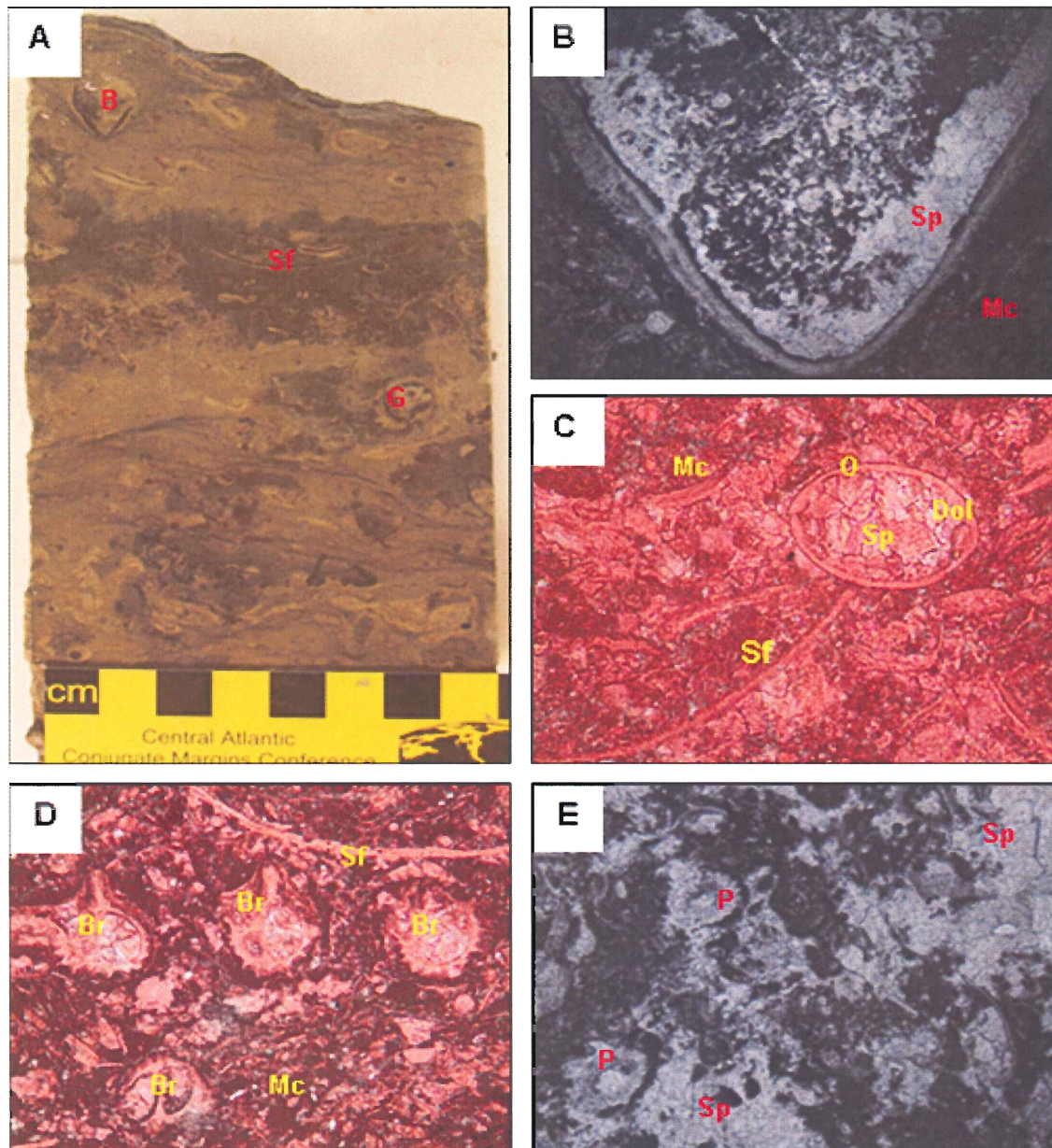


Figure 4.14- Representative cored, and thin-sectioned samples of lithofacies J. **A**, cored sample of lithofacies J showing dark and light layers, rich in coarse whole and fragmented shells. **B** x6.3 – PPL. Photomicrograph of thin section 04, shows a large, well-preserved brachiopod (marked with a ‘B’ in figure A). Note the presence of sparite within the grain and the micritic nature outside the grain. **C**, x200 – PPL. Stained sample GR-001 from lithofacies J. Note the lack of porosity (no blue background), the presence sparite within a well-preserved ostracod, the equal micrite to sparite relationship, the abundance of shell fragments and the weak presence of dolomite (white specs within ostracod grain). **D**, x100 – PPL. Stained sample GR-001 showing and abundance of bryozoans, interparticle sparite, micritic matrix and shell fragments. **E**, x6.3 – PPL. Unstained thin section sample 04, showing the presence of pelmatozoans as well as large void spaces infilled with sparite (Sp-upper right and lower left corners).

4.4.5 Depositional Setting: Upper Unit:

According to Scholle and Ulmer-Scholle (2003), abundant well-preserved micrite and micritic peloids suggest deposition above the euphotic zone. The abundance of fragile bryozoan fronds indicates that the depositional environment was likely low energy. According to Scholle and Ulmer-Scholle (2003), peloids are commonly preserved in settings including back barrier or back-bar grass flats, lagoons and protected deeper shelf settings. The presence of pelmatozoans restricts the depositional setting to normal salinity conditions on the shelf or shelf margin, ruling out a brackish environment of deposition. Therefore this unit was probably deposited in a normal salinity, shallow marine, low-energy, protected environment (Fig 4.16). The presence of interbedded green shale, interpreted as paleosol layers, indicates brief periods of surface exposure followed by a minor flooding event.

4.5.0 Well-log responses of Core Units

4.5.1 Lower Unit

Gamma ray log fluctuations are heavily influenced by the presence of silt and shale beds. Thick (~1m) massive carbonate mudstone beds of lithofacies A typically have a low peak around 40 API and gradually grade to highs of 140 API representing the clay-rich shale layers of lithofacies C (Figs 1.2, 4.1, & 4.15). The wavy laminated shale/mudstone layers yield gamma-ray values typically near 75API. Overall the gamma-ray log seems to coarsen upward. The porosity log peaks tend to increase with the presence of shaley layers, reflecting its fissile nature. Troughs associated with the massive carbonate units indicate that they are well-consolidated and non-porous (Fig 4.15).

4.5.2 Middle Unit

The gamma-ray log shows a clean (15-30 API) blocky unit nearly 5.0m thick (Figs 1.2, 4.1, 4.10, & 4.15). The boundary between the lower and middle units is represented by a sharp increase in the gamma log to nearly 55 API near 900m depth. Despite the abrupt lithological change between the middle and upper units, the gamma response is gradational because of the similar mineralogical properties of lithofacies D of the middle unit and lithofacies J of the upper unit. Limestone density porosity logs indicate the shoaling-up cycles documented in the middle unit (Fig 4.10). The porosity values typically range from 5 -15% (Figs 4.1 & 4.10) and are consistent with the values determined by GR Petrologies (chapter 5).

4.5.3 Upper Unit

The gamma-ray log response of facies #1 is influenced by the presence of the clay-rich shale layers and ranges from 45 API in the mudstone units to 80 API in the green shale layers. Porosity logs indicate low levels of porosity within the carbonate mudstone, ranging from 0-3% and typically increasing to 6% with the presence of shale (Figs 1.2, 4.1, & 4.15).

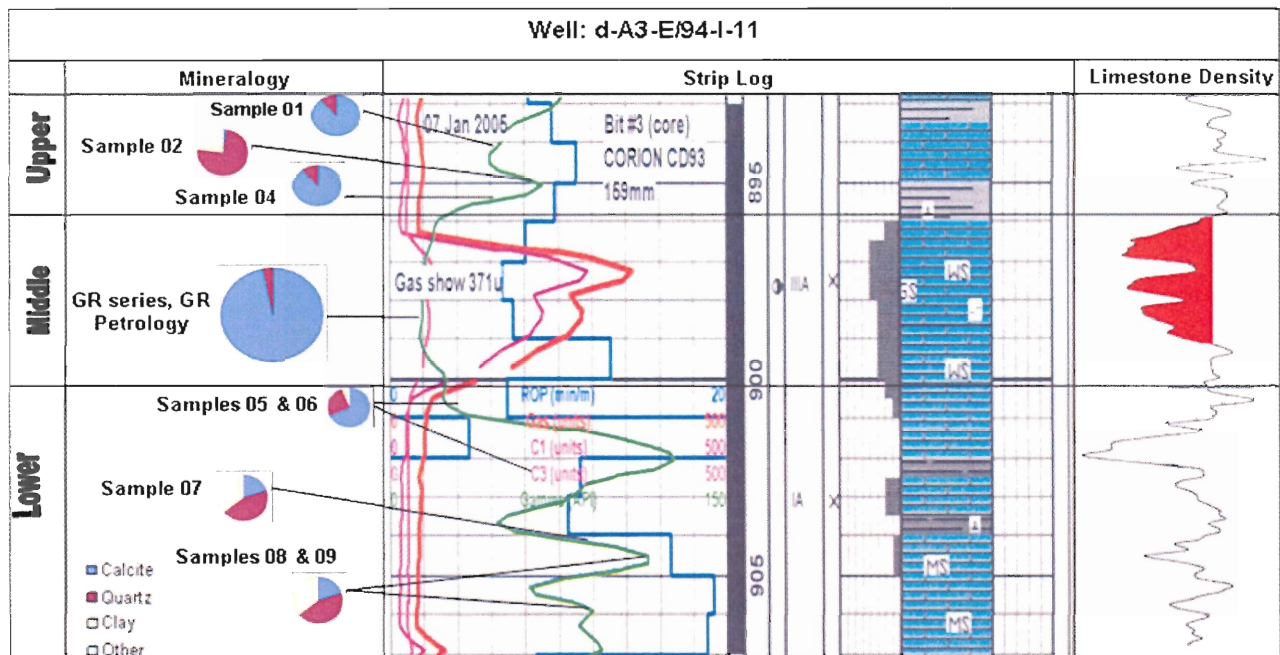


Figure 4.15- Mineralogical comparison of the upper, lower and middle units with the core gamma-ray log (green line, middle left column), strip-log (middle right column) and limestone density log (right column). Note that the clay-rich, shaley layers tend to correspond with high gamma values and shale layers in the strip log (dark grey beds). Upper and lower mineralogical abundance data determined using XRD methods.

4.6.0 Stratigraphic Succession

Overall, the interpreted depositional settings for the units suggests that the 14 m core represents a dominantly regressive period, during which the tidal-influenced carbonate sand (middle unit) and protected facies (upper unit) prograded basinward over storm-deposited open-marine successions (lower unit), which probably accumulated at the base of the sandwave complex. According to Halley et al. (1993), there are four main influences on the production and the development of carbonate sand bodies: (1) antecedent topography; (2) physical processes – tidal, wind, and wave-generated currents; (3); diagenesis; and (4) sea-level history.

The positioning of a sand body along a bank, platform or shelf margin can be directly related to the underlying topography, which can promote localized conditions of water agitation (Hallam et al., 1993). The study area is located atop the Beaton High

(Figs 2.2 and 2.3) which likely had a large influence on the formation of the Banff C sand unit that clinoforms basinward off the high (Figs 2.3 and 2.5). According to figure 2.3, the Beaton high is more than 60 km wide. This explains the unusually great width of the Banff C sand complex (>40 km). Evidence of physical processes presents itself in the varied thickness of the sand body which creates pod-like expressions on the isopach map. The topographic lows surrounding the pod-like structures may represent the scouring surfaces of a network of subtidal channels which formed as sediments were being washed down-slope by storm currents. Early cementation (see Chapter 5) resulted in the well-preserved nature of the sand body. Early cementation filled the intergranular pores creating a solid intergranular network, preventing the deformation of the grains, resulting in poor grain connectivity and a low-quality reservoir. The Banff Formation is interpreted as a dominantly regressive unit, and falling sea-level probably caused the basinward progradation of the sand complex giving it its clinoforming nature.

Settings change in the core from an open marine base of the sand complex (Lower Unit) to a restricted lagoon above (Upper Unit). The upward change in facies to a lagoon with periodic subaerial exposure indicates a dominantly regressive system. Four stacked shoaling-upward successions were logged within the middle sand facies. Records of the subsequences are observed in the limestone density log (Figs 4.10; 4.15). They record a skeletal grainstone facies with minimal porosity which shoals upward into a porous oolitic facies. According to Lasemi et al. (1998) the appearance of ooids in a skeletal sand facies is a function of increasing wave energy. This can be attributed to decreasing accommodation space caused by the upward accretion of skeletal grains. Upward accretion of the sand complex caused by the accumulation of grains will cause a fall in

relative sea-level, increasing the wave energy and resulting in more vigorous reworking of the topmost sediments. Down-slope progradation (Figs 2.2 and 2.3) of these sediments would then raise relative sea-level, creating more accommodation space allowing for the accretion of another sand body. This helps explain the increased micrite coating thickness in the coarser layers, and coarsening and shoaling-upward nature of the successions occur within the upper unit. Regression to subaerial conditions is recorded in the upper units by fining upward successions in which lagoonal lime muds grade-upward into terrigenous green shales (paleosols).

A depositional model for the cored interval suggests that it was centered upon a barrier complex that prograded basinward, off the Beatton High towards the southwest as indicated by regional and local cross-sections (Figs 2.3 and 2.5). The barrier complex is represented by the middle unit, a sand barrier complex (Fig 4.16). Quiet marine settings landward of the sand barrier complex, allowed for the settling and accumulation of micritic peloids and well-preserved skeletal grains, which are locally abundant in the upper unit. Minor shallowing events resulted in periodic exposure, allowing for the accumulation of green shale paleosols. Basinward, at the base of the barrier system, mixed, fine-grained siliciclastic-carbonate grains and skeletal fragments accumulated in repeating fining-upward successions. Easily transported, fine-grained sediments and skeletal material from the barrier complex were gradationally redeposited basinward on the seaward part of the ramp.

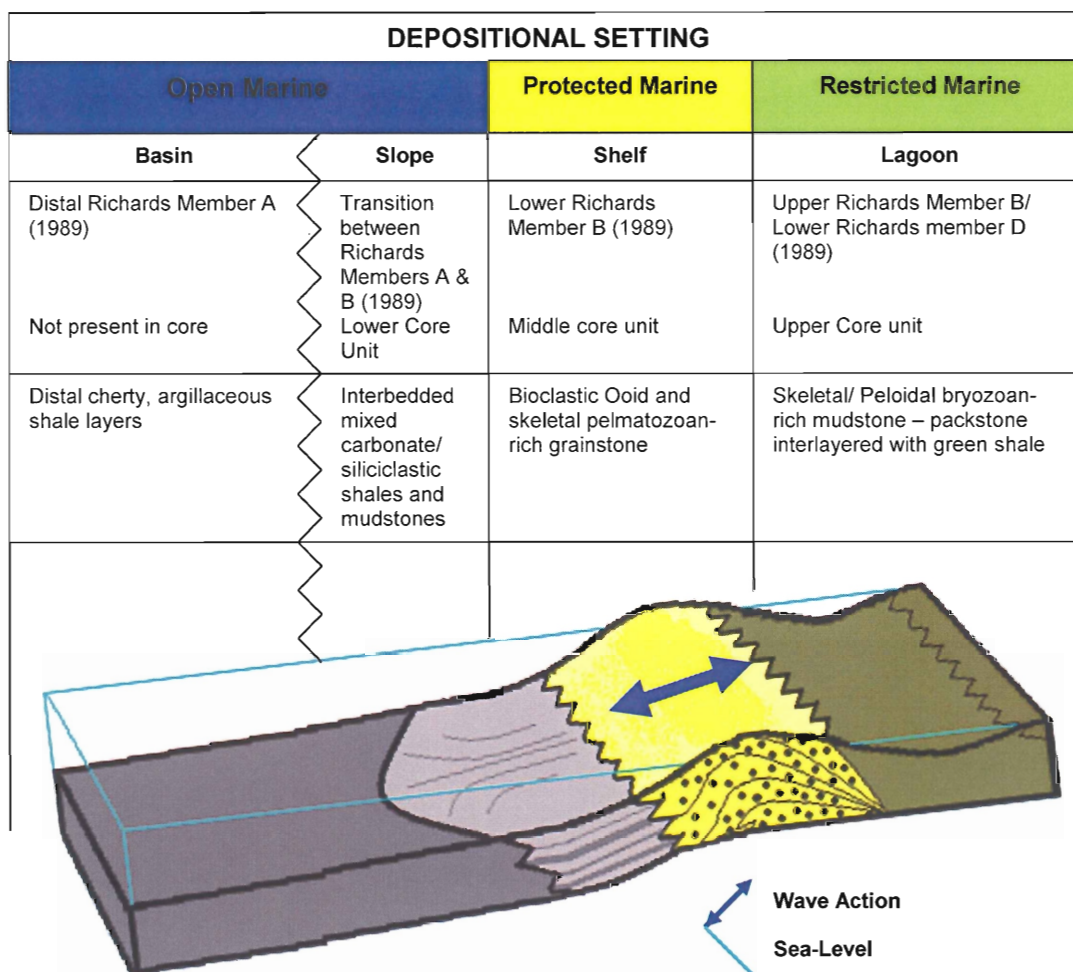


Figure 4.16- 3-D schematic model of the depositional environments responsible for generating the lower, middle and upper core units in well d-A3-E/94-I-11. Note the prograding and clinoforming nature of the middle sand belt unit.

4.7.0 Modern Analogue –Bahamas Bank

The following is a summary of the marine sand belt facies of the Bahamas Bank described by Halley et al. (1983). The Bahamas Bank is the largest and best documented modern carbonate sand-shoal analogue and serves as an appropriate modern analogue for the cored unit described above. Morphologically, sand belt bodies are described as linear bank-margin carbonate sands, oriented roughly parallel to the bank, platform, or shelf edge. Seismic profiling and sediment cores suggest that sand belts from the Bahamas are

commonly less than 10m thick, similar to the Banff C thicknesses. The shoals extend as long as 75 km along the margin of the Bahamas Bank, and are no more than 4 km wide (similar to the width of the bank they are deposited on). Three marine sand belts occur in the Bahamas: (1) the Cat Cay ooid sand belt lies on the protected northwestern coast of the Bahamas, along the Straits of Florida; (2) The platform behind Berry islands on the northern coast of the Great Bahama Bank; (3) and Lily Bank shoal which occurs on the unprotected northern coast of the Little Bahamas Bank. These sand belts are maintained by daily tidal flows and are significantly influenced by storms which may be responsible for developing channels. The short channels scour the tops of the sand belts at angles approximately normal to their axes and commonly terminate basinward in spillover lobes.

The active sand belts of the Bahamas are compositionally similar to the middle sandwave facies (Fig 4.17). They are described as a mixture of oolitic, skeletal, and peloidal sands that separate low-energy, deeper-water sediments from low-energy, shallow water lagoonal deposits. Landward, the sand belt changes into a grass and algal covered, burrowed bottom of lime mud or muddy peloidal and superficially coated ooid sand. Basinward, the sediments are described as a mixture of peloidal and skeletal grains. Both changes between the sand belt and landward and basinward facies are described as abrupt.

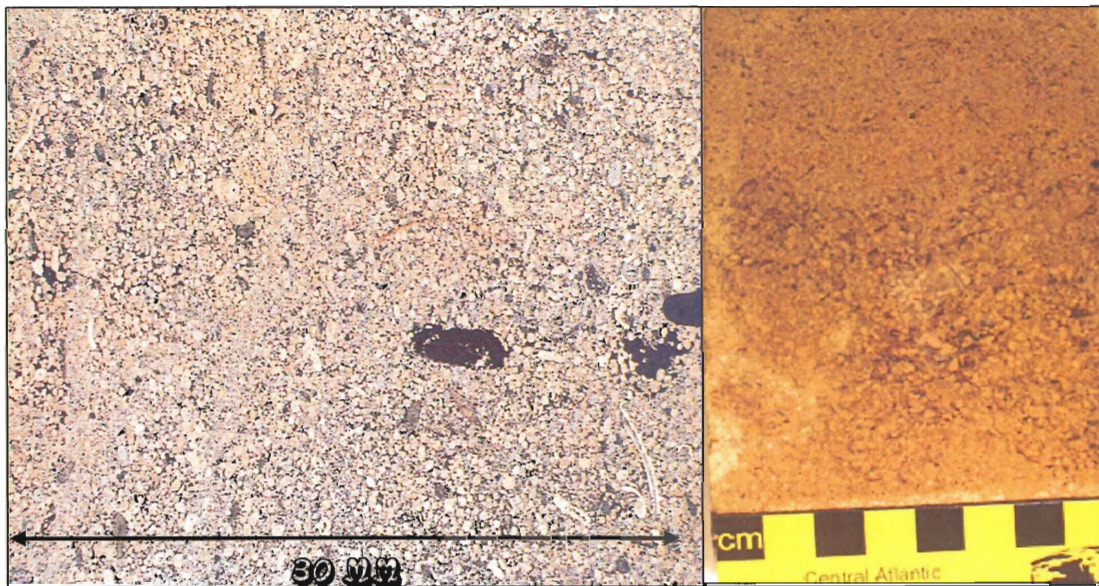


Figure 4.17- Comparison of oolitic grainstone lithofacies from the modern Bahamas Bank (left) and the Banff C unit of the ancient Mississippian Banff Formation (right).

CHAPTER 5 - Porosity, Permeability and Diagenesis

GR Petrology Consultants Incorporated (2005) provided assessments of porosity, permeability, and diagenesis of the GR sample series (middle core unit, well d-A3-E/94-I-14) to test the reservoir quality of the middle unit of the Banff C cored interval (Table 5.1). The results are summarized below.

Sample #	Depth (m)	Lithofacies	Pore Size (um)	Total Porosity (%)	Effective Porosity (%)	Qualitative porosity evaluation (North, 1985)	Permeability (mD)	Qualitative Permeability evaluation (North, 1985)	Reservoir Quality
GR-001	895.00	J	0	1.0	0.0	Negligible	0.50	Negligible	Low
GR-002	896.50	D	44	18.5	13	Fair-good	2.10	Poor-fair	Low-moderate
GR-003	897.50	E	18	5.2	1.3	Negligible-poor	0.81	Negligible	Low
GR-004	898.00	D	18	12.6	5.3	Poor-fair	1.80	Poor-fair	Low-moderate
GR-005	899.00	F	16	3.3	0.7	Negligible	0.80	Negligible	Low

Table 5.1- Summary table of porosity, permeability, and reservoir quality of the GR sample series, middle core unit, well; d-A3-E/94-I-11.

5.1.0 Diagenesis and Porosity Types:

Diagenesis is the main processes involved in the formation/destruction of pore space and thus is the main controlling factor in permeability levels and reservoir quality. Scholle and Ulmer-Scholle (2003) defined diagenesis as any post-depositional physical or chemical changes in sediments or sedimentary rocks. The processes and timing associated with diagenesis in the middle sand unit are summarized in figure 5.1. According to GR Petrology, initial compaction and deformation of micritic mud and grains lowered the primary intergranular porosity of the Banff C reservoir. Lithification of the limestone was enabled by the early emplacement of calcite cement, which mitigated grain-compaction causing the grains to remain relatively undeformed.

Microspar and sparite cements infilled void spaces of the Banff C unit, cementing the grainstone and packstone, and negatively affecting porosity, permeability and reservoir quality. Moldic porosity and micropores within the Banff C are controlled by the extent of incipient dolomitization and dissolution of micritic grains, processes which enhanced the overall reservoir quality of the middle Banff C unit. (Fig 5.2)

Paragenesis of Middle Sand Unit		
Diagenetic Processes	Early stages of burial	Late stages of burial
Compaction	————— — — —	
Micritization of Grains	— ————— — —	
Sparite Cementation	— ————— — — —	
Dissolution of Micrite and Dolomite	— ————— —————	
Pyrite precipitation	— ————— — —	
Dolomitization	— ————— — —	

Figure 5.1 Paragenesis of the middle sand unit.

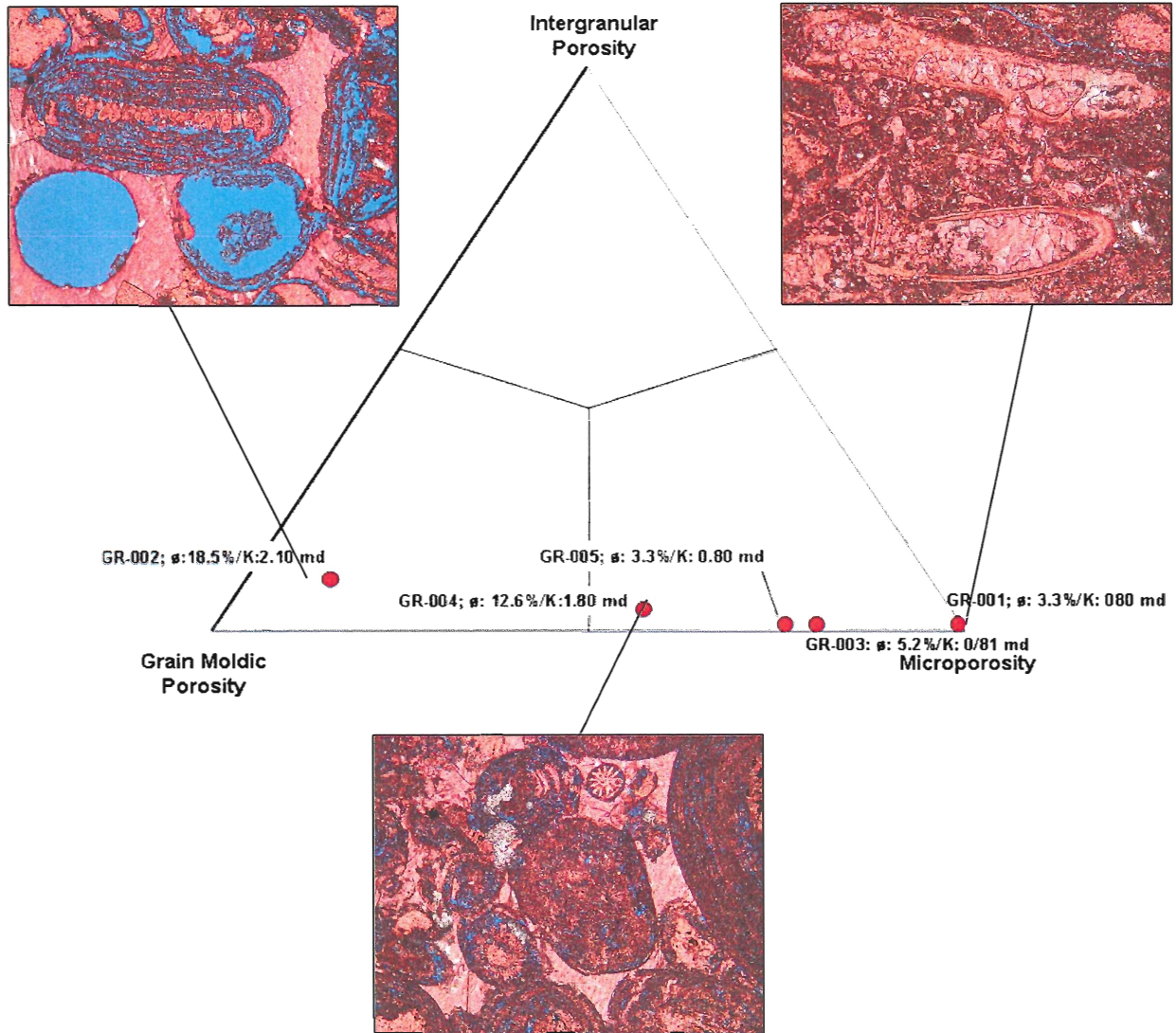


Figure 5.2- Ternary diagram illustrating the various pore types and abundances associated with the GR sample series, middle core unit, well; d-A3-E/94-I-14. After GR Petrologies (2005).

5.2.0 Porosity:

Total porosity values obtained using conventional core analysis within the Banff C cored interval ranged from 1% in sample GR-001 of lithofacies J, to 18.5% in sample GR-002 in lithofacies D (Table 5.1; Fig 5.3). Porosity averages between 8 and 9% throughout the middle and the lowermost upper Banff C cored interval. The total porosity consists of effective interparticle and intraparticle pores, moldic pores, and non-effective micropores. According to GR Petrology, the average microporosity content of the middle Banff cored interval is moderately high, and results in effective porosity values considerably lower than the Total porosity values (Fig 5.3). The effective porosity of the measured samples ranges from 0% in sample GR-001 to 13.6% in sample GR-002 (Table 5.1, Fig. 5.3) and averages 5% throughout the measured interval.

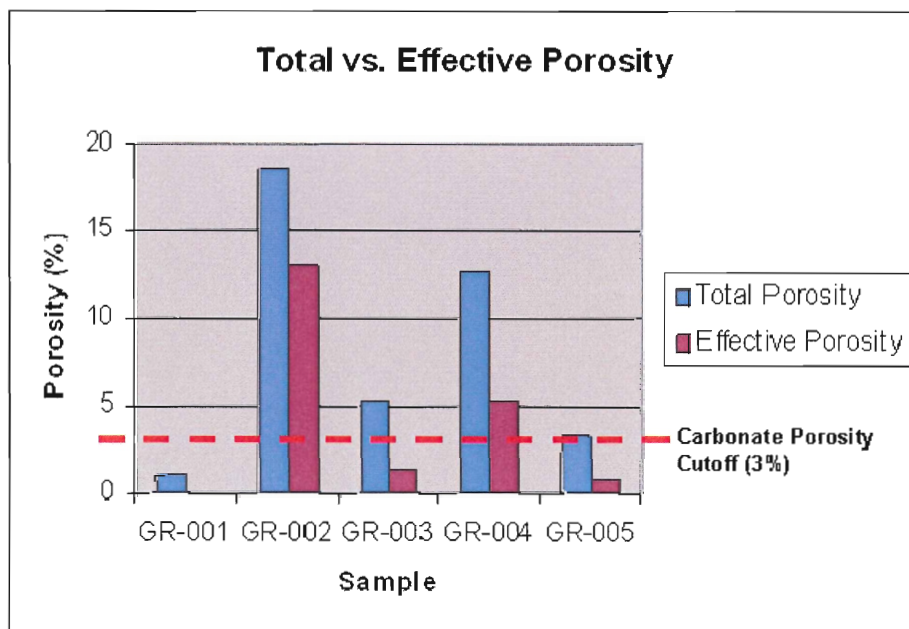


Figure 5.3- Histogram comparing total and effective porosities for each of the GR samples, middle core unit, well; d-A3-E/94-I-14.

5.2.0 Permeability Values:

Permeability was calculated as a function of the volume of porosity, the type and distribution of pores, the pore and pore-throat size, and the pore connectivity, and has a great effect on the reservoir quality. Core analysis shows that the permeability values of the Middle Banff C ranges from 0.49 mD in sample GR-001 to 2.10 mD in sample GR-002 (Table 5.1; Fig 5.4). The average permeability for all the measured samples is 1.20 mD. The permeability values for samples GR-001 and GR-005 determined using conventional core analysis are higher than expected. The GR Petrology consultants suggest that the fabric and texture of these samples have lower true permeability than the values measured by conventional core analysis. They expect true permeability values near the 0.01mD range for these samples. Similarly, GR petrologists expect the true permeability value of sample GR-004 to be lower than the calculated amount. The calculated permeability value for sample GR-004 is similar to GR-002, however the effective porosity values of sample GR-004 are considerably lower than those of sample GR-002. Because of this, true permeability values for sample GR-004 are expected to be within the 0.10 - 0.50 mD range. At best, permeability is considered low to moderate, and is highest within sample GR-002 which shows good total porosity and locally good effective porosity. The relatively low permeability values are a function of the poor connectivity between the semi-isolated moldic pores.

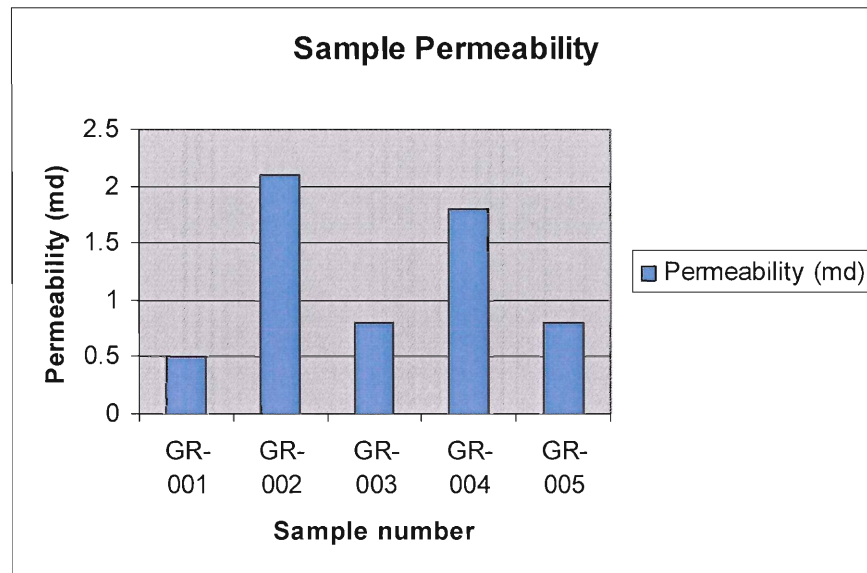


Figure 5.4- Permeability diagram of the GR sample series, middle core unit, well d-A3-E/94-I-14

5.3.0 Summary/Reservoir Quality middle core unit:

Porosity associated with the middle core unit is interpreted as mainly secondary. Total porosity of the middle Banff core unit ranks as poor according to North (1985), averaging between 8 and 9%. Effective porosity also ranks as poor but averages considerably lower at 5% because micropores are the main pore space contributor associated with the middle core unit (Figure 5.1). Moldic porosity is the second main pore-type contributor. The leached molds are typically poorly connected and bound by early stage sparite cements which destroyed primary, intergranular porosity. Consequently, permeability values are low, averaging 1.20 mD which ranks as poor according to North (1985). According to GR Petrologies, the middle core unit is low-moderate in reservoir quality and capable of gas or light oil production. It is recommended that acid fracture stimulation be used to optimize production.

CHAPTER 6 – Hydrocarbon potential of Banff C, northeastern BC

6.1.0 Carboniferous reserves (WCSB)

Within the WCSB, Carboniferous deposits rank third in conventional oil and gas accumulations behind the Devonian and the Cretaceous (Hay et al., 1994). According to Hay et al. (1994), Carboniferous strata of the WCSB contain approximately 13% ($365 \times 10^6 \text{ m}^3$, 2295 million barrels) of the proven conventional oil reserves and 16 % ($580 \times 10^9 \text{ m}^3$, 20.5 TCF) of the marketable natural gas reserves. As of 1994, the Carboniferous has produced 13.1% and 19.8% of Western Canada's cumulative oil and gas, respectively. Predictions indicate that 11 of the 14 largest oil pools yet to be discovered in Western Canada will occur within Paleozoic strata (Hay et al., 1994). Fifty-two of the 92 largest undiscovered gas pools are predicted to occur within the Carboniferous and Devonian.

6.2.0 Petroleum Systems

In order to evaluate the hydrocarbon potential of the Banff C, many factors must be considered. Not only must the reservoir quality of the middle Banff C unit be examined in terms of factors controlling porosity and permeability, but also structures and lithologies of material within and surrounding the potential Banff reservoir must be examined in order to interpret the effectiveness of the Banff petroleum system.

Together, five basic elements are essential to form an oil and gas deposit, and are known as components of a petroleum system:

- 1) A source of hydrocarbons, typically organic-rich shale or carbonate, buried through time and heated to temperatures (within the oil and gas window) at which the organic material “matures” and liberates oil and gas.
- 2) A path of migration that allows the hydrocarbons to move from their point of formation into a suitable reservoir.
- 3) A porous and permeable, relatively homogeneous reservoir, generally clean sandstones or carbonates.
- 4) Low porosity and permeability seal rocks capable of containing the hydrocarbons within the reservoir over geological timescales.
- 5) A trapping mechanism impeding further migration of the hydrocarbons within a reservoir, confining them to a local, drillable area.

6.2.1 Exshaw Formation – potential source rocks

According to Creaney et al (1994), the Exshaw Formation – which immediately underlies the Banff Formation and interfingers with the basal Banff strata has total organic content (TOC) values as high as 20% with hydrogen indices suggesting a marine, type II organic matter. Maximum temperature (T_{max}) values range from 386 – 469° C and generally fall within the oil window (Table 6.1). In 2004, Stasiuk and Fowler studied the organic facies in potential WCSB Devonian and Mississippian source rocks, and defined five (A-E) petrographic organic facies based on alginite, acritarchs, sporinite, siliceous microfossils, and algal mat microtexture assemblages. They concluded that the

Exshaw contained the organic facies A-D, with TOC values as high as 29.75%. In northeastern BC, Stasiuk and Fowler (2004) found that the most prominent facies are the organic occurrence of prasinophyte alginites and acritarchs of intermediate-water facies B and the siliceous microfossil-bearing deep to intermediate-water facies D. Although TOC and Tmax data were not available from within the study area, TOC data in areas with the same facies assemblage as those present within the study area averaged 9% and Tmax averaged 434° C. According to Richards et al. (1994), black shales of the lower Exshaw Formation extend throughout the WCSB and correlate with the basal shale of the northern Banff Formation (Richards Member A). Therefore the basal shales of the Banff Formation may serve as intraformational source rocks for the Banff C reservoir.

Tmax (C)	Maturity
<435	Immature
435-465	Mature (oil window)
>465	Overmature

Table 6.1- Required Tmax levels for hydrocarbon maturation (After North, 1985)
Note that most of the Exshaw data falls within the Mature category

6.2.2 Banff C – Potential Reservoir

The proposed petroleum system is centered on the potential Banff C reservoir. Despite being a rather thin interval (<10 m) the Banff C reservoir, which is part of Richards Member D is laterally extensive throughout the WCSB. Porosity and permeability values presented by GR Petrologies of this reservoir suggest that it is of low – moderate quality and capable of producing light oil or gas.

The porosity values encountered are fairly consistent with porosity determined using well logging techniques throughout the study area. Gas shows, recorded using strip-logging techniques, consistently present themselves within the porous intervals of the middle Banff C reservoir, indicating that it is hydrocarbon charged (Fig 6.1). The porous intervals observed in the well-logs range from 5% to 18% with net pay thicknesses ranging from 1 m to 8 m (Fig 6.2-A). The net pay values typically increase with the thickness of the middle Banff C unit which ranges from 3 m to 11 m (Fig 6.2). An unrisks reserve evaluation determined that the Banff C contains 0.9 BCF OGIP/DSU (BCF = billion cubic feet, OGIP = original gas in place, DSU = drilling spacing unit = 1400 m x 1000 m area), the parameters are summarized in table 6.2.

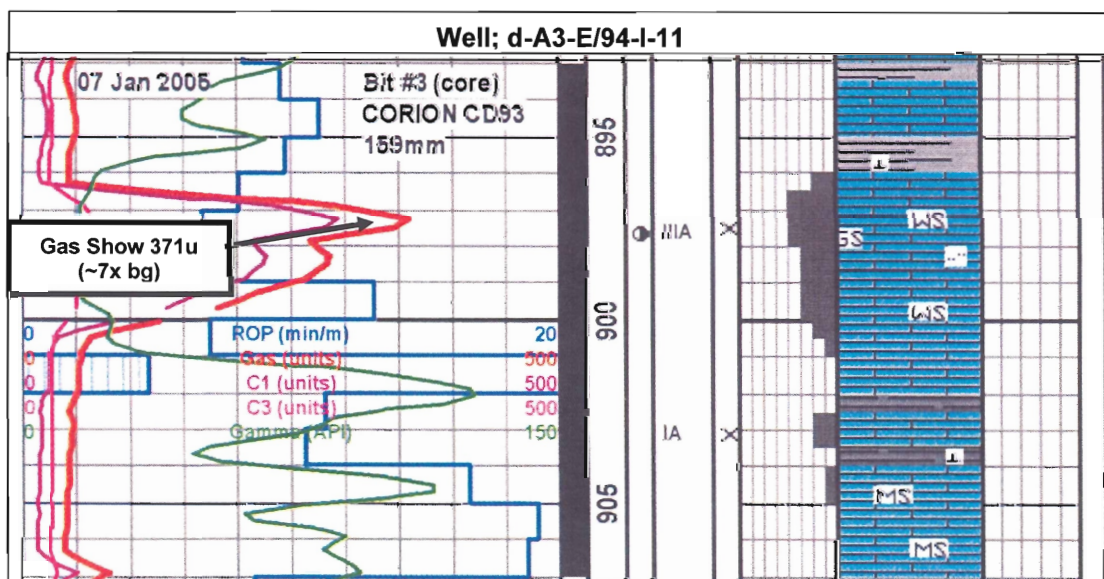


Figure 6.1- Strip log through the Banff C unit, shows strong gas peak (red line, left column) typical for the entire study area. Note the gas show peaks within the most porous interval of the Banff C unit. Gas shows typically range between 5 and 51x the background (bg)

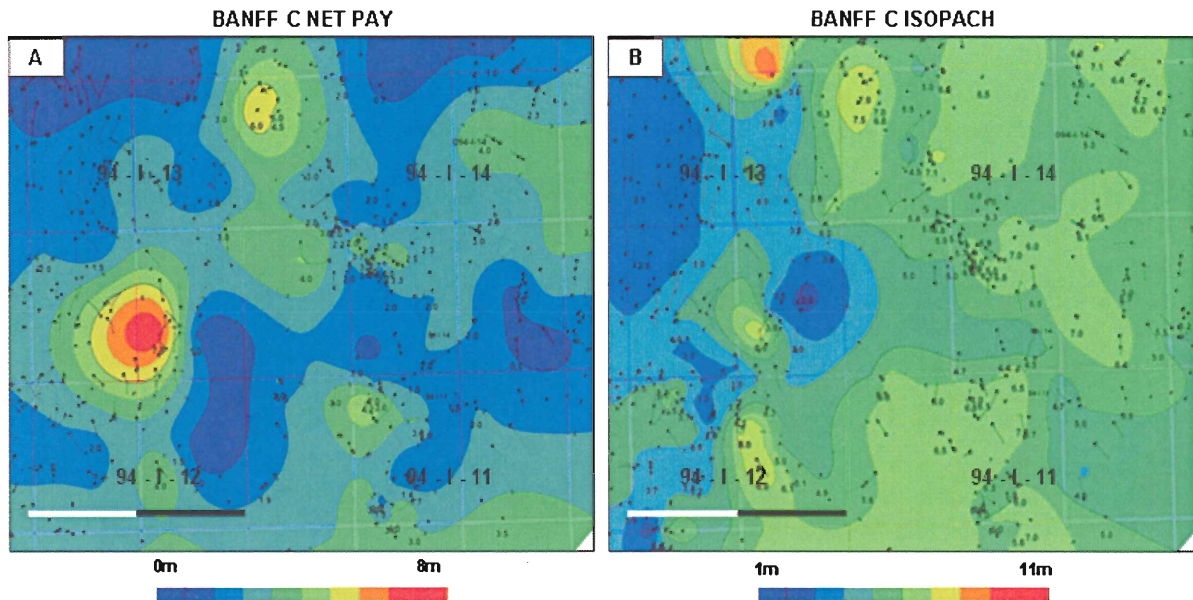


Figure 6.2- Net pay and isopach maps of the Banff C unit within the study area, created based on well-log and core data. **Figure 6.2-A,** Net pay map of the Banff C interval, values range from 0 to 8 m in thickness. **Figure 6.2-B,** Isopach map of the Banff C unit. Note that the net pay values are typically controlled by the thickness of the Banff C unit.

Parameters		Comments
Area (km ²)	988	Used Banff C intervals > 4m thick
Net Pay (m)	3	Average net pay throughout study area
Gas Saturation (%)	50	Typical for Mississippian producers
Porosity (%)	12	Average well-log porosity
Results:		0.9 BCF OGIP/DSU

Table 6.2- Summary of Banff C unrisked reserves analysis calculated during authors 2007 summer work term.

6.2.3 Seal/Cap Rocks

Overlying the Banff C reservoir seen in the D-A3-E/94-I-14 core sample are tight, micritic lime mudstones, packstones and shales. Lithological data provided by strip log observations indicates that these lithologies are consistently extensive throughout the

study area. GR Petrology studies show the sample GR-001 has no effective porosity and petrographic analysis of overlying samples reveal tight, micritic mudstones and wackestones. Underlying the Banff C reservoir are mixed siliciclastic and carbonate mudstones and shales which are also tight and extensive throughout the reservoir. Well-logs indicate that the units which directly underlie the Banff C reservoir have low-porosity. The petrographic and well and strip-log data available for the material that surrounds the Banff C reservoir indicates that the underlying and overlying material are capable of serving as good cap and seal rocks, respectively, within this petroleum system.

6.2.4 Trapping Mechanisms

Regional cross sections and isopach maps show that the Banff C is a laterally extensive unit which strikes along the former Carboniferous paleo-shoreline and builds out with clinofolds perpendicular to the shoreline in a southwesterly direction. Mapping as well as lithological interpretations of the Banff C suggest that it is an amalgamated shoal structure. Shoal structures are generally extensive along-strike and tend to be relatively narrow perpendicular to strike with abrupt lateral facies transitions. The subsurface morphology of the Banff C suggests that, if the reservoir were charged with hydrocarbons, they would likely accumulate and become trapped to the northeast (up-dip of the clinofolding structure, Fig 2.5).

6.2.5 Type of Petroleum System

Creaney et al. (1994) define two types of petroleum systems, open and closed. They define a closed petroleum system as, “one in which petroleum generated from a

particular source generally does not migrate out of rocks of the same age.” Source rocks of the Banff Assemblage are likely derived from the organic-rich Exshaw Formation and its lower Banff correlatives. Although the Exshaw is late Devonian and the Banff early Carboniferous, they were deposited in the same T-R sequence within the study area. Therefore the potential Banff Assemblage system in northeastern BC can be classified as a closed petroleum system.

CHAPTER 7 – Conclusions

7.1.0 - Core Observations

Combining my subsurface mapping of the Banff Formation and megascopic core description with the petrology of the Banff core interval and porosity and permeability data supplied by GR Petrologies, I was able to draw several major conclusions about the middle Banff C unit.

1. The deposition of the Mississippian Banff Formation in northeastern BC was controlled topographically by the Beatton High, a forebulge situated directly below the study area. Together with falling sea-level, The Beatton High controlled basinward progradation of the Banff Formation, the basal part of which was deposited as a suite of clinoforms off the high, to the southwest.
2. The Banff cored interval represents lithologies of Richards' member D. It can be subdivided into the upper, middle, and lower units based on megascopic analysis. Thin section microscopy reveals that each unit contains multiple lithofacies. The lithofacies indicate depositional environments in relatively shallow-water settings, ranging from open marine to barrier complex to protected lagoonal.
 - a. The lower unit contains massive carbonate mudstones rich in siliciclastic grains rhythmically bedded with layers of dark, fissile shale. It is rich in foraminifera and brachiopods and is interpreted as an open marine facies, the sediments of which was transported basinward by storm events and settled in quiet conditions, after which shales capped the layers.
 - b. The middle unit contains repeated successions of pelmatozoan, bryozoan-rich skeletal grainstone that coarsen upward into oolitic grainstones, and is

interpreted as a barrier complex that accumulated on the shelf margin. It represents the Middle Banff C unit which was mapped by the author in the summer of 2007.

- c. The upper unit comprises pelmatozoan and bryozoan-rich skeletal-peloidal wackestones, packstones and mudstones interbedded with layers of green shale. The upper unit originated landward of the middle sand unit in a quiet, protected, marine setting, with periodic exposure.
3. The upper and middle units of the Banff cored interval represent lithologies of Richards member D. The lower unit represents a transitional phase between the Member D and Member A, which conforms with the contact relationship, described by Richards (1993) as gradational.
4. Porosity values within the middle Banff core unit rank qualitatively from negligible to good. The values obtained from the GR Petrologies studies correlate well with values obtained from well-logs which are prominent throughout the central and eastern portion of the study area.
5. Net pay values recorded within the Banff C, using well-logging techniques, average approximately 3 m and typically correlate with the overall thickness of the Banff C unit. Presumably, thicker intervals contain more shoaling-upward successions yielding a larger number of porous intervals.
6. Shoaling-upward successions within the middle core unit (Banff C) and early cementation have negatively affected reservoir quality. Three lithofacies were identified within the middle core unit. Of these lithofacies the ooid grainstone lithofacies, qualitatively (North 1985) ranked the highest ranging from fair to

good. The lithofacies repeat themselves in packages interpreted as shoaling-upward successions. The coarser oolitic-rich tops of these sequences contain the highest porosity values and are generally separated by skeletal layers of negligible to poor porosity. Early cementation destroyed intergranular porosity and created a lithological framework disabling further compaction and deformation of grains which resulted in poor connectivity of pore spaces between grains and low permeability levels.

7. Gas show peaks observed in strip-logs indicate that the middle Banff core unit is hydrocarbon-charged.
8. Unrisked reserves analysis of the Banff C unit within the study area yielded results of 0.9 BCF OGIP/DSU.

7.2.0 Recommendations for Further Analysis

In order to fully understand the reservoir potential of the Banff C the following measures should be taken:

1. More lithological data should be collected and evaluated from the Banff C and surrounding intervals in adjacent areas. Attempts should be made at correlating the shoaling-upward sequences and determining their lateral extent. In order to do so, more thin section sampling should be done within the Banff C (middle core) unit. Samples were taken on metre intervals and each shoaling-upward succession is between 50 and 100 cm thick. The successions are not well-represented in the thin section data using a 1 m sample interval. Sampling at smaller intervals would

give better indication as to the thickness and frequency of the porous ooid grainstone intervals.

2. Sampling the thicker Banff C units could be an asset, the cored unit representing the Banff C is only 5 m in thickness, the unit can be as thick as 10 m (Fig 2.4) and thicker intervals typically contain larger net pay values. Drilling the thicker units would likely yield more hydrocarbons.

7.3.0 Recommendations for Drilling

According to GR Petrologies (2005) the Banff C unit is capable of producing light oil or gas. In order to successfully produce hydrocarbons from this reservoir the following measures should be followed:

1. Drill the thicker units first as they seem to contain greater net pay intervals.
2. When drilling, use stacking method to reduce risk. Target multiple potential reservoirs to avoid drilling a dry well.
3. Re-enter existing wells to reduce drilling costs. There are plenty of wells within the study area that penetrate the Banff C unit.
4. Use fracturing methods to artificially fracture the reservoir, this will destroy the low porosity baffles caused by the tight skeletal and peloidal grainstone lithofacies.

8.0 REFERENCES

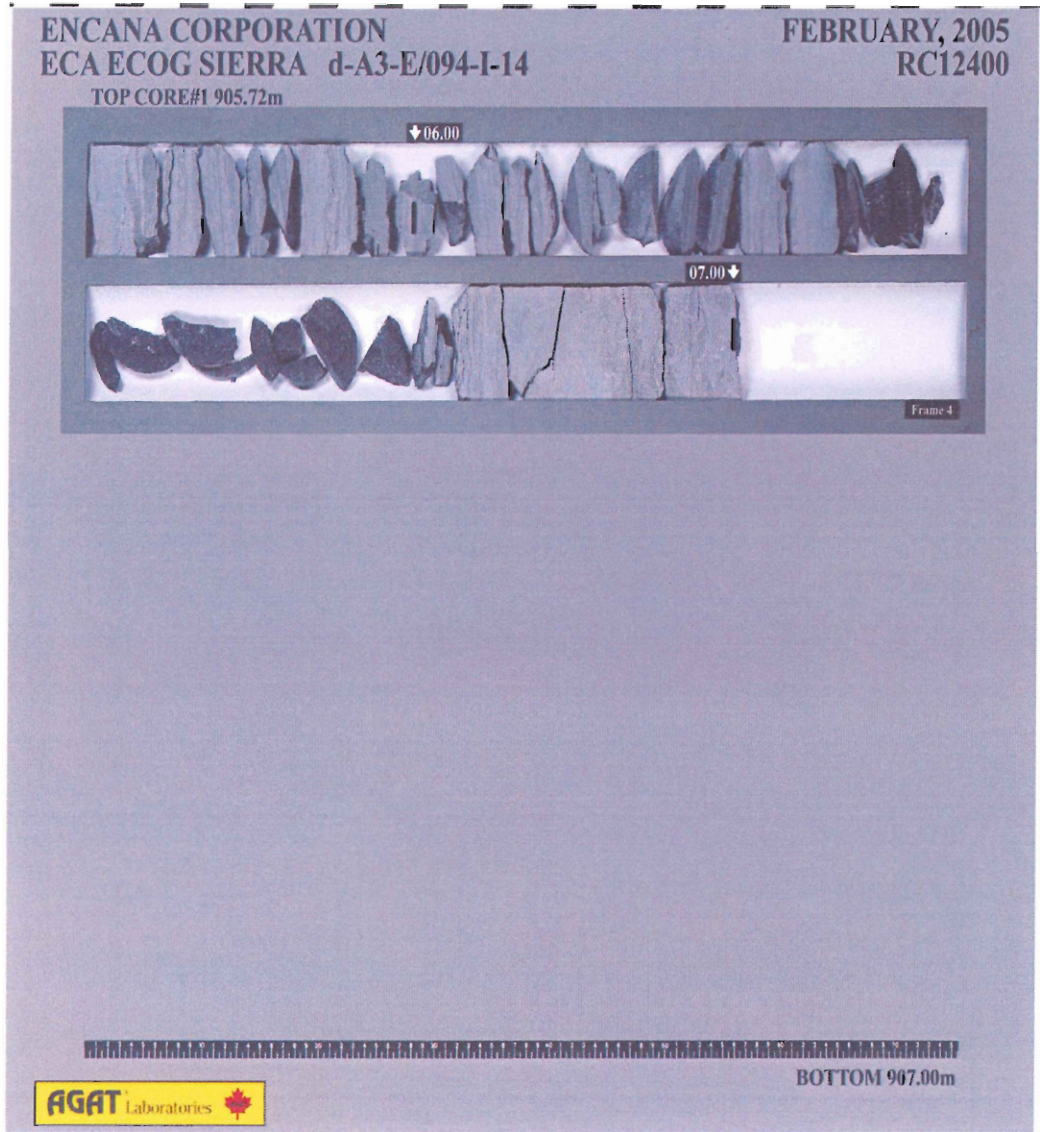
- Caplan, M.L. and Bustin, R.M. 2001. Paleoenvironmental and paleoceanographic control on black, laminated mudrock deposition: Example from Devonian–Carboniferous strata, Alberta, Canada, *Journal of Sedimentary Geology*, **145**: 45-72.
- Creaney, S., Allan, J., Cole, K.S., Fowler, M.G., Brooks, P.W., Osadetz, K.G., Macqueen, R.W., Snowdon, L.R., and Riediger, C.L. 1994. Petroleum generation and migration in the Western Canada Sedimentary Basin - Chapter 31. *In Geological Atlas of the Western Canadian Sedimentary Basin Edited by G. Mossop and J. Dixon. Canadian Society of Petroleum Geologists and the Alberta Research Council, Calgary, Alberta, Canada, pp. 455-468.*
- DeCelles, P.G. and Giles, K.A. 1996. Foreland basin systems, *Basin Analysis*, **8**: 105-123.
- Dragoie, C. 2005. EnCana corporation ECA ECOG sierra d-A3-E. d-A3-E/94-I-14, Cabra Consulting, Calgary, Alberta.
- Dunham, R.J. 1962. Classification of carbonate rocks according to depositional texture. *In Ham, W. E.(ed), classification of carbonate rocks: American Association of Petroleum Geologists Memoir, 108-121.*
- Gordon, A.A. 2005. Petrographic and Reservoir quality assessment Banff Formation limestone d-A03-E/94-I-14 EnCana corporation. GR 7677 05, GR Petrology Consultants Inc., Calgary, Alberta.
- Hallam, A. 1984. Pre-quatarnary sea-level changes, *Annual Review of Earth Planetary Science*, **12**: 205-243.
- Halley, R.B., Harris, P.M., and Hine, A.C. 1983. Bank margin environments. *In Carbonate Depositional Environments Edited by P.A. Scholle, D.G. Bebout and C.H. Moore. the American Association of Petroleum Geologists, Tulsa, Oklahoma, U.S.A., pp. 465-506.*
- Hay, P.W. 1994. Oil and gas resources of the Western Canada Sedimentary Basin. *In Geological Atlas of the Western Canadian Sedimentary Basin Edited by G. Mossop and J. Dixon. Canadian Society of Petroleum Geologists and the Alberta Research Council, Calgary, Alberta, Canada, pp. 469-470.*
- Kendall, C. 2006. USC Sequence Stratigraphy Web [online]. Available from <http://strata.geol.sc.edu/thinsections/classification.html> [cited 03/10 2008].
- Lasemi, Z., Norby, R.D., and Treworgy, J.D. 1998. Depositional facies and sequence stratigraphy of a lower Carboniferous bryozoan-crinoidal carbonate ramp in the

- Illinois Basin, mid-continent USA. *In Carbonate Ramps Edited by V.P. Wright and T.P. Burchette*. The Geological Society of London, UK, pp. 369-395.
- Law, J. 1981. Mississippian correlation, northeastern British Columbia, and implications for oil and gas exploration, *Bulletin of Canadian Petroleum Geology*, **29**: 378-398.
- Magoon, L.B. 1988. The petroleum system - a classification scheme for research, exploration, and resource assessment, United States Geological Survey, *Bulletin*, **1870**.
- Mann, U. and Muller, G. X-ray mineralogy of deep sea drilling project legs 52 through 53, western north Atlantic. *In Donnelly, T, et al. Edited by initial reports of the deep sea drilling project*, U.S. Government Printing Office, Washington, 721-728.
- Nesse, W.D. 2000. Introduction to X-ray crystallography. *In Introduction to Mineralogy Edited by Oxford Printing Press*, New York, New York, pp. 160-168.
- North, F.K. 1985. Petroleum geology. Allen & Unwin Inc., 8 Winchester Place, Winchester, Mass.
- O'Connell, S.C. 1990. The development of the Lower Carboniferous Peace River Embayment as determined from Banff and Pekisko Formation depositional patterns, *Bulletin of Canadian Petroleum Geology*, **38A**: 93-114.
- Parrish, R.R. 1992. Miscellaneous U-Pb zircon dates from southeast British Columbia. *In Radiogenic age and isotope studies: Report 5*, Geological Survey of Canada Paper, **91-2**: 143-153.
- Procter, R.M. and MacAulay, G. 1968. Mississippian of Western Canada and Williston Basin, the American Association of Petroleum Geologists Bulletin, **52-10**: 1956-1968.
- Pysklywec, R. and Mitrovica, J.X. 2000. Mantle flow mechanisms of epeirogeny and their possible role in the evolution of the Western Canada Sedimentary Basin, *Canadian Journal of Earth Sciences*, **37**: 1535-1548.
- Richards, B.C. 1989. Upper Kaskaskian sequence: Uppermost Devonian and Lower Carboniferous. *In Western Canada Sedimentary Basin A case history Edited by B.D. Ricketts*. Canadian Society of Petroleum Geologists, Calgary, Alberta, Canada, pp. 165-202.
- Richards, B.C., Bamber, E.W., Higgins, A.C., and Utting, J. 1993. Subchapter 4E Carboniferous. *In Sedimentary Cover of the Craton in Canada Edited by P.J. Griffin and A.V. Okulitch*. Canada Communications Group - Publishing, Ottawa, Canada, pp. 202-271.

- Richards, B.C., Barclay, J.E., Bryan, D., Hartling, A., Henderson, C.M., and Hinds, R.C. 1994. Carboniferous strata of the Western Canada Sedimentary Basin. *In* Geological atlas of the Western Canada sedimentary basin *Edited by* G. Mossop and J. Dixon. Canadian Society of Petroleum Geologists and the Alberta research Council, Calgary, Alberta, Canada, pp. 221-250.
- Scholle, P.A. and Ulmer-Scholle, D.S. 2003. A color guide to petrography of carbonate rocks: Grains, textures, porosity, diagenesis. AAPG, Canada. .
- Smith, M.T. and Gehrels, G.E. 1992. Structural geology of the Lardeau Group near trout lake, British Columbia: Implications for the structural evolution of the Kootenay arc, Canadian Journal of Earth Sciences, **29**: 1305-1319.
- Stasiuk, L.D. and Fowler, M.G. 2004. Organic facies in Devonian and Mississippian strata of Western Canada Sedimentary Basin: Relation to kerogen type, paleoenvironment, and paleogeography, Bulletin of Canadian Petroleum Geology, **52**: 234-255.

APPENDICES

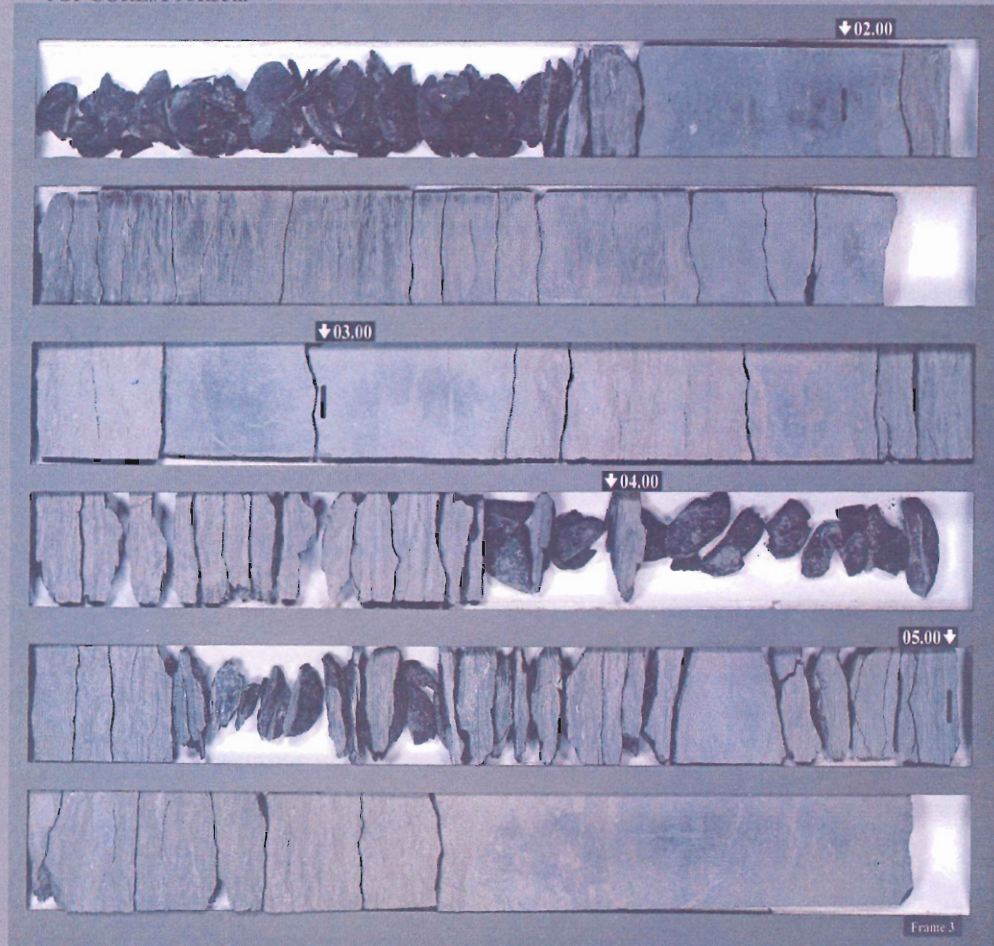
APPENDIX A – Core Photographs




ENCANA CORPORATION
ECA ECOG SIERRA d-A3-E/094-I-14

FEBRUARY, 2005
RC12400

TOP CORE#1 901.35m



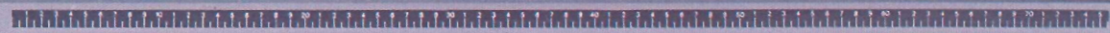
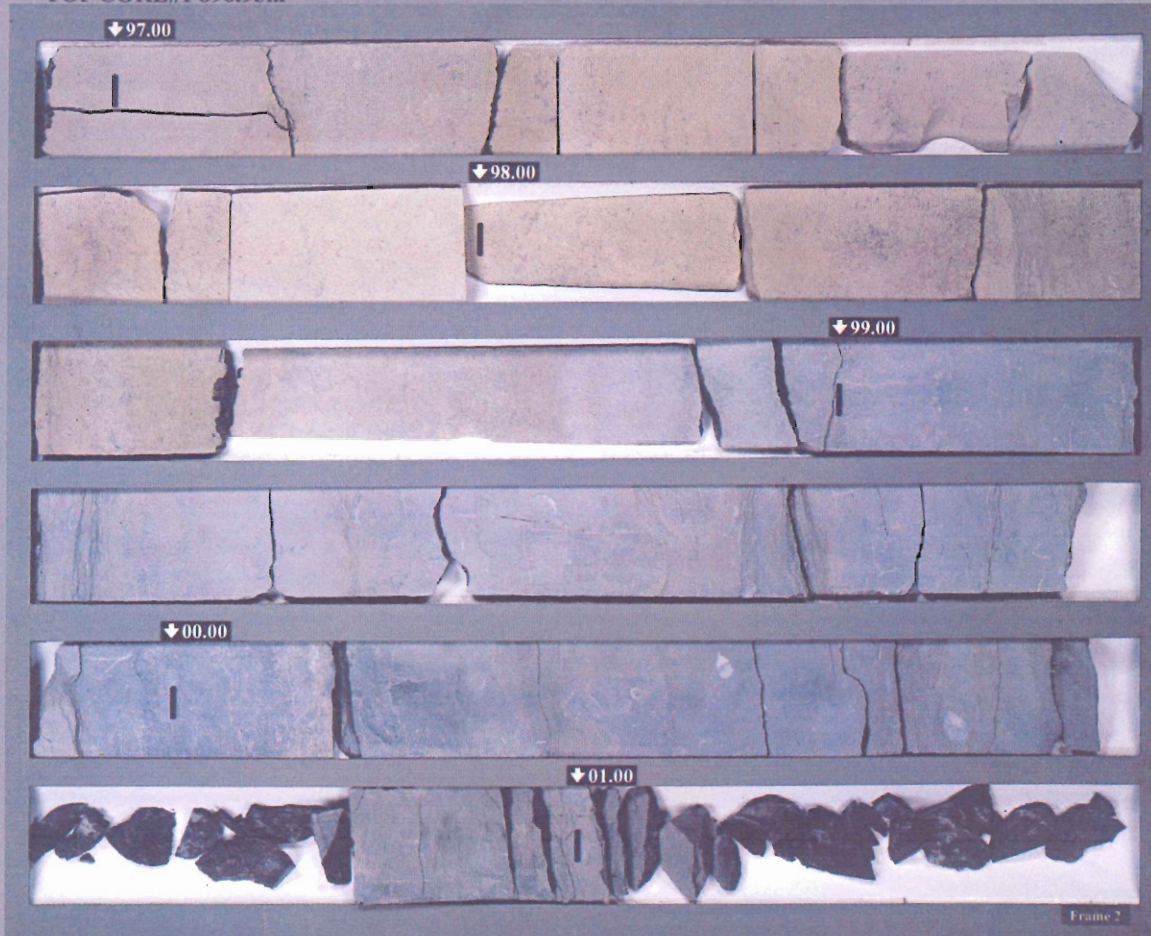
AGAT Laboratories 

BOTTOM 905.72m

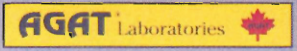
ENCANA CORPORATION
ECA ECOG SIERRA d-A3-E/094-I-14

FEBRUARY, 2005
RC12400

TOP CORE#1 896.95m



BOTTOM 901.35m



APPENDIX B
Detailed Thin Section Descriptions

WELL: D-A3-E/94-I-14

FORMATION: Banff

THIN SECTION: 01

DEPTH: 894.35m

CORE UNIT: Upper, protected backshoal **LITHOFACIES:** G

GRAINS:

Relative Abundance	Skeletal Grain Types	Non-Skeletal Grain Types
Abundant >20%	Bryozoans Ostracods	Peloids
Moderate 10-20%	Pelmatozoans Phylloid Algae? Bivalves Brachiopods	
Rare <10%	Gastropods	

Preservation/Overall Abundance: Grain preservation ranges from well-preserved to fragmented. Well preserved grains are generally larger and stronger whereas poorly preserved fragmented grains tend to be small, fragile organisms (e.g. ostracods). Grains are ~20-40% abundant

Other: Many of the small fragments are difficult to identify, although they are likely ostracods.

Fenestrae- occur as large void spaces which may represent soft bodied organisms which were not preserved and filled in with sparite. Could also result from dissolution of some components. Also occur as pore space between peloidal grains.

MATRIX: Micritic

CEMENT: Sparry calcite

MINERALIZATION: Traces of pyrite ~10% abundant, crystal size range: 0.02 - 0.10 mm

CLASSIFICATION:

Dunham: Skeletal/Peloidal Wackestone

Folk: Poorly washed skeletal/peloidal Biosparite

OTHER: Layering can be observed with the naked eye by holding the thin section up to a light. Layers alternate between coarser grained sparite dominate layers and finer grained micritic layers.

WELL: D-A3-E/94-I-14

FORMATION: Banff

THIN SECTION: 03

DEPTH: 894.90m

CORE UNIT: Upper protected backshoal **LITHOFACIES:** I

GRAINS:

Relative Abundance	Skeletal Grain Types	Non-Skeletal Grain Types
Abundant >20%	Pelmatozoans Ostracods	
Moderate 10-20%	Bryozoans	
Rare <10%	Gastropods Brachiopods	Peloids

Preservation/Overall Abundance: Rare biota are well preserved and larger than other grains. Smaller, more dominant, weaker grains appear less well preserved and more fragmented (e.g. ostracods, pelmatozoans and bryozoans). Grains are generally <10% abundant

Other: Minor occurrences of fenestrae, represent soft bodied organisms replaced by sparite – or dissolved components
Evidence for bioturbation provided by elongate bodies with abundant grain material inside present in the heavily micritic matrix.

MATRIX: Micritic

CEMENT: Minor sparite

MINERALIZATION: Pyrite crystals (0.03 -1.00 mm) accumulate in sparry cemented areas

CLASSIFICATION:

Dunham: Mudstone

Folk: Fossiliferous Biomicrite

OTHER: Minor, thin, laterally extensive, wavy laminations recognized by their brownish color. Layers or lenses rich in fragmented skeletal grains (possibly sponge spicules?) Present in the micritic matrix that is generally poorer in skeletal grains which are however less fragmented.

WELL: D-A3-E/94-I-14

FORMATION: Banff

THIN SECTION: 04

DEPTH: 895.36m

FACIES: Upper, protected

LITHOFACIES: J

GRAINS:

Relative Abundance	Skeletal Grain Types	Non-Skeletal Grain Types
Abundant >20%	Bryozoans Pelmatozoans Ostracods	Peloids
Moderate 10-20%		
Rare <10%	Brachiopods Bivalves	

Preservation/Overall abundance: Small, grains more fragmented (e.g. bryozoans, ostracods). 50-85% abundant

Other: Large variation in grain-size, brachiopods typically the largest, pelmatozoans range from large to small
Fenestrae present

MATRIX: Micritic, peloids, accumulates around skeletal grain walls.

CEMENT: sparite, forms in sheltered and interparticle pore space

MINERALIZATION: pyrite crystals (0.01-0.03mm in size) occur mostly in sparry cements

CLASSIFICATION:

Dunham: Peloidal/Skeletal Packstone

Folk: Poorly washed Biosparite

WELL: D-A3-E/94-I-14

FORMATION: Banff

THIN SECTION: GR-001

DEPTH: 895.00m

FACIES: Upper, protected

LITHOFACIES: J

GRAINS:

Relative Abundance	Skeletal Grain Types	Non-Skeletal Grain Types
Abundant >20%	Bryozoans Bivalves Ostracods	
Moderate 10-20%	Pelmatozoans Brachiopods	Peloids Intraclasts
Rare <10%		Ooids

Preservation/Overall abundance: Generally fragmented, a few well preserved grains. Lots of small unidentifiable skeletal fragments that are relatively thin. 50-80% grain abundance

MATRIX: Micritic

CEMENT: Sparite– infills, interparticle and shelter porosity

MINERALIZATION: minor 0.01 – 0.05mm dolomite crystals occur within the micritic matrix. Minor pyrite (0.01 – 0.03mmsized crystals) accumulations occur within the coarser calcite cements

CLASSIFICATION:

Dunham: Skeletal Peloidal Packstone

Folk: Packed Biomicrite

WELL: D-A3-E/94-I-14

FORMATION: Banff

THIN SECTION: GR-002

DEPTH: 896.5m

CORE UNIT: Middle Sandbelt

LITHOFACIES: D

GRAINS:

Relative Abundance	Skeletal Grain Types	Non-Skeletal Grain Types
Abundant >20%		Ooids Intraclasts
Moderate 10-20%	Pelmatozoans Bryozoans	
Rare <10%	Gastropods	

Preservation/Overall abundance: Fragmented. Grains are 90% abundant.

Other: Ooid nuclei include pelmatozoan, bryozoan, and shell fragments, as well as intraclasts

MATRIX: Micritic, forms around coated grains

CEMENT: Sparite forms within bioclastic pores and in intraparticle pore space.

MINERALIZATION: Dolomite occurs within partially leached grains, Pyrite tends to form around outer grain boundaries

CLASSIFICATION:

Dunham: Oolitic Grainstone

Folk: Oosparite

WELL: D-A3-E/94-I-14

FORMATION: Banff

THIN SECTION: GR-003

DEPTH: 897.5m

CORE UNIT: Middle Sandbelt

LITHOFACIES: E

GRAINS:

Relative Abundance	Skeletal Grain Types	Non-Skeletal Grain Types
Abundant >20%	Bryozoans Pelmatozoans	Intraclasts Peloids
Moderate 10-20%	Bivalves Ostracods	Ooids
Rare <10%		

Preservation/Overall Abundance: Fragmented. Grains are 80-90% abundant

MATRIX: Micritic, forms peloids and also in and around skeletal grains

CEMENT: Sparite, forms within coarser grains and intraparticle pore spaces

MINERALIZATION: traces of dolomite crystals ranging in size from 0.01 – 0.05 mm replacing sparite.
Minor, small (<0.05 mm) traces of pyrite occur throughout the sample

CLASSIFICATION:

Dunham: Peloidal Grainstone

Folk: Sorted Biosparite

WELL: D-A3-E/94-I-14

FORMATION: Banff

THIN SECTION: GR-004

DEPTH: 898.00m

CORE UNIT: Middle Sandbelt

LITHOFACIES: D

GRAINS:

Relative Abundance	Skeletal Grain Types	Non-Skeletal Grain Types
Abundant >20%		Ooids Intraclasts
Moderate 10-20%	Bryozoans Pelmatozoans	
Rare <10%	Shell fragments	

Preservation/Overall Abundance: Fragmented. Grains 80-90% abundant

Other: Ooid nuclei consists dominantly of intraclasts as well as Bryozoan, pelmatozoan, and shell fragments

MATRIX: Micrite – coats nuclei forms in and around grains.

CEMENT: Calcite – forms in intraparticle pores

MINERALIZATION: Dolomitization occurs within partially leached grains, Pyrite tends to form around outer grain boundaries

CLASSIFICATION:

Dunham: Oolitic Grainstone

Folk: Oosparite

WELL: D-A3-E/94-I-14

FORMATION: Banff

THIN SECTION: GR-005

DEPTH: 899.00m

CORE UNIT: Middle Sandbelt

LITHOFACIES: F

GRAINS:

Relative Abundance	Skeletal Grain Types	Non-Skeletal Grain Types
Abundant >20%	Bryozoans Pelmatozoans Ostracods	Intraclasts
Moderate 10-20%	Bivalves Ostracods	
Rare <10%	Gastropods	Ooids

Preservation/ Overall abundance: Bryozoans, pelmatozoans, and bivalves are generally fragmented, Ostracods range from well preserved to fragmented, gastropods appear well preserved. Grains are 80-90% abundant

Other: Fenestrae present

MATRIX: Micritic, forms in and around grains

CEMENT: Sparite, forms in inter and intra-particle pore space

MINERALIZATION: Minor dolomite replacing micrite. Minor amounts of pyrite accumulated within coarser calcite cements and range in size from 0.01 – 0.03mm.

CLASSIFICATION:

Dunham: Skeletal Grainstone

Folk: Unsorted Biosparite

WELL: D-A3-E/94-I-14

FORMATION: Banff

THIN SECTION: 05

DEPTH: 900.50m

CORE UNIT: Lower Mixed Carbonate
Siliciclastic

LITHOFACIES: A

GRAINS:

Relative Abundance	Skeletal Grain Types	Non-Skeletal Grain Types
Abundant >20%	Pelmatozoans Brachiopods	Detrital Quartz grains
Moderate 10-20%	Bryozoans Corals	
Rare <10%	Radiolarian??? (small round networks lined with dark micritic walls, infilled with calcite or pyrite)	

Preservation/Overall abundance: Fragmented. Fossilized grains are generally 10% abundant

Other: No fenestrae (unlike upper and middle facies)

A lot of brachiopod spines may indicate heavy fragmentation in lower facies, as brachiopod spines not present in upper facies despite the fact that it does contain brachiopods
Brachiopods seem more diverse, indicated by different shell fabrics and ornamentations

MATRIX: Microspar with sub-angular to sub-rounded, well-sorted quartz grains (~0.04mm in size)

Brownish in colour may indicate sideritic carbonate. Carbonate component appears different from upper and middle facies.

CEMENT: The presence of sparry calcite is minor compared to the middle and upper facies, it occurs mainly in interparticle pores. (e.g. within brachiopod spines, coral and bryozoan walls)

MINERALIZATION: Pyrite, present throughout matrix.

CLASSIFICATION:

Dunham: Quartzose Lime Mudstone

Folk: Quartzose Biomicrite

OTHER: moderate evidence for a horizontal "fabric:" both fossil and quartz grains seem to be oriented with their long axes parallel to bedding.

WELL: D-A3-E/94-I-14

FORMATION: Banff

THIN SECTION: 06

DEPTH: 902.36m

CORE UNIT: Lower Mixed Carbonate
Siliciclastic

LITHOFACIES: A

GRAINS:

Relative Abundance	Skeletal Grain Types	Non-Skeletal Grain Types
Abundant >20%	Pelmatozoans Radiolarian??	Detrital Quartz Grains
Moderate 10-20%	Brachiopods Ostracods Chambered forams?? – (microgranular calcite crystals make up walls)	Calcite Intraclasts
Rare <10%		

Preservation/Overall abundance: Mostly fragmented, brachiopod spines appear altered – outer layer fabric hard to see still possesses two distinct layers. Fossilized grains are 30% abundant.

Other: Grains are randomly oriented. A lot of unrecognizable, yet well preserved grains. These grains are typically best observed in 16x optical power.

Four dominant morphologies:

- 1) Circular (bunch of grape-like) networks, Chamber walls typically brown in colour, appear micritic? Inter-chambers filled with calcite cement (typically) sometimes pyrite infillings. Appear fragmented.
- 2) Elongate – coral-like networks, long subparallel, semi-enclosed chamber walls, with typically one opening. Wall and chamber composition similar to #1. Appear fragmented.
- 3) Chambered foram with gastropod-like elongate spiral form. Only a few well preserved tests however a lot of grains probably present but poorly preserved.
- 4) V-shaped, chambered grains, with a center division running sub-parallel to outside walls. Sub-perpendicular to the center division are multiple other divisions. Appear well-preserved.

MATRIX: Microspar?, with sub-angular to sub-rounded, well-sorted quartz grains (~0.04mm in size) Brownish in colour – could this indicate sideritic carbonate. Carbonate component appears different from upper and middle facies.

CEMENT: Sparite

MINERALIZATION: Occurrences of pyrite throughout the matrix

CLASSIFICATION:

Dunham: Quartzose lime Wackestone

Folk: Sparse Biomicrite

WELL: D-A3-E/94-I-14

FORMATION: Banff

THIN SECTION: 07

DEPTH: 904.36m

CORE UNIT: Lower Mixed Carbonate
Siliciclastic

LITHOFACIES: B

GRAINS:

Relative Abundance	Skeletal Grain Types	Non-Skeletal Grain Types
Abundant >20%	Brachiopods Bivalves	
Moderate 10-20%	Pelmatozoans Silicified coccoid cells (dark black circles look like zircons) Cyanobacterial Filaments	
Rare <10%	Sponge Spicules Bryozoans Orbitolinid forams	

Preservation/Overall abundance: Fragmented, lots of brachiopod spines. Grains 60% abundant

Other: Sub-horizontal fabric, aligned sub-parallel to bedding
Solution seams between touching grain boundaries
Brachiopods seem diverse, impunctate and punctate shell structures
Absence of bryozoans, ostracods and fenestrae (fragile organisms) suggests higher energy environment

MATRIX: Micritic, light brown in PPL, darker and pleochroic in crossed-polarizers

CEMENT: calcareous, sparite traces occur in centers of brachiopod spines

MINERALIZATION: Pyrite occurrences throughout matrix

CLASSIFICATION:

Dunham: skeletal lime packstone

Folk: packed biomicrite

OTHER: A lot of fractures

WELL: D-A3-E/94-I-14

FORMATION: Banff

THIN SECTION: 08

DEPTH: 904.73m

CORE UNIT: Lower Mixed Carbonate
Siliciclastic

LITHOFACIES: C

GRAINS:

Relative Abundance	Skeletal Grain Types	Non-Skeletal Grain Types
Abundant >20%	Brachiopod fragments Sponge spicules? Other Shell fragments	
Moderate 10-20%		
Rare <10%		

Preservation/Overall abundance: Fragmented. Trace amounts of fossils

MATRIX: micritic to microsparic (see notes below) with abundant, sub-angular quartz grains (typically size ~.05mm). Rare (<10%) amounts of titanite, white mica, chlorite, pyroxenes and biotite – likely igneous origin
A lot of minor occurrences of weird minerals (one reddish brown one, some circular stuff) –

CEMENT: Sparite

MINERALIZATION: pyrite present throughout matrix

CLASSIFICATION: Calcareous siltstone

OTHER: Lenticular bedding, dark finer grained layers alternating with lighter, coarser grained layers and lenses. The darker layers contain a micritic component whereas the lighter layers contain microspar.

WELL: D-A3-E/94-I-14

FORMATION: Banff

THIN SECTION: 09

DEPTH: 905.70m

CORE UNIT: Lower Mixed Carbonate
Siliciclastic

LITHOFACIES: C

GRAINS:

Relative Abundance	Skeletal Grain Types	Non-Skeletal Grain Types
Abundant >20%	Pelmatozoans Brachiopod spines Shell fragments Bryozoans	
Moderate 10-20%		
Rare <10%		

Preservation/Overall abundance: Fragmented. Trace amounts of fossils.

Other:

MATRIX: Micritic – Microsparic, abundant quartz sub-angular to sub-rounded grains (~.03mm in size)
Rare (<10%) amounts of titanite, white mica, chlorite, pyroxenes and biotite – likely igneous origin

CEMENT: calcareous

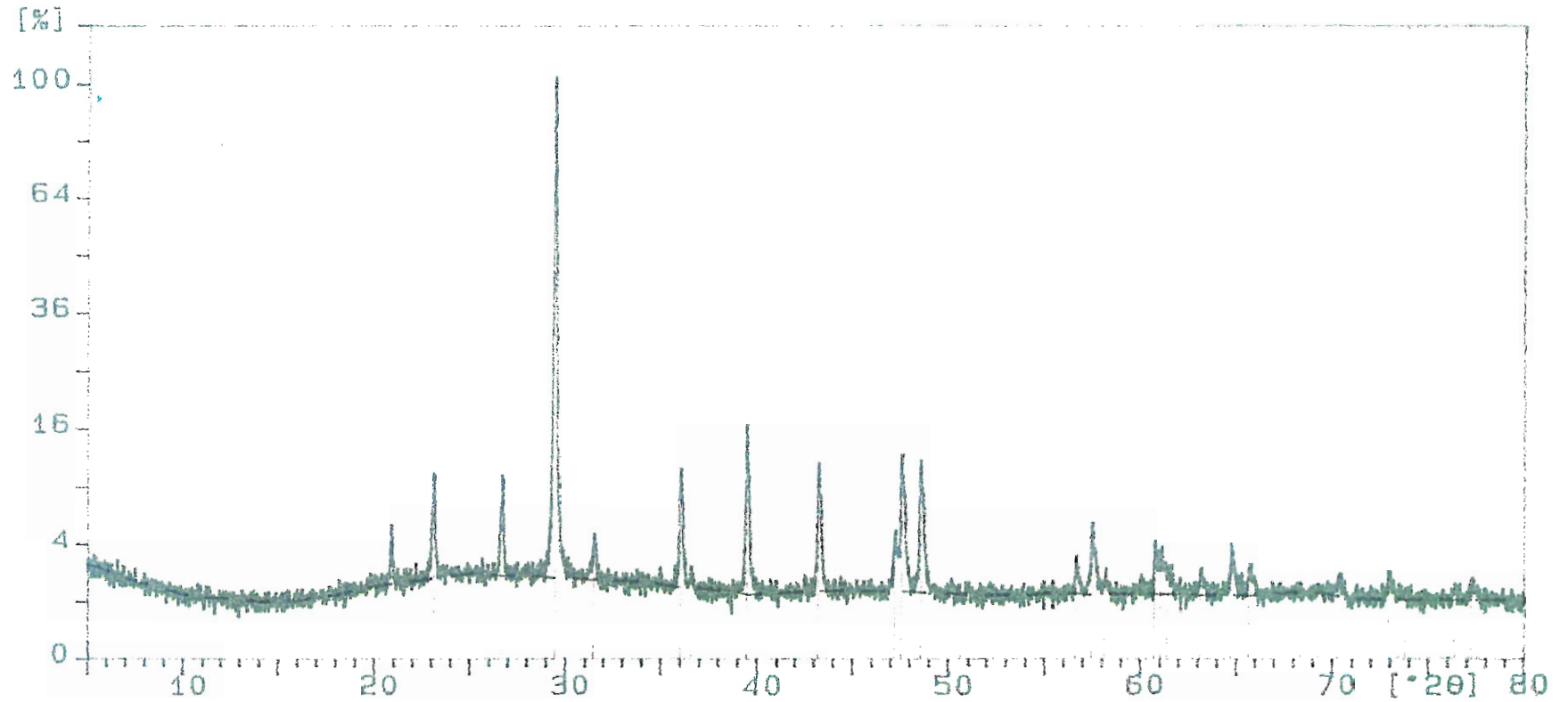
MINERALIZATION: pyrite occurrences throughout matrix

CLASSIFICATION: Calcareous Shale

APPENDIX C
XRD Charts

Sample ident.: 894.35

30-Jan-2008 11:58



89435

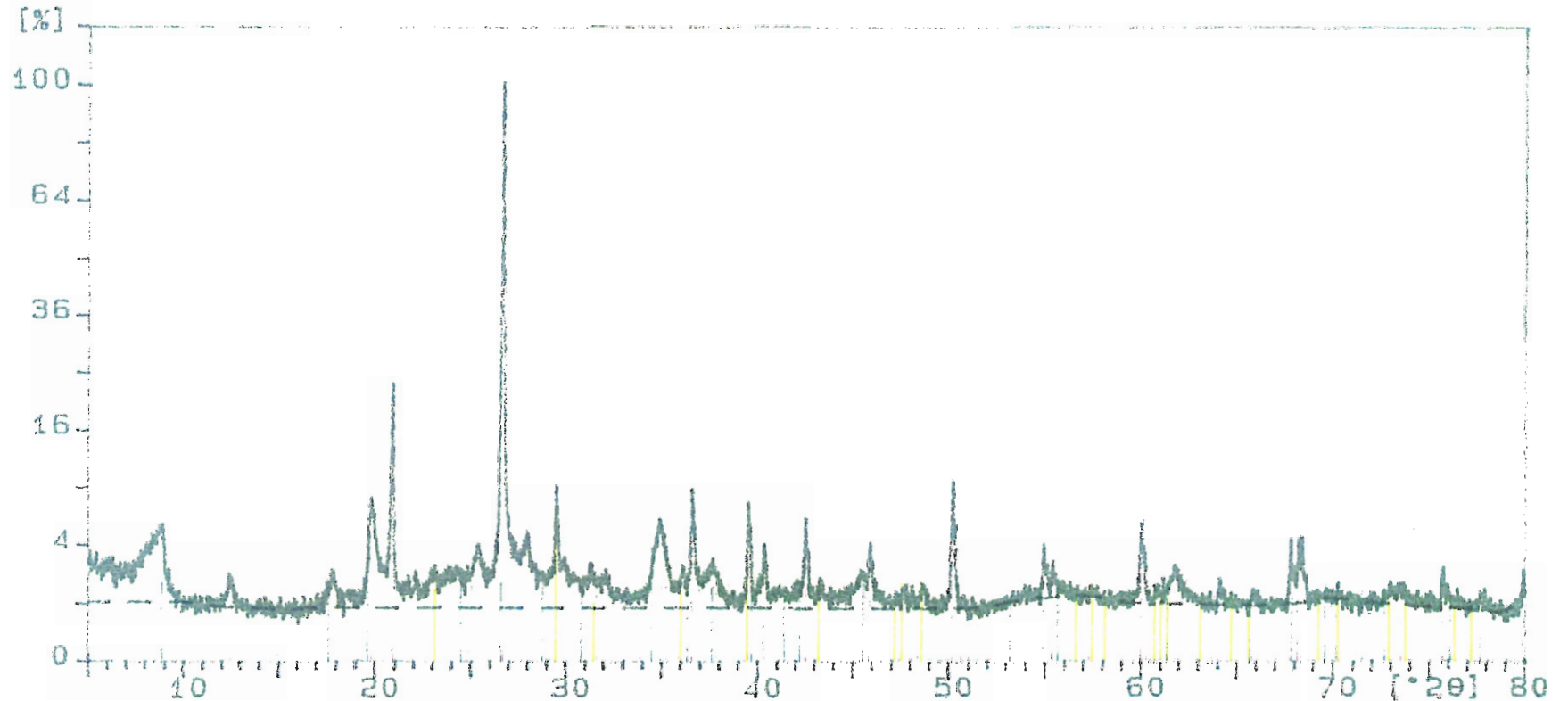


05-0586 Calcite, syn

33-0161 Quartz, syn

Sample ident.: 89445

30-Jan-2008 12:34



89445

33-1161

Quartz, syn

05-0586

Calcite, syn

01-0714

Clinoclere, 2M, 2B

02-0462

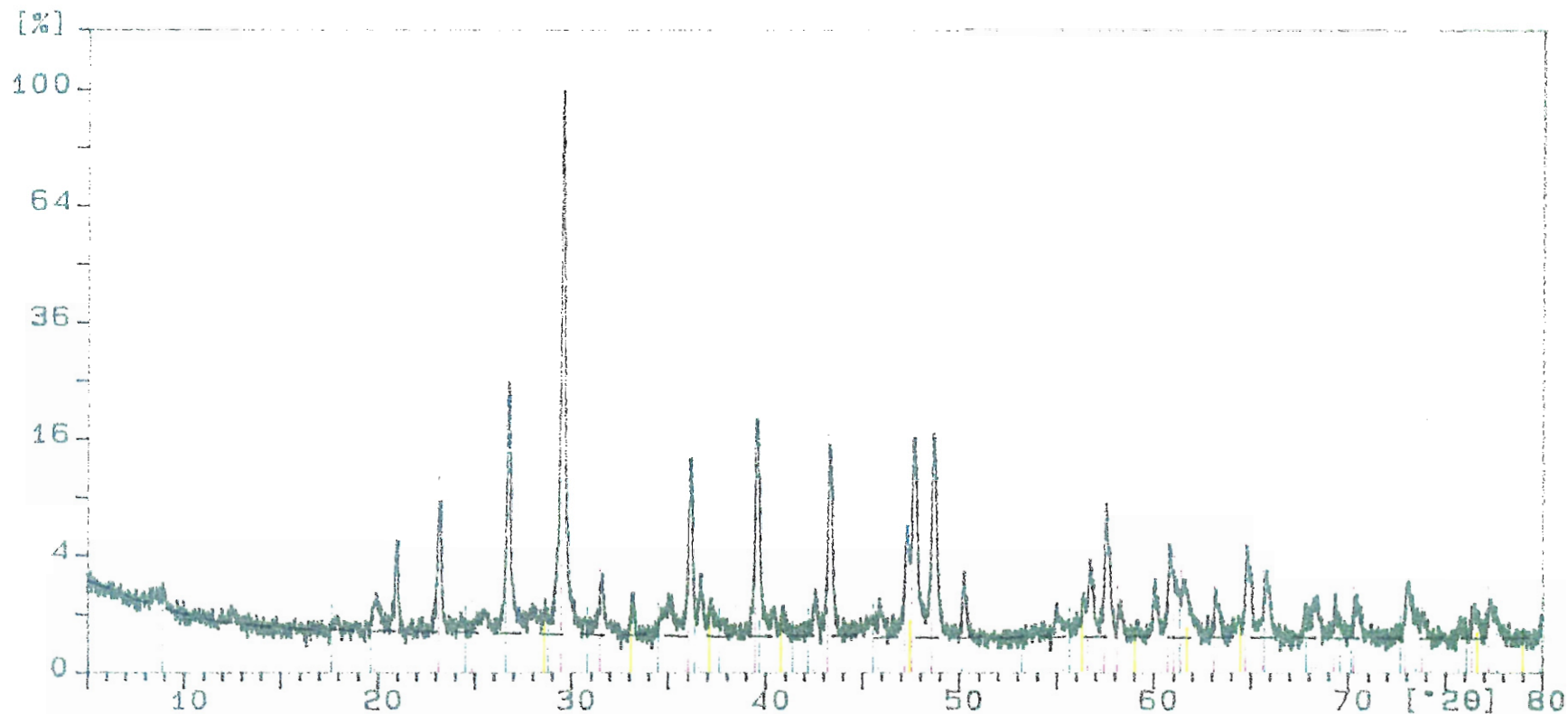
Illite, 1M

01-0714

Basalite, 1M

Sample ident.: 89490

30-Jan-2008 11:22



89490



05-0586 Calcite, syn

33-0461 Quartz, syn

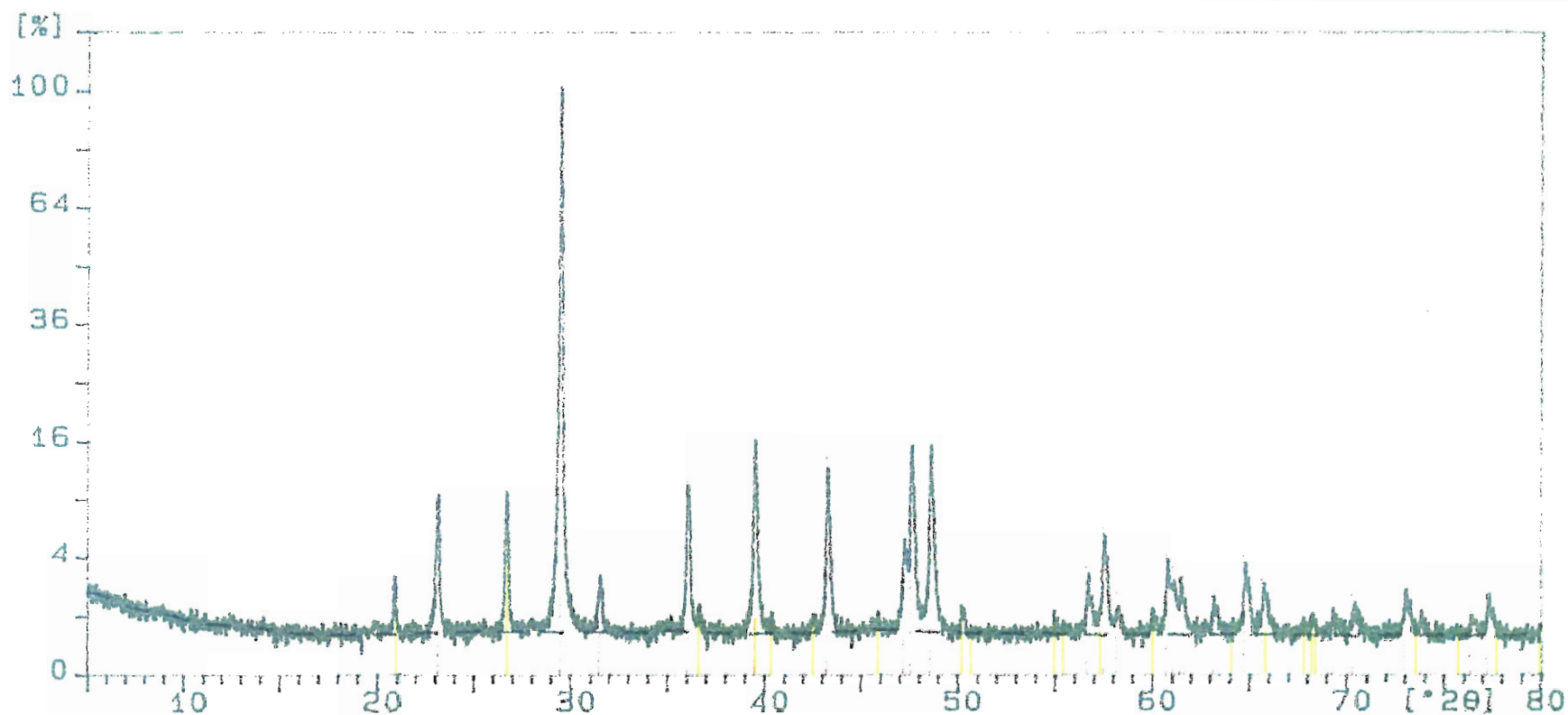
06-0710 Pyrite, syn

02-0462 Illite, 1M

01-0711 Kaolinite, 1M

Sample ident.: 895.36

30-Jan-2008 12:14



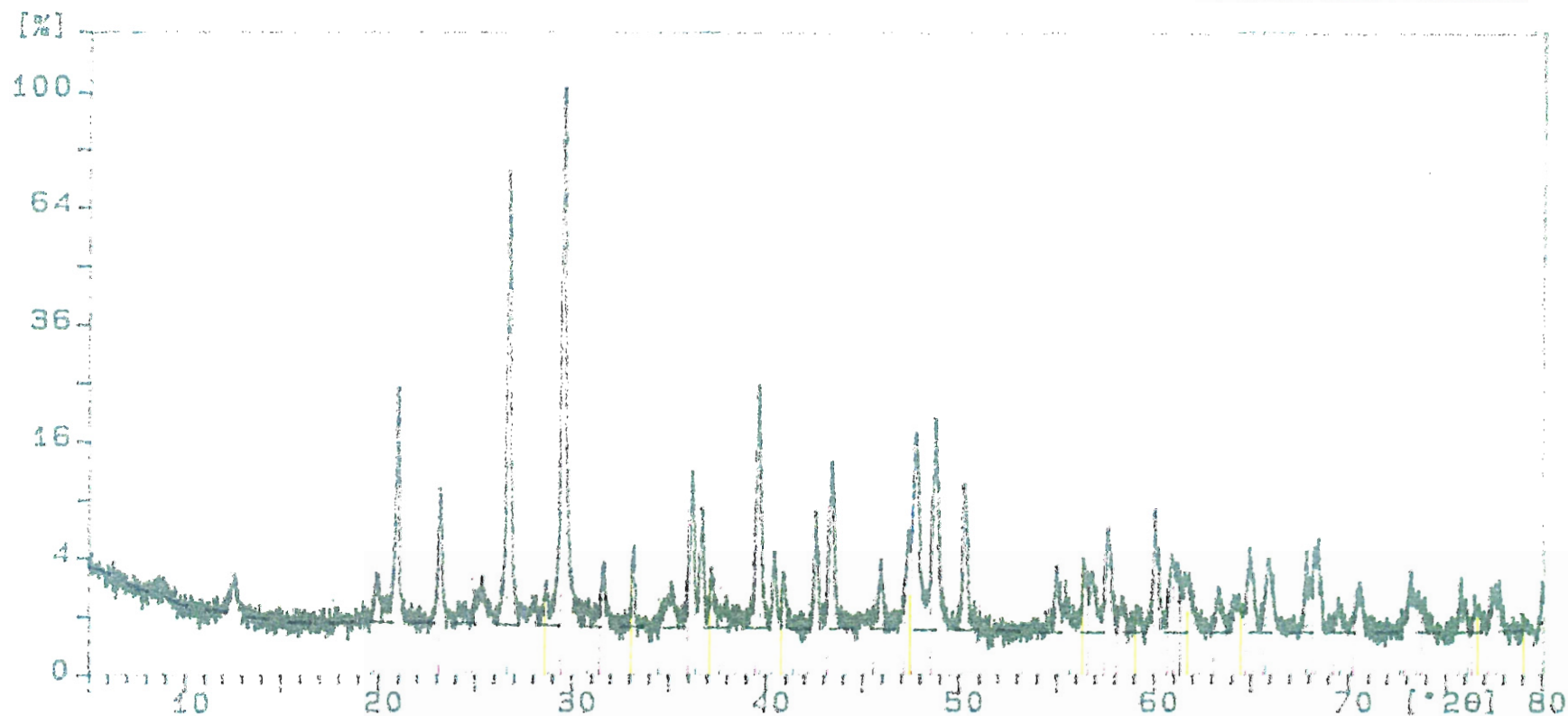
89536

05-0586 Calcite, syn

33-1161 Quartz, syn

Sample ident.: 90050

29-Jan-2008 18:01



90050

05-0586 Calcite, syn

33-1164 Quartz, syn

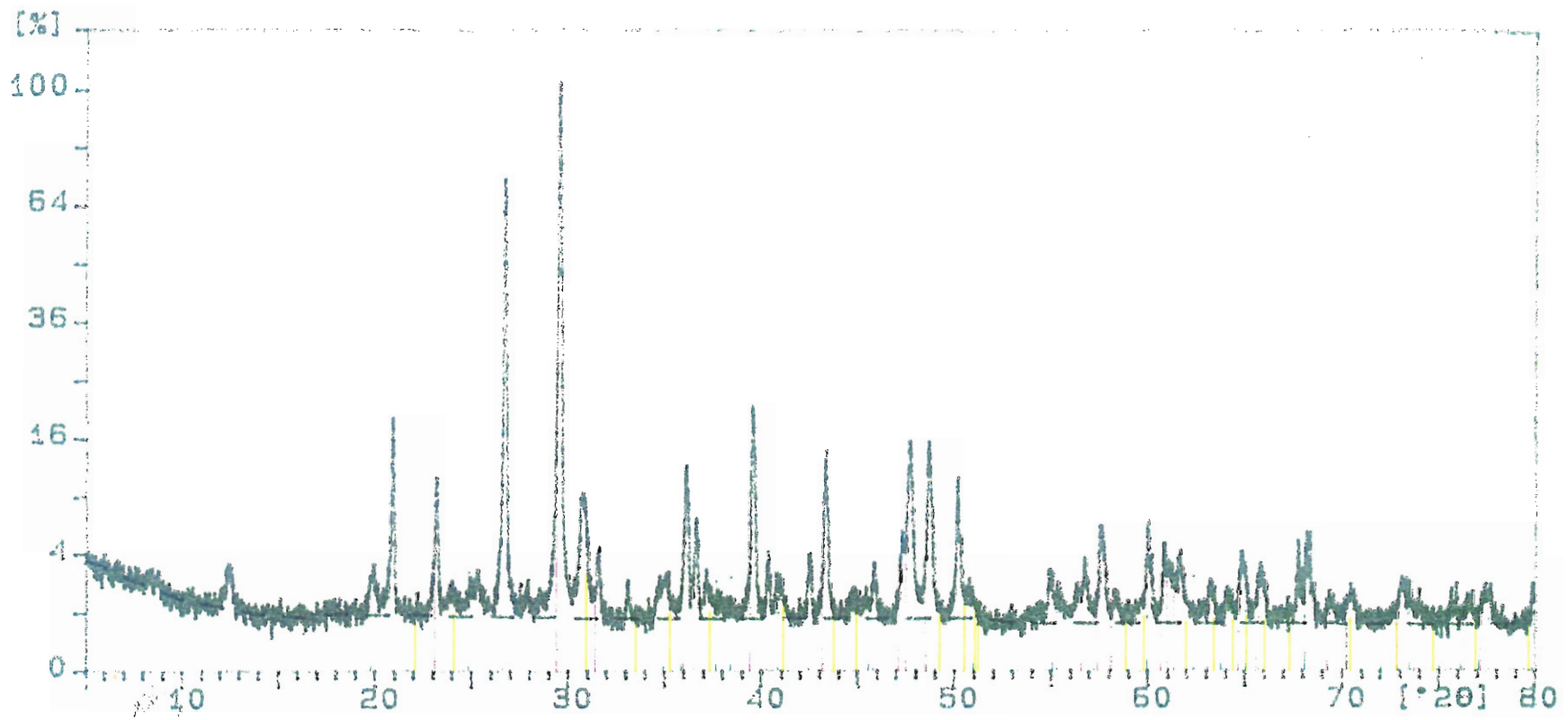
06-0710 Pyrite, syn

02-0462 Illite, 1M

06-0321 Kaolinite, 1M

Sample ident.: 90283

29-Jan-2008 17:46

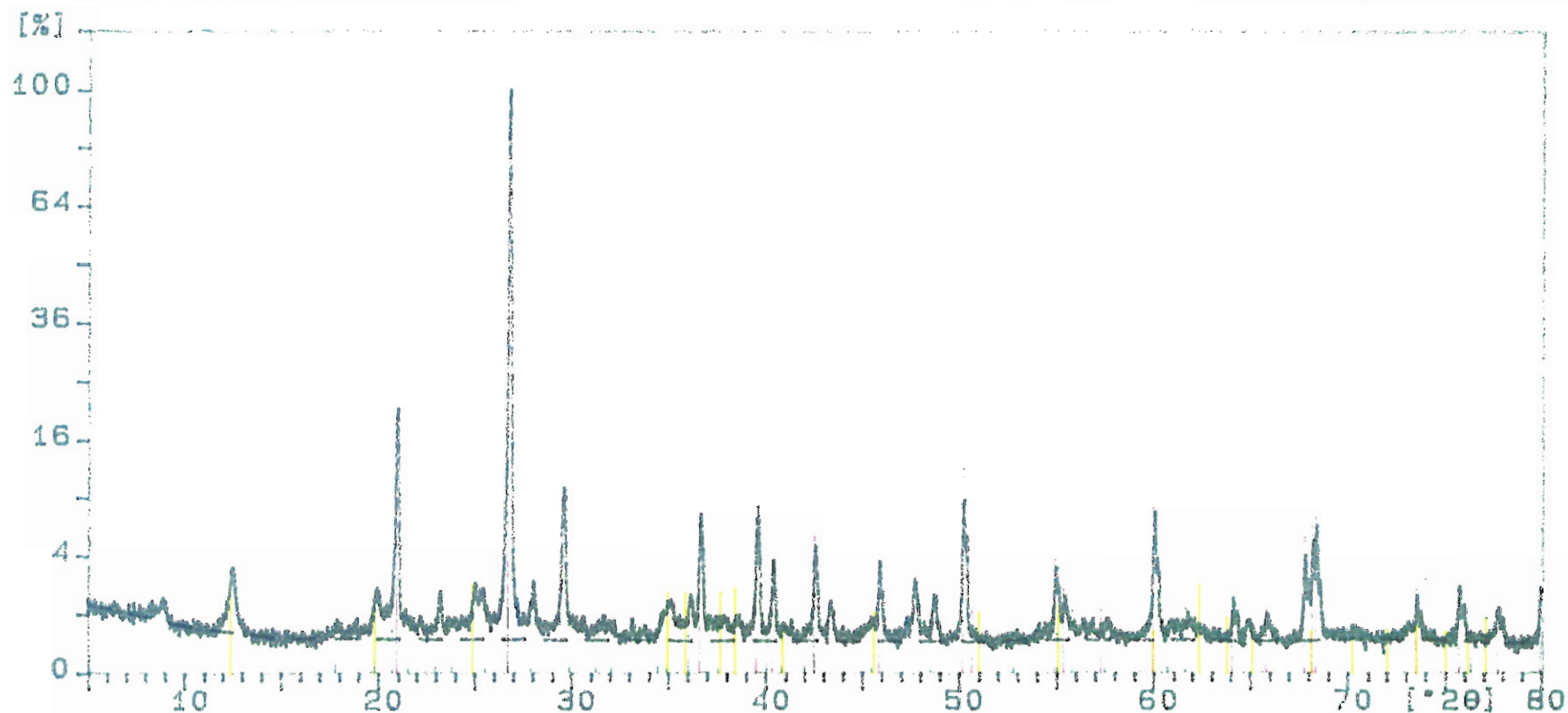


90283

- 05-0586 Calcite, syn
- 33-1161 Quartz, syn
- 11-0078 Dolomite
- 06-0221 Kaolinite 1Md

Sample ident.: 90436

29-Jan-2008 17:26



90436

33-1161 Quartz, syn

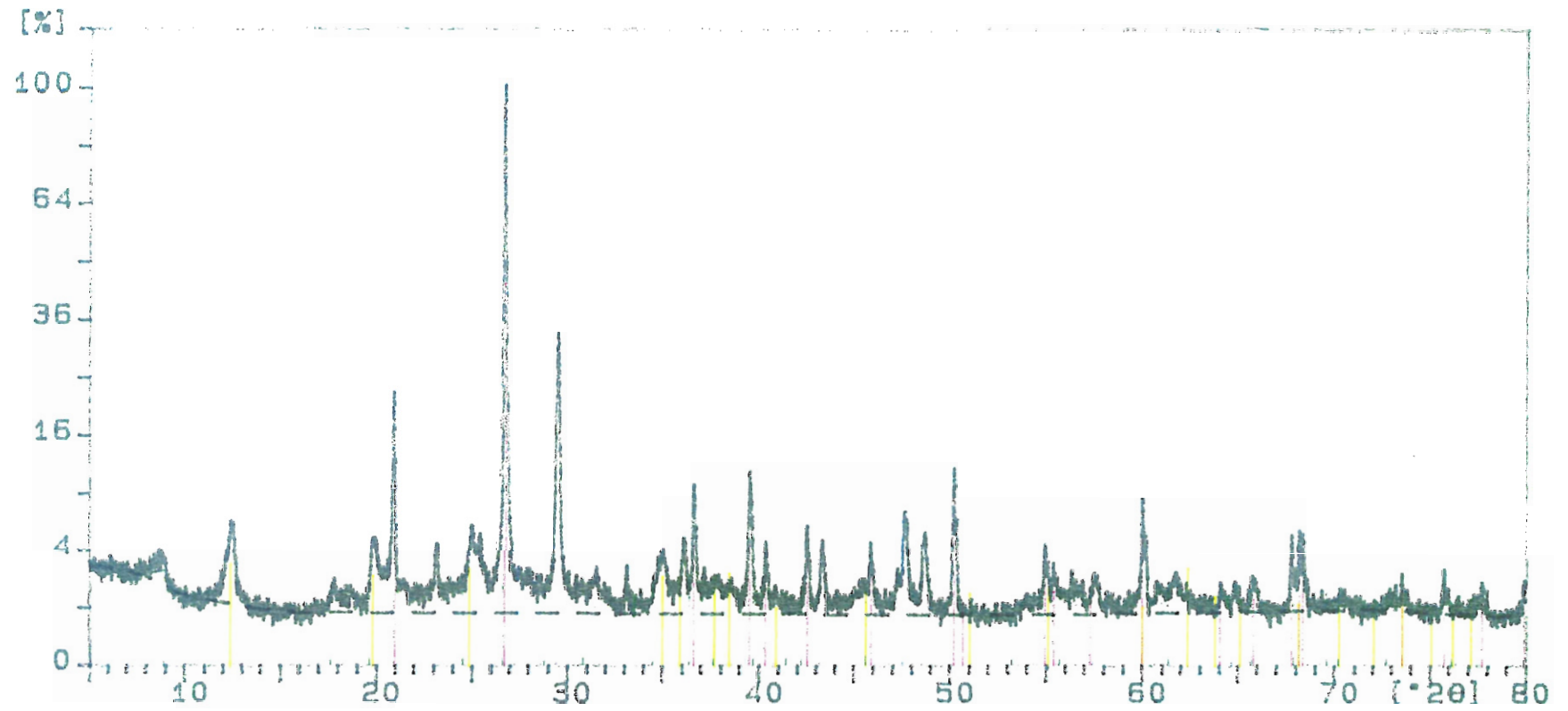
05-0586 Calcite, syn

06-0221 Kaolinite 1Md

19-0814 Muscovite-2M1, vanadian

Sample ident.: 90473

29-Jan-2008 17:08



90473

33-1161 Quartz, syn

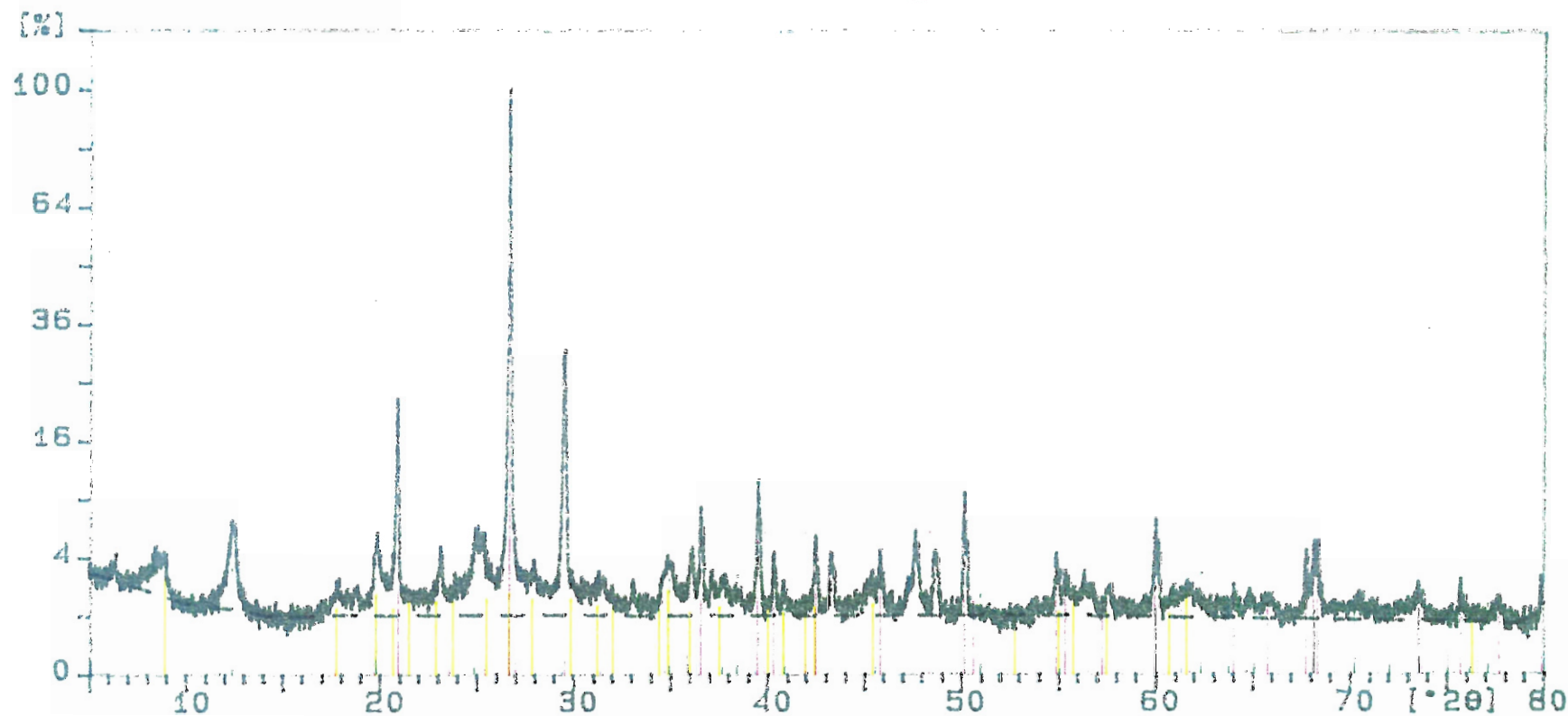
05-0586 Calcite, syn

06-0221 Kaolinite 1Md

02-0462 Illite, 1M

Sample ident.: 90570

29-Jan-2008 16:43



90570

33-1161

Quartz, syn

05-0585

Calcite, 50

19-0814

Muscovite-2M1, vanadian

06-0221

Kaolinite 1Md

13-0134

Diagenetic kaolinite